INVESTIGATIONS ON PERFORMANCE ENHANCEMENT OF CYLINDRICAL CONFORMAL ANTENNAS FOR GPS, WI-FI AND WIMAX APPLICATIONS

Submitted in partial fulfillment of the requirements
for the award of the degree of
DOCTOR OF PHILOSOPHY

by

RATIKANTA SAHOO

(Roll No: 715044)

Supervisor:

Dr. D. Vakula
Associate Professor

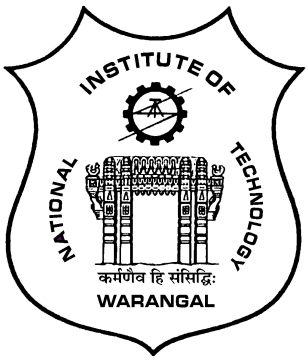

DEPARTMENT OF ELECTRONICS AND COMMUNICATION ENGINEERING
NATIONAL INSTITUTE OF TECHNOLOGY WARANGAL
TELANGANA STATE-506004, INDIA

2020

Dedicated to

My family

Approval Sheet

This thesis entitled "**Investigations on Performance Enhancement of Cylindrical Conformal Antennas for GPS, Wi-Fi and WiMAX Applications**" by **Ratikanta Sahoo** is approved for the degree of Doctor of Philosophy.

_____

_____

_____

Examiners

_____

_____

_____

Supervisor (s)

_____

Chairman

Date: _____

DECLARATION

This is to certify that the work presented in the thesis entitled "**Investigations on Performance Enhancement of Cylindrical Conformal Antennas for GPS, Wi-Fi and WiMAX Applications**" is a bonafide work done by me under the supervision of **Dr. D. Vakula**, Associate Professor, Department of Electronics and Communication Engineering, National Institute of Technology Warangal, India and was not submitted elsewhere for the award of any degree.

I declare that this written submission represents my ideas in my own words and where others' ideas or words have been included, I have adequately cited and referenced the original sources. I also declare that I have adhered to all principles of academic honesty and integrity and have not misrepresented or fabricated or falsified any idea / data / fact / source in my submission. I understand that any violation of the above will be a cause for disciplinary action by the Institute and can also evoke penal action from the sources which have thus not been properly cited or from whom proper permission has not been taken when needed.

Ratikanta Sahoo

(Roll No: 715044)

Date: .....

DEPARTMENT OF ELECTRONICS AND COMMUNICATION ENGINEERING

NATIONAL INSTITUTE OF TECHNOLOGY WARANGAL

TELANGANA STATE-506004, INDIA

CERTIFICATE

This is to certify that the thesis entitled "**Investigations on Performance Enhancement of Cylindrical Conformal Antennas for GPS, Wi-Fi and WiMAX Applications**", which is being submitted by **Mr. Ratikanta Sahoo (Roll No: 715044)**, in partial fulfillment for the award of the degree of Doctor of Philosophy to the Department of Electronics and Communication Engineering of National Institute of Technology Warangal, is a record of bonafide research work carried out by him under my supervision and has not been submitted elsewhere for any degree.

Dr. D. Vakula
(Supervisor)
Associate Professor
Department of E.C.E.
N.I.T. Warangal
Warangal - 506004, India

ACKNOWLEDGEMENTS

Firstly, I would like to express my sincere gratitude to my supervisor Dr. D. Vakula for the continuous support of my Ph.D study and related research, for her patience, motivation, and guidance. My sincere thanks to her for providing me an opportunity to join the institute as a Ph.D research scholar and giving me access to the research facilities. I find words inadequate to thank them for enabling me to complete this work in spite of all obstacles. The thesis would not have seen the light of the day without her insistent support and cooperation.

I am also grateful to Prof. L. Anjaneyulu, Head of the department, Department of Electronics and Communication Engineering, NIT Warangal for his valuable suggestions and support that he shared during my research tenure.

Besides my supervisor,I take this privilege to thank Prof. N. Bheema Rao, previous Head of the department, Department of Electronics and Communication Engineering, NIT Warangal for his helpful discussion and extensive comments during the course of my doctoral work. I am very grateful to Prof. N.V.S.N Sarma, Professor, Department of Electronics and Communication Engineering, NIT Warangal for his enlightening wisdom, suggestions and advices during the course of this doctoral work. I also thank Doctoral Scrutiny Committee member, Dr. A. Prakasa Rao, Associate Professor, Department of Electronics and Communication Engineering, NIT Warangal for his encouragement during the course of my doctoral work.

I also take this privilege to acknowledge Prof. V. T Somasekhar , Professor, Department of Electrical Engineering, NIT Warangal for their continuous support, suggestions and advices given during my research period whenever required.

I also thank Mr. C. Sairam, Scientist, Defence Electronics Research Laboratory, Hyderabad for his help to measure all my antennas. I thank Mr. Sriniva Reddy from Cosmic Enterprises, Hyderabad in supporting the fabrication of all my antennas.

It is my pleasure to show my indebtedness to my co-scholars at NIT for their help during the course of this work. I find no words inadequate to express any form of acknowledgment to my family members for their love, support and patience for making my dream come true.

Finally, I thank God, for filling me every day with new hopes, strength, purpose and faith.

ABSTRACT

Rapid expansion of wireless communications industry has created a need for better connectivity among various terrestrial wireless systems and wireless systems mounted on mobile platforms such as aircrafts, cars, ships and satellites. These wireless communication systems require antennas to meet the platform specifications in addition to the radiation characteristics. The platform on which antenna to be mounted is not always flat. Hence, the structure of the antenna is to be modified according to the surface on which it is to be mounted. The antennas which are bent on the non planar surface are known as conformal antennas. Fixed and mobile wireless systems need antennas for GPS, Wi-Fi and WiMAX applications with omnidirectional and directional radiation characteristics. The conformal antennas designed for GPS, Wi-Fi and WiMAX applications have to be wideband to allow all the frequencies, must be compact to reduce the space requirements and high gain for better connectivity. In the proposed thesis , the design of conformal antennas are proposed to meet the demands of the present day communication systems. Different novel techniques are adopted to improve performance of antennas..

Initially, cylindrical conformal antennas with slots and fractal structures are designed and fabricated on 60 mm radius of curvature for GPS application. The wideband characteristics are obtained by using partial ground concept and wide-slot on ground plane.

Later gain enhancement of the wideband conformal directional antenna with parasitic elements and metamaterial is discussed. The gain enhancement of the basic conformal antenna is achieved by integrating triangular shaped parasitic elements and low index metamaterial unit cells. The application of metamaterials for conformal antenna design is discussed. The unit cell metamaterial and unit cell as an array is designed and integrated with antenna for enhancement of gain of antenna.

Cylindrical conformal antennas are designed for Wi-Fi and WiMAX applications subsequently. The conformal antennas with dual U slot on the patch are designed on cylinders of various radius of curvatures for Wi-Fi application. A compact metamaterial based cylindrical conformal dual-band antenna is designed, fabricated and validated experimentally for Wi-Fi and WiMAX applications. The compactness, wideband and dual-band characteristics are obtained by incorporating meanderlines, fractal inductor and parasitic elements respectively. In the proposed work, the fractional bandwidth is achieved up to 81.4% and the gain is increased up to 1.6 dBi. All the antennas have shown better characteristics when compared with existing antennas.

Contents

List of Figures

List of Tables

List of Abbreviations

3-D	Three Dimensional
2-D	Two Dimensional
4G-LTE	4th Generation Long-Term Evolutio
ATGM	Anti-Tank Guided Missile
ARINc	Aeronautical Radio, Incorporated
BW	Bandwidth
CP	Circular Polarisation
CRLH-TL	Composite Right-and-Left-Handed Transmission Line
CST	Computer Simulation Technology
CPW	Co-planar Waveguide
DC	Direct Current
EM	Electromagnetic
EGR	Embedded GPS Receiver
EWCA	European Workshop on Conformal Antennas
FR4	Flame Retardant
GNSS	Global Navigation Satellite System
GLONASS	Global Navigation Satellite System
GPS	Global Positioning System
HPBW	Half-Power Beamwidth
HP	Hewlett-Packard.
HFSS	High-Frequency Structure Simulator
IFS	Iterated Function System
LHM	Left Handed Metamaterials
LP	Linear polarisation
LEO	Low Earth Orbit
LIM	Low Index Metamaterial
MTM	Metamaterial

MSRR	Modified Split-Ring Resonator
MMIC	Monolithic Microwave Integrated Circuit
MIMO	Multiple-Input and Multiple-Output
PSL	Parallel Strip Line
PEC	Perfect Electric Conductor
PMC	Perfect Magnetic Conductor
PBG	Photonic Band Gap
PCB	Printed Circuit Board
RF	Radiofrequency
RHM	Right Handed Metamaterials
SRF	Self-Resonance Frequency
SRR	Split-Ring Resonator
SWR	Standing Wave Ratio
SMA	SubMiniature version A
T/R	Transmitter/Receiver
UWB	Ultra Wide Band
Wi-Fi	Wireless-Fidelity
WLAN	Wireless Local Area Network
WiMAX	Worldwide Interoperability for Microwave Access
ZIM	Zero Index Metamaterial
ZOR	Zero Order Resonace

List of Symbols

ε_r	Relative permittivity
μ_r	Channel Length
λ_g	Guide wavelength
ε	Permittivity
μ	Permeability
n	Refractive index
k	propagation constant
Z	Impedance
c	velocity of light
V_p	Phase velocity
C_R	Shunt capacitance
C_L	Series capacitance
L_R	Series capacitance
L_L	Shunt inductance
β	Phase constant
G	Conductance
f_r	Resonant frequency
Q	Quality factor

Chapter 1

Introduction

1.1 Overview

Wireless communication system is an electronic system which utilizes radio waves for transmission of information. Since wireless systems have some attractive and unique benefits over the wired system, wireless systems are used extensively for many applications [1].An antenna, as a fundamental part of any wireless system, is characterized as a device which can receive and radiate electromagnetic energy in a desired and efficient way.

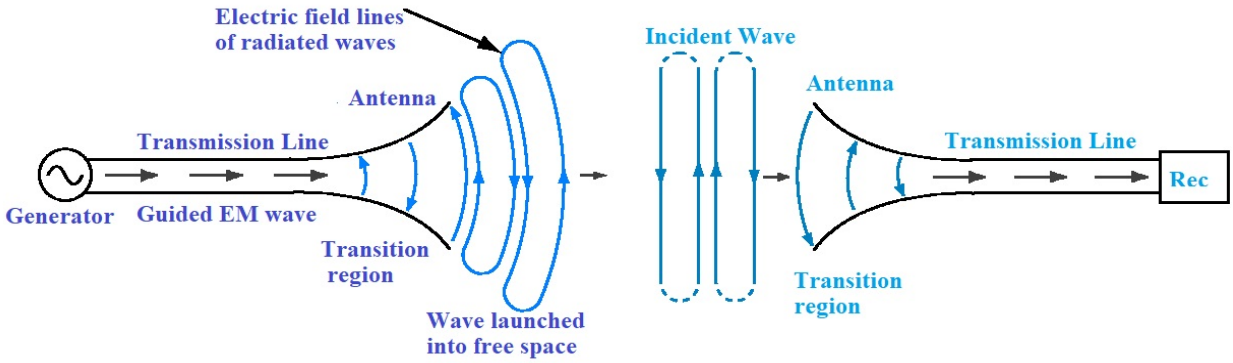

Figure 1.1 A radio communication system.

A typical radio communication system is shown in Figure 1.1. The source information is amplified and modulated in the transmitter and sent to the transmitting antenna by means of a transmission line, which has a characteristic impedance usually of 50 Ω . The antenna radiates the information in the form of an electromagnetic wave in a proficient and desired way to the destination, where the information is picked up by the receiving antenna and sent to the receiver

through transmission line. The signal is demodulated and the original information is recovered at the receiver.

Basically, antenna is a resonant device which radiates a particular range of frequencies. Each frequency band is allocated for a specific application. Antenna frequency bandwidth is defined in terms of operating frequencies, where maximum power is radiated. Generally, the bandwidth of the antenna is defined using fractional bandwidth. Depending on the frequency range, antennas can be classified as narrowband and wideband. The fractional bandwidth of narrowband antenna is less than 20%, where as fractional bandwidth of wideband antenna is considered greater than or equal to 20%. Wideband antennas are used for transmitting high data rates. The direction of radiated fields, beamwidth, gain and efficiency are the other parameters, which define the antenna performance. The characteristics of radiation pattern depend on the size and shape of the radiating antenna element. The size of the antenna is determined in terms of wavelength 'λ' which vary within the operating frequency range. It is always desirable to get the same pattern of radiated field/power over the entire operating frequency range and however it is difficult to get similar characteristics over a broad frequency range. In addition, the input impedance of the antenna should be matched at the feed line to transfer maximum power without reflection.

Antennas like monopole,dipole, loop, log-periodic, helical and Yagi–Uda antennas are three-dimensional antennas which are used for many applications for VHF communications. The antennas for which the energy is received over an area are termed as aperture antennas. The main types of aperture antennas include horn antenna, slot antenna and parabolic reflector.

The three-dimensional antennas are not suitable for portable wireless devices due to their large size. Therefore, two-dimensional printed antennas are widely used in portable wireless devices. Planar antennas such as microstrip antennas have became very popular since 1970s for many applications. Microstrip antennas are low profile antennas, compatible with Monolithic Microwave Integrated Circuit (MMIC) and mechanically robust when mounted on rigid surface. These antennas comprise of a metallic patch on a substrate and with a conductor on the bottom side of the surface which act like a ground plane. The shape of the radiating patch decides the radiation characteristics of the antenna. Conventional rectangular and circular geometries are preferred due to the simplicity in design and fabrication. Microstrip antennas are also convenient to make them conformal to the mounting platform due to their planar nature [2, 3, 4, 5, 6]. But, microstrip antennas have low efficiency and low power handling capacity. In addition, microstrip antennas are narrow bandwidth devices with low gain. However,these limitations can be overcome with novel techniques. Bandwidth enhancement is done by stack-

ing configuration and also by using reconfigurable structure [6]. The gain of antenna can be increased with parasitic elements and metamaterials.

Wireless communication plays a significant role in everyday life. Antennas are the eyes and ears for wireless devices which are experiencing a drastic change from the prior long wire antenna for communication links in military applications to modern compact antennas. Different wireless communication technologies such as Radar, satellite communication, cellular communication, Global Positioning System (GPS), Bluetooth, Radio frequency identification, Wi-Fi and WiMAX are emerging rapidly. However, for future needs, many number of antennas are to be integrated for a wide range of communication needs. For some situations, the platform for mounting the antenna is not always flat. Consequently, it is important to make the antenna conformal to the device to make it less noticeable to the human eye. Due to space constraints on the device, design of compact antenna is also required. For military and commercial applications, there is an expanding requirement for compact conformal antennas that can fulfill the communications needs and also utilizing as meager space as possible. The conformal antennas for airborne systems also require wide bandwidth.

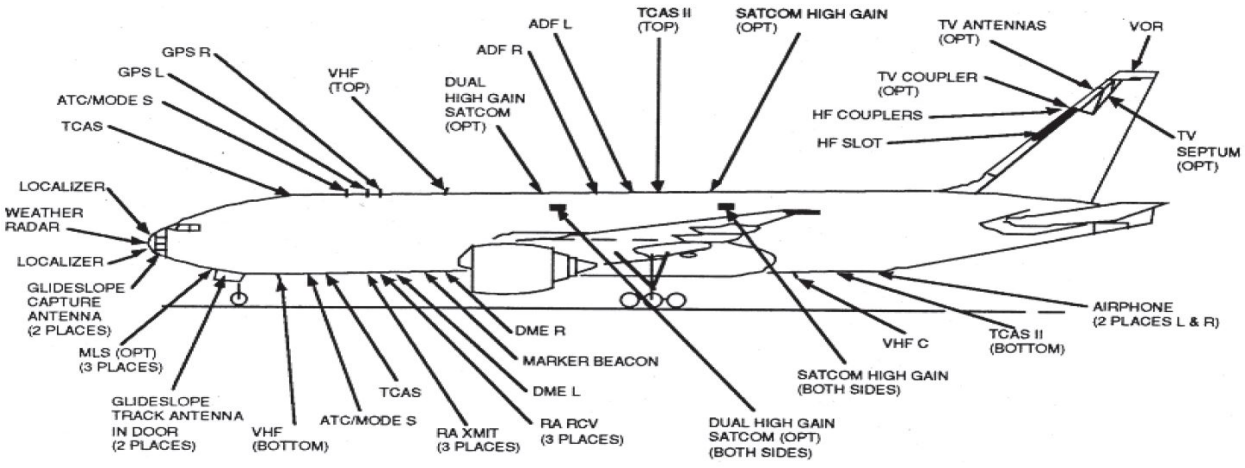

Figure 1.2 At least 20–30 antennas protrude from the skin of a modern aircraft [8].

A modern aircraft has numerous antennas projecting from its structure, for radar altimeter, navigation, instrument landing systems and data communication system. There can be 20 to 70 unique antennas on a typical military aircraft as illustrated in Figure 1.2, these antennas cause extensive drag and increased fuel consumption [7, 8]. Integrating these antennas into the aircraft skin is profoundly desirable [9, 10, 11].

Antenna mounted on aircraft on ARINC (Aeronautical Radio Inc) is shown in Figure 1.3. To minimize shadowing effects on the aircraft, the antenna is located close to the center line, conformed to the surface of the aircraft.

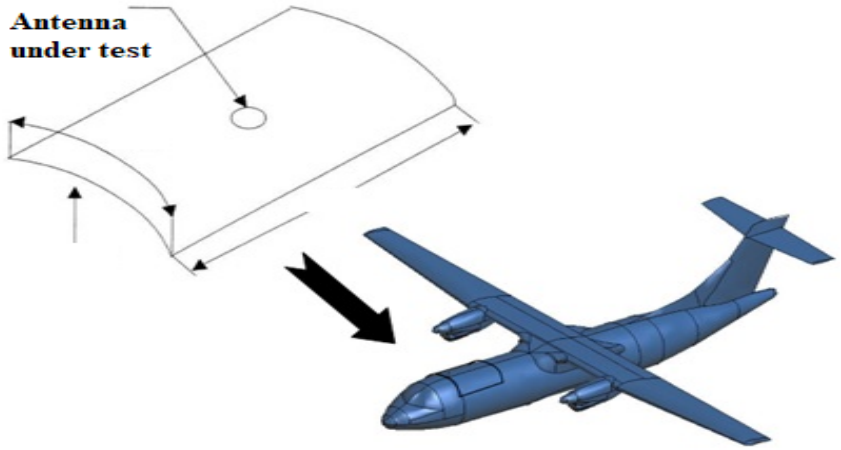

Figure 1.3 Antenna mounted on aircraft [María Del Carmen Redondo González].

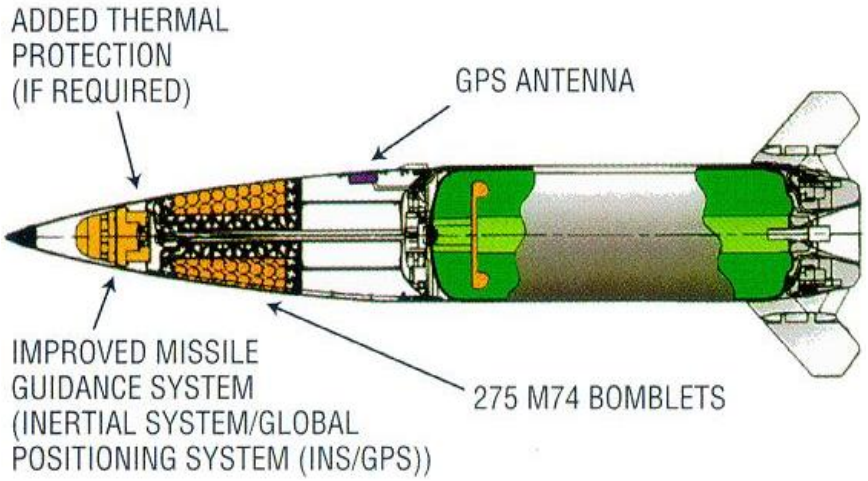

Figure 1.4 Long-range precision tactical missile system.

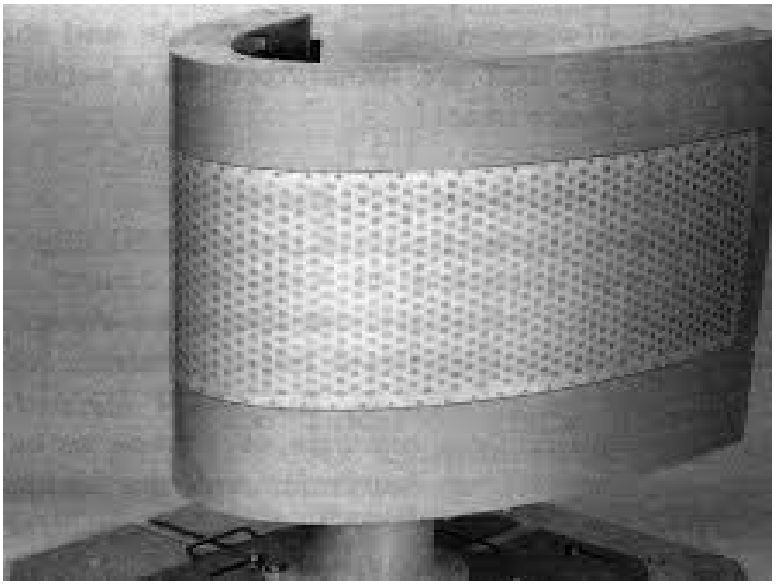

Figure 1.5 Conformal array antenna for aircraft wing integration [12].

Figure 1.6 A conical conformal array for data communication from a satellite [13-14].

A GPS conformal antenna is used in long-range precision tactical missile system to guide the missile as shown in Figure 1.4.By integrating an onboard Global Positioning System (GPS) with antenna, the payload can be reduced to accomplish the required precision and expanded range. The missile guidance set uses an embedded GPS receiver to receive and process GPS satellite navigation signals and integrates the GPS data into the inertial guidance scheme to improve navigational accuracy.

The X-band array conformal on the elliptical cross-section shape of the leading edge of an aircraft wing is shown in Figure 1.5 [12].This elliptical antenna was developed by the Technical Research and Development Institute of Japan Defence Agency in 1996.This antenna has circular polarized microstrip antenna elements on the elliptical cylinder. A total of 570 active antenna elements are arranged in 57 rows $\times$ 10 columns. The row elements are used to control azimuth plane pattern and column elements are used for control of elevation plane pattern. Each active element is connected to the T/R module. Two-dimensional digital beam forming and suppression of side lobes are obtained by the array.

A conical, faceted, satellite antenna array is shown in Figure 1.6 [13]which is built at Alcatel in France. The X-band array has semi active elements with electronic scanning capability. The X-band array is used to simultaneously connect with several ground stations. Microstrip antennas mounted on cylindrical, elliptical and paraboloid structures are shown in Figure 1.7. These antennas are designed and developed by Ball aerospace and European workshop on conformal antennas (EWCA).

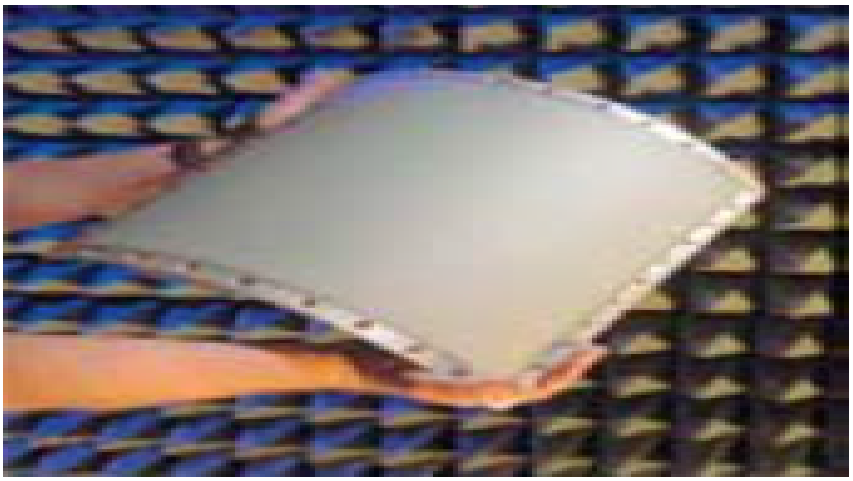

(a)

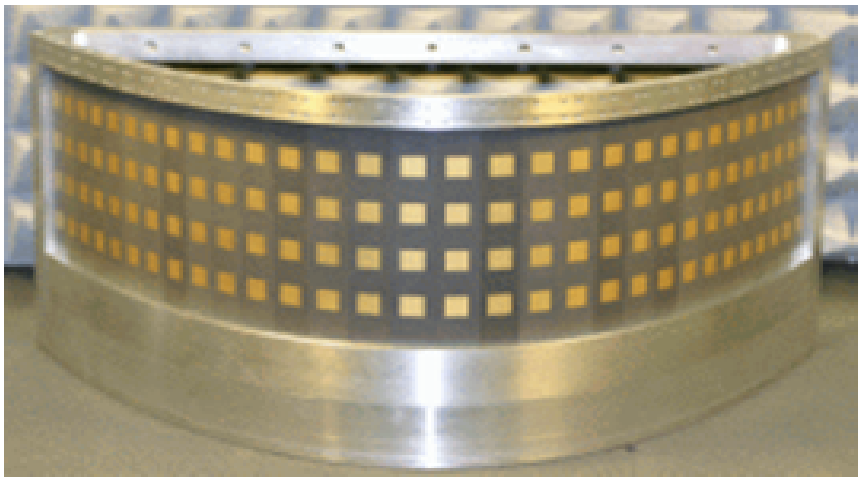

(b)

(c)

Figure 1.7 Examples of conformal antennas from Ball aerospace and European workshop on conformal antennas (EWCA) (a) cylindricalmicrostrip antenna (b) elliptical microstrip array (c) aperture array on the paraboloid.

1.2 Motivation

Different applications are developed in wireless communication like GPS, Wi-Fi and WiMAX. Global Positioning System is used to identify the coordinates of the user. GPS is used widely for civilian safety,military purpose, aircraft and mobile devices. The other application in wireless communication widely used now a days is Wi-Fi. Wi-Fi is a router used to connect portable devices with an internet connection.In portable device, antennas for GPS and Wi-Fi applications are required. WiMAX is used for wireless data transfer over long distances.WiMAX has potential application in military communications. GPS and WiMAX wireless communication systems are intended for a long range complex systems such as aircraft, radar, missiles and space applications. For moving vehicle there is need of antennas for WiMAX and GPS applications.The antennas projecting from its structure, causes extensive drag and increased fuel consumptions. Hence, there is a requirement to integrate the antenna conformal to the mounting platform.

The usage of conformal antennas in navigation and communication purposes is increasing drastically. Conformal antennas also give broader beams than planar antennas, which is an advantage in particular when omnidirectional patterns are required, which normally are accomplished by applying an array. Another purpose for using conformal antennas is to make them less visible to the human eye since there are integrated on the structure. This property might be helpful for design of antennas for urban or military environments.

Conformal antennas can be practically of any geometry, in spite of the fact that the main structures explored so far are conical, cylindrical and spherical .The cylindrical conformal antenna can be selected over other shapes like conical, spherical, etc. due to simple geometry, omnidirectional pattern, continuous wide-angular coverage. Cylindrical conformal antennas can be used on all applications like aircraft, missile and satellite. For long-distance communication, there is a prerequisite of the wideband and high gain antenna. In addition, GPS antennas also require omnidirectional coverage. Wi-Fi antennas which are used on portable devices have to be compact and must give omnidirectional coverage. There is a requirement to design and develop antennas to meet the emerging demand of modern wireless communication systems. Hence, there is a need to study and design novel compact high gain conformal antennas for GPS, WiMAX and Wi-Fi applications.

1.3 Literature Survey

This section deals with a brief overview of the published literature on conformal antennas followed by various techniques published on bandwidth and gain enhancement techniques applied for planar antennas and conformal antennas.. The techniques adopted in the literature are highlighted and their drawbacks are illustrated.

E. A. Navarro et al exhibited the model and experimental results of a conformal stacked antenna design with synthetic dielectric substrate [14]. As the material can easily be bent and retains its shape after heating, it is especially attractive for conformal designs. But fractional bandwidth is obtained as 13–16%.

H Zhu et al proposed a cylindrically conformal four-element slotted array with improved axial radiation [15]. Although the proposed conformal array exhibits a low profile and maximum axial radiation gain of 5.12 dBic (decibel w.r.t isotropic circular polarisation), but has narrow impedance bandwidth of 400 MHz.

M. V. T. Heckler et al designed a circularly polarized circumferential array [16]. A prototype of a sub-array of four CP microstrip patches are manufactured to validate the design procedure, but impedance bandwidth is around 100 MHz only.

M Xiaoping and G Xueyuan designed the Global Position System antenna array which is conformal with missile [17]. The antenna array consists of 4 elements with each antenna of 57.8×57.8 mm^2 size. But the impedance bandwidth is 20 MHz only.

Based on the concept of folded slot antennas, a new flexible conformable reconfigurable antenna is proposed by S. M. Saeed et al [18]. When the p-i-n diode is ON, the antenna has a single band at 2.42 GHz with 160 MHz impedance bandwidth for WLAN wireless devices. However, when the p-i-n diode is OFF, the antenna is dual-band with different polarizations at 2.36 and 3.64 GHz for WLAN and WiMAX wireless devices, with 180 and 270 MHz impedance bandwidth respectively. The size of the antenna is 59×31 mm^2 and maximum gain is 1.75 dBi at 3.64 GHz.

The circular cylindrical multilayer stacked patch antenna with omnidirectional radiation pattern was considered by R. Zentner et al [19].The dimensions of the inner and outer patch are 53×25.3 mm^2 and 54.2×100 mm^2. The fractional bandwidth of the antenna is 13.4%. The

measured gain in the direction of the patch center varies between -3 and 1.5 dB within the band 1.8-2.1 GHz. The measured cross-polarization level is near -20 dB.

J. H. Bang et al presented a two-element conformal antenna for receiving the GPS L_1, L_2 and GLONASS L_1 signals for precision artillery applications [20]. The –6 dB impedance bandwidths are 26 MHz (1.213–1.239 GHz) and 64 MHz (1.558–1.622 GHz). The maximum gain of the antenna is 0 and 0.5 dBi at L_2 and L_1 bands, respectively.

N. Herscovici et al presented the cylindrical omnidirectional patch antenna [21].The antenna is operating at 1.06 GHz. But, the dimension of the patch is 50.8×119.38 mm^2 with a fractional bandwidth of 7.8% and a maximum gain of 1.2 dBi. A conformal circularly polarized dual-band antenna for global navigation satellite system is presented by K. A. Yinusa [22]. The antenna is resonanting at the Galileo E5a/b(1.189 GHz) and E1(1.575 GHz) including GPS and Glonass bands. But the diameter of the antenna is 116 mm.

R. Munson presented a new class of conformable antennas using microstrips to form the feed networks and radiators [23].The application of these antennas is limited due to small bandwidths.

X. Wang et al proposed cylindrical conformal antenna and an array with photonic bandgap (PBG) structures, both are operating in X-band (10.2 GHz) [24]. The proposed PBG patch antenna is operating at 10.175 GHz with a fractional bandwidth of 11%. The antenna array consists of 4 elements with each element of size 9 mm × 6 mm. The cylindrical microstrip array with PBG structure is operating at 10.2 GHz and a fractional bandwidth of 6.4%.

Z. Zhang et al proposed a cylindrical conformal switchable antenna system at 2.4 GHz [25]. The volume of the tri-polarization antenna is 94×94×5.8 mm^3. Y. Bayram et al presented a conformal and light weight antenna based on E-textile conductors and polymer-ceramic composites [26]. The antenna dimensions are 50 × 50 mm^2 on a polymer substrate of 7.62 mm thickness and permittivity of 4. E-textile patch with 35 mm× 35 mm dimensions is embedded on a polymer substrate. The sample patch antenna based on the proposed technique achieved 6 dB gain. The gain of the cylindrical conformal antenna is reduced by 2.5 dB than that of antenna realized with a PEC surface. The impedance bandwidth is around 120 MHz. C. H. Ahn et al presented a X-band conformal array dual-polarized antenna for unmanned aerial vehicles [27]. The proposed antenna array is operating at 9.8 GHz yields about 100 MHz impedance bandwidth.

J. W. Niu and S. S. Zhong designed cylindrical conformal bow-tie antennas with small radii [28]. The size of each element is $23.97 \times 83.04 \times 0.8$ mm^3. The antennas are resonating at 9 GHz with a 5% fractional bandwidth.

For bandwidth improvement of a patch antenna, a few methodologies have been proposed [29-38]. N. Herscovici presented a three-dimensional microstrip feed line [29] in which an additional plastic supporting post is placed in between ground plane and radiating patch to obtain a fractional bandwidth of 31%.

Combined utilization of both L-probe feeding and patch loaded with U-slot planar antenna are used in [30] by K. Luk et al where an extra foam substrate is required between ground and patch for the fractional bandwidth of 42.7%. A foam layer is used in L-probe feed antenna designed by Y. X. Guo, et al in [31]. A fractional bandwidth over 30% and an average gain of 7.5 dBi have been achieved. A capacitive probe-fed structure has been implemented in the microstrip antenna design by M. G. de Aza et al to enhance fractional bandwidth upto 35% by using hard foam material [32]. Hard foam may not be suitable for aircraft or missile applications. A planar microstrip antenna loaded with chip resistor is proposed by K. L. Wong and Y. F. Lin in [33]. These antennas are designed using lossy material which is a drawback and obtained fractional bandwidth is 9.8%.

T. Huynh and K. F. Lee designed a planar patch antenna with U-shaped slot for reactive loading in [34]. The difficulty is the presence of air or foam medium in between the ground plane and patch. The fractional bandwidth obtained in this design is 12.4%. A planar antenna with two gap-coupled parasitic patches and a directly coupled patch is proposed by C. K. Wu and K. L. Wong to obtain broadband characteristics with 12.7% of fractional bandwidth in [35]. But in the design, four stacked patches are used which increases the occupied volume. Various resonators and thick substrates with low dielectric constant have been utilized by E. Chang et al to design the patch antenna on a planar surface for obtaining fractional bandwidth to 20% [36]. H. F. Pues and A.R. Van De Capelle have designed an impedance matching system to enhance fractional bandwidth up to 12% [37]. S. Y. Ke described a ground plane loaded with an H-shaped slot in which achieved fractional bandwidth is 21% [38].

For gain enhancement, different techniques are reported in the previous literature [39-42]. Incorporating parasitic elements in antenna for gain enhancement is a well-known technique. A gain enhancement of 4.4 dBi is achieved at 2.96 GHz by using a triangular shaped parasitic element for planar antenna which is reported by Y. Tawk et al in [39].

Design of a planar printed log-periodic dipole array antenna with the gain enhancement of 2 dBi in the high-frequency range of 21-40 GHz is attempted by G. Zhai et al in [40]. Gain enhancement of antenna by using superstrate technique is presented by J. H. Kim et al for planar antenna in [41]. However, use of superstrate increases the weight of antenna which is not suitable for conformal application due to difficulties in bending. The gain enhancement of planar printed antenna is also attempted by S. Enoch et al utilizing zero index metamaterial as superstrate in [42]. However, use of zero index metamaterial as superstrate makes the patch antenna systems heavy in weight. So superstrate type of antenna is not suitable especially for conformal antenna due to heaviness and difficulty in bending.

To achieve compactness of the antenna, different techniques are reported in the published literature [43-45]. Many efforts such as using shorted pin by R. Chair et al [43], employing substrate with high dielectric constant by T. Lo [44] and utilizing loaded slots and capacitances by J. H. Lu and K. L. Wong [45] are done for miniaturization of microstrip antenna. The size of antenna can be reduced by using high dielectric constant of the substrate but with an increase in quality factor and also decrease in operating bandwidth. Research methods are developed to simultaneously increase the bandwidth and minimize the size of the microstrip antenna. This is a very challenging task but useful for many applications.

An extensive literature survey is undertaken [14-28] in order to determine the current state of the art of conformal antennas. From the published literature, it can be established that the printed antenna is suitable as a low profile antenna. Printed antennas have simple structures that are easily manufactured at a low cost, light weight and suitable to integrate with any wireless electronic devices. But the microstrip antenna has a narrow bandwidth and low gain.

From the above literature survey [14-45], a compact, wideband and high gain planar and conformal antennas are obtained by using different techniques. But, bandwidth improvement of the conformal antenna is a major issue for different applications.

In the present thesis work, it is attempted to investigate various compact wideband cylindrical conformal antennas of omnidirectional and directional radiation pattern for different wireless applications. In addition, different slots, fractal structures are added in the radiating patch to achieve compactness of the antenna. Partial ground and wide-slot in ground plane are incorporated to enhance the bandwidth. The enhancement of gain and compactness of the antennas are also achieved by using metamaterial. But, sometimes the metamaterial unit cell will not work in the entire frequency range.

In order to overcome these problems, non-resonant structure metamaterials are considered. In the proposed thesis, metamaterial unit cell is designed by non-resonant double S-shaped structure of the sub-wavelength dielectric substrate. Here, the proposed metamaterial is used on both sides of substrate for bandwidth improvement. If double S-shaped structure is integrated in front of the radiating elements, propagating surface wave of the radiating element is focused by the metamaterial lens which results in gain enhancement.

The antennas are designed to meet the required specification and simulation is performed using commercial either three dimension EM simulator, Ansysy HFSS 15 or CST Microwave studio. Dielectric material like RT/duroid 5880 of thickness 0.787 mm is used for fabrication of prototype antenna in the proposed work. The fabricated antennas are tested in compact test range anechoic chamber, where the measurement conditions are controlled when compared with outdoor ranges. EM wave absorbing materials are fixed to the walls, ceilings and floor in the measurement chamber room to get accurate results.

1.4 Research Objectives

The research primarily focuses on achieving the following objectives:

I. Design, fabricate and validate cylindrical conformal antennas.

II. Implementation of structural modifications and slots for achieving a compact and wide-band structure.

III. Introduction of fractal concept on the patch and partial ground concept for obtaining compact and wide bandwidth.

IV. Improvement of the radiation pattern and gain of the cylindrical conformal antenna by using low index metamaterial.

V. Use of metamaterial concept for achieving dualband frequency operations.

VI. To compare the simulation result with the experimental result of the above-designed antennas and also, compare with the existing published work.

1.5 Thesis Outline

The thesis presents the state of the art of cylindrical conformal antennas. The analysis and design of conformal antennas and performance improvement in terms of compact size, bandwidth and gain enhancement are illustrated. The results are improved using slots, fractal and metamaterial concepts.

Chapter 1: Introduction

This chapter presents an introduction to the conformal antenna and its applications. A detailed survey of published literature is illustrated. The drawbacks of the existing antennas are discussed. A detailed explanation is presented for the design of cylindrical conformal antennas. Some of the novel methods that can be applied to overcome the existing drawbacks are mentioned. A brief outline of the thesis is presented.

Chapter 2: Wideband Slotted Cylindrical Conformal Antenna for GPS Application

In this chapter, cylindrical conformal antennas with different slots on a cylinder are designed and fabricated for GPS application. The cylindrical conformal antennas are designed with dumbbell-shaped slot and cross-slot on the rectangular patch and on bow-tie patch. Wideband characteristics are obtained by using partial ground concept.

Chapter 3: Cylindrical Conformal Fractal Antenna for GPS Application

This chapter presents the design of fractal-based planar as well as a conformal antenna. Fractal structures are incorporated in the radiating patch structure for improving the performance of antenna. The cylindrical conformal antenna with Koch fractal andMinkowski fractal on the radiating patch and partial ground are proposed for GPS applications.

Chapter 4: Conformal Wideband Antenna with Parasitic Elements and Metamaterial for WiMAX Application

This chapter explains the design of a conformal antenna for WiMAX application. The gain enhancement of the basic conformal antenna is achieved by integrating triangular shaped parasitic elements and low index metamaterial unit cells. The application of metamaterials for conformal antenna design is discussed. The unit cell of metamaterial is designed and later extended as array. Metamaterial is integrated with antenna for gain enhancement.

Chapter 5: Metamaterial Inspired and Slotted Conformal Antenna for Wi-Fi and WiMAX Applications

Cylindrical conformal antennas are designed for Wi-Fi and WiMAX applications. The conformal antennas with dual U slot on the patch are designed with various radius of curvatures for Wi-Fi application. A compact metamaterial based cylindrical conformal dual-band antenna is designed, fabricated and validated experimentally for Wi-Fi and WiMAX applications. The proposed cylindrical conformal antenna is compared with the existing planar antenna. The compactness, wideband and dual-band characteristics are obtained by incorporating meanderlines, fractal inductor and parasitic elements respectively.

Chapter 6: Conclusions and Future Scope

A consolidation of the results is presented. Cylindrical conformal antennas with different radius of curvature are designed for commercial applications with wide bandwidth and better gain, radiation pattern than that are available in the literature. Thus the results obtained indicate that the designed cylindrical antennas are good candidate for different wireless and commercial application.

Future work: The proposed work can be extended for structures other than cylindrical. In addition, conformal antenna with fractal shaped metamaterial can be also be extended as conformal array. Conformal antenna arrays can be designed for beam steering application.

1.6 Contributions of Research Work

The key contributions of this work are summarized as follows:

1. A detailed survey of published literature is performed and drawbacks of the existing cylindrical conformal antennas are listed. Some of the novel methods are extracted to overcome the existing drawbacks.

2. A wideband cylindrical conformal antenna with dumbbell shape slot on three sides of the patch is designed. The conformal antenna exhibits a fractional bandwidth (for the definition of -10 dB) of 75.94% operating from 1056 to 2349 MHz.The gain of the proposed conformal antenna is 2.09 to 4.9 dBi within the operating frequency range.

3. The conformal antenna with a printed cross-slot on the radiating patch and the partial ground is designed which exhibits a fractional bandwidth of 79.28% operating from 1091 to 2524 MHz and gain of the proposed conformal antenna is 2.37 to 5.33 dBi within the operating frequency range.

4. A bow-tie shaped patch antenna with a bow-tie shaped slot in the ground plane with a larger dimension is designed. It is observed that the conformal antenna exhibits a fractional bandwidth of 81.4% operating from 0.75 to 1.78 GHz and gain of the proposed antenna is 3.5 to 4.78 dBi within the operating frequency range.

5. The conformal antenna designed using Koch fractal on the patch exhibits a bandwidth of 20 MHz and also has a peak gain of 5.9 dBi at the center frequency of 1.575 GHz.

6. The fractal antenna antenna with partial ground concept are incorporated to achieve wideband fractional bandwidth of 43.72% operating from 1.09 to 1.7 GHz and gain variations from 2.3 to 3.5 dBi within the operating frequency range.

7. The conformal antenna integrated with parasitic elements and low index metamaterial unit cells is proposed to narrow the beamwidth by 24^0 in the H-plane and gain is enhanced by 1.8 dBi compared to the basic conformal antenna. The impedance bandwidth of the proposed conformal antenna achieves a bandwidth of 22.3% from 3.1 to 3.88 GHz.

8. A conformal antenna with dual U slot is proposed. The planar antenna is transformed to conformal cylindrical of 25 mm,45 mm and 60 mm radii. The gain values are decreased from 5.9 to 2.81 dB but the bandwidth values vary from 23 to 22.1 MHz by changing the radius of curvature from 60 to 25 mm.

9. A metamaterial inspired cylindrical conformal antenna with a shunt fractal inductor and a bottom patch is proposed. The cylindrical conformal antenna achieves a wideband -10 dB fractional bandwidth of 44.5% and a gain of 1.26 dBi at the operating frequency 2.45 GHz and 4.5% of bandwidth and a gain of 2.2 dBi at the operating frequency 3.5 GHz.

10. All antennas are fabricated and experimentally tested in vector network analyzer and anechoic chamber. The simulated and measured results are compared.

1.7 Conclusions

The various applications of conformal antenna are elaborated. The published literature presented on cylindrical conformal antennas is discussed. The research objectives of the pro-

posed work are outlined. The use of slots, fractals and metamaterials on printed antenna for obtaining compact, wideband and high gain are stated. A brief summary of the thesis work on cylindrical conformal antennas is mentioned. Key contributions of the proposed work are also highlighted.

Chapter 2

Wideband Slotted Cylindrical Conformal Antenna for GPS Application

2.1 Introduction

With the improvement of communication technologies, bandwidth improvement is becoming vital for practical utilization of microstrip antennas [46, 47, 48, 49, 50, 51, 52, 53, 54, 55]. For instance, wideband antennas are required for GPS receivers installed on hand held devices, moving vehicles and missiles. These antennas are pivotal part of the GPS receiver as they need to work in remote zones and also receive weak signals from satellites.

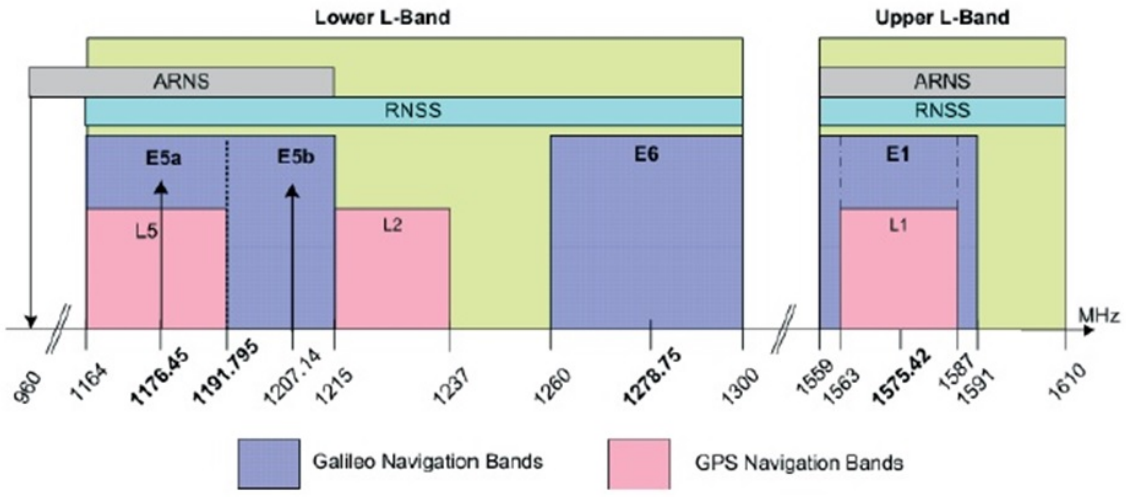

Figure 2.1 Global positioning system band.

Applications are developed for Global Positioning System in L_1 (1.57 GHz), L_2 (1.22 GHz), L_3 (1.38 GHz), L_4 (1.37 GHz) and L_5 (1.17 GHz) bands which are shown in Figure 2.1. The L_1 band is required for C/A procurement, and the L_2 is necessary for military and P(Y) codes. The L_5 band is used for safety life of civilian, and the L_3 band is used for atomic explosion identification. The L_4 band is under development for climatic analysis. Along these lines, it can be viewed that use of GPS bands extend from L_5 to L_1 bands.

In some applications, GPS antennas are to be placed where the omnidirectional scope is guaranteed with no signal distortion. Sometimes the antenna mounting platform is not planar. In those cases, there is requirement of the conformal antenna to make it less noticeable to the enemy eye, reduce aero dynamical drag and have omnidirectional coverage like on aircraft and missile[11, 56, 57]. Hence, development of omnidirectional coverage conformal antennas are required for GPS receivers.

A few circularly polarized antenna designs have been reported [58, 59, 60, 61, 62] for GPS application on planar surfaces. But according to [63], in the multi path environment, the linearly polarized signal is less vulnerable to distortions compared to circularly polarized signal. So, the omnidirectional linearly polarized antenna can also be applied for receiving purpose. Literature is published on planar GPS antennas working at only single band with narrow operating bandwidth. A cylindrical conformal antenna array for GPS in L_1 band with 20 MHz bandwidth and a gain of 1.65 dBi is proposed in [17].

Although a wideband GPS Antenna has been reported [64], but it is designed on flat surface. Two elements conformal antenna array is designed for multi-GNSS reception with narrow bandwidth [20]. A circular patch with cross-slot fed with a proximity coupled has been demonstrated on the flat surface with less bandwidth [65]. So, wideband antenna design has become a challenging topic with the rapid development of wireless communication systems.

S. Y. Ke described a ground plane loaded with an H-shaped slot in which achieved bandwidth is 21% [38]. Antennas with a wide slot and different shapes of the feed line have been described on a planar surface for large impedance bandwidths [53, 54, 55].

The design of bow-tie microstrip antenna, which has more extensive bandwidth than the dipoles are reported [2, 66]. The radiation characteristics of the bow-tie microstrip printed antenna are also reported in [67]. The bandwidth of this antenna depends upon the flare angle of the bow-tie shape.

In this chapter, cylindrical conformal antennas with different slots are designed on a cylinder of 60 mm radius of curvature for GPS application. The wideband characteristics of the proposed cylindrical conformal antenna are obtained by incorporating partial ground and wide-slot on ground plane. The designed antennas are simulated, fabricated and tested.

2.2 Design of planar rectangular microstrip antenna

The geometry of rectangular microstrip antenna is shown in Figure 2.2. The dimension of the antenna depends on the resonant frequency of operation and parameters of the substrate. The width, *'W'* of the patch can be calculated as given below.

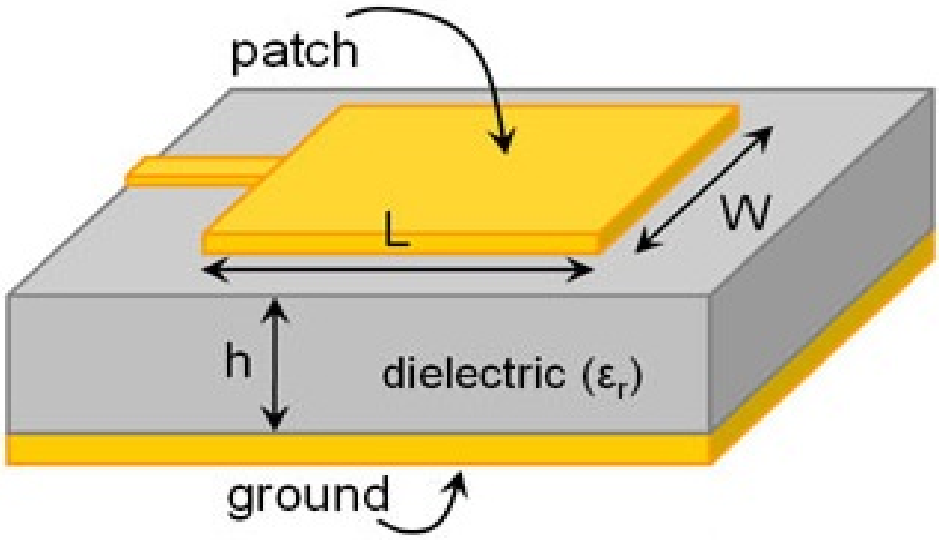

Figure 2.2 Geometry of rectangular microstrip antennas.

$$W = \frac{c}{2f_r\sqrt{\frac{\varepsilon_r+1}{2}}} \tag{2.1}$$

where *'c'* represents the velocity of the Electromagnetic wave, 'f_r' is the resonant frequency of the antenna, 'ε_r' is the dielectric constant of the substrate.

The effective dielectric constant 'ε_e' is determined as given in equation (2.2)

$$\varepsilon_e = \frac{\varepsilon_r+1}{2} + \frac{\varepsilon_r-1}{2}\left(1+\frac{12h}{W}\right)^{-1/2} \tag{2.2}$$

where *'h'* is the thickness of the substrate.

Due to the fields extending into the dielectric, the change in electrical length of the material is given by

$$\frac{\Delta l}{h} = 0.412 \frac{(\varepsilon_e + 0.3)\left(\frac{W}{h} + 0.264\right)}{(\varepsilon_e - 0.258)\left(\frac{W}{h} + 0.8\right)} \tag{2.3}$$

The length of the patch is then obtained by using the equation (2.4)

$$L = \frac{c}{2 f_r \sqrt{\varepsilon_e}} - 2\Delta l \tag{2.4}$$

2.2.1 Feeding methods

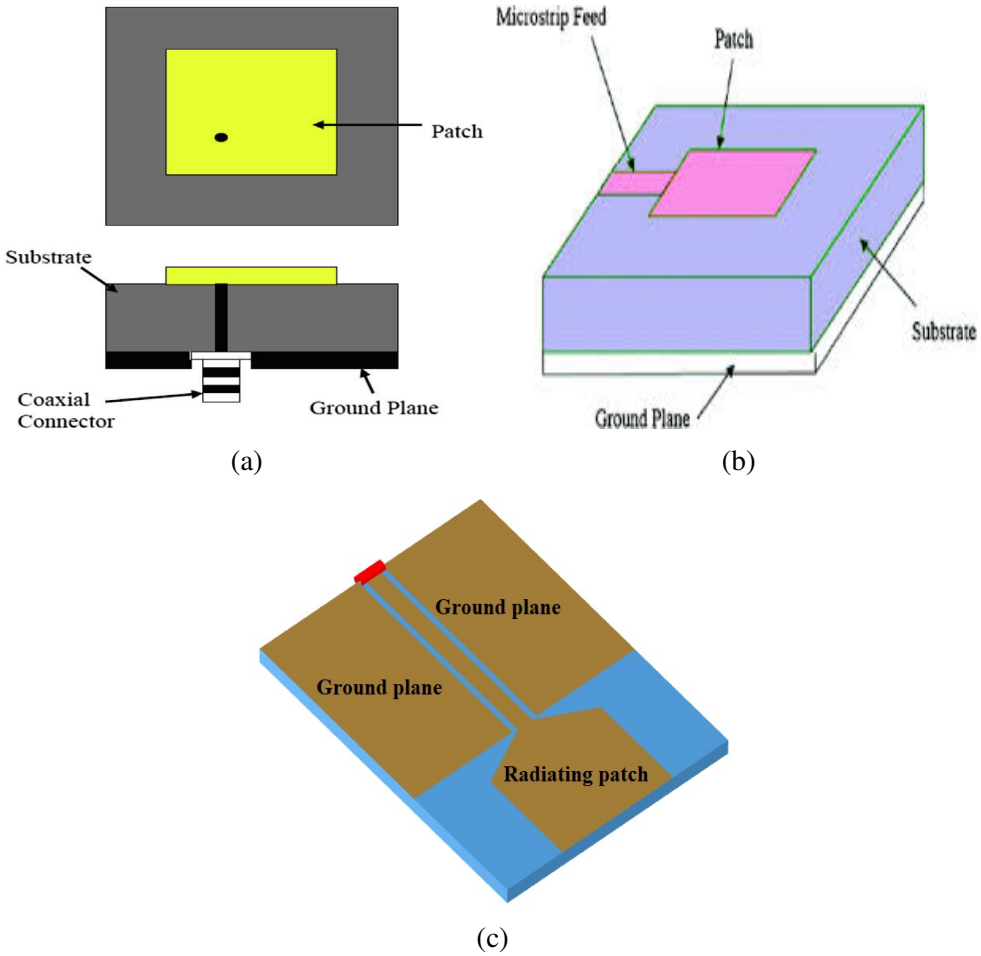

Figure 2.3 Feeding techniques (a) coaxial probe feed (b) microstrip line feed (c) coplanar wive guide feed (CPW).

The power fed to the microstrip antenna depends on the feeding techniques. It also depends on the effective design of feed. The antenna impedance is to be matched to the standard 50 Ω line impedance. Microstrip antennas are fed using coaxial feed, microstrip line feed,coplanar waveguide(CPW) feed in the proposed work are shown in Figure 2.3. The antenna is fed by a coaxial cable, the center conductor is connected to the radiating patch and outer conductor is connected to the ground plane as shown in Figure 2.3a. The coaxial feed technique is simple and also the feed lies below the radiating surface. The radiating patch is connected to the feed using a microstrip line as shown in Figure 2.3b. The microstrip line is designed to match the feed impedance to 50 Ω. This technique is easy to design and also useful for array design by parallel or corporate feeding technique. But, drawback of this technique is that the radiation from feed line causes interference with radiation from the patch. In CoPlanar Wave guide feeding (CPW-feeding), the ground plane is placed on the same plane as the patch as shown in Figure 2.3c. This feed technique also improves the bandwidth of operation of the antenna and hence adopted for many applications.

2.3 Design of conformal antenna

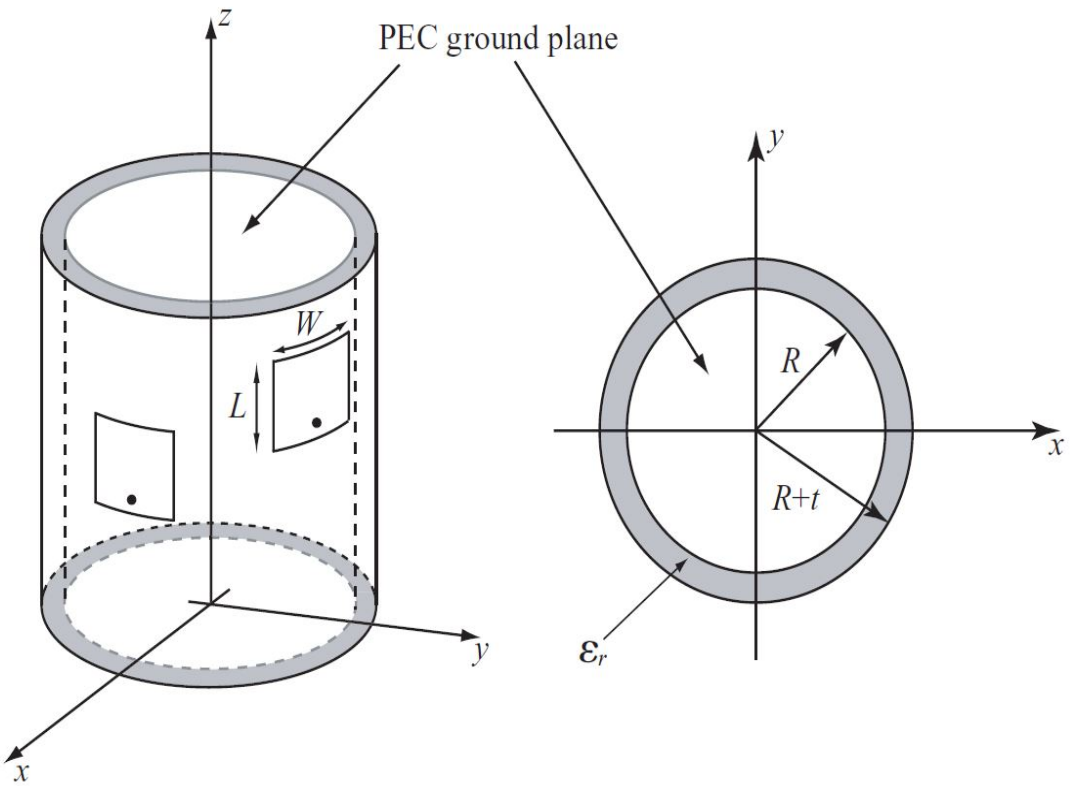

Figure 2.4 Geometry of rectangular microstrip antennas located on a circular cylinder [11].

The transformation of planar rectangular patch antenna to conformal antenna is explained in this section. The planar antenna is conformed to the cylindrical shaped dielectric substrate with relative permittivity $\varepsilon_r > 1$, thickness *'t'* and with an inner radius *'R'*. A perfectly conducting, cylindrically shaped ground plane between the substrate and the cylinder is assumed to be infinite in the z- direction. A typical geometry is shown in Figure 2.4.

An approximate value of the resonant frequency can be found by using equation of planar antenna. But the length and width of antenna corresponds to the antenna dimension after transformations. Thus, the resonant frequency of the TM_{mn} mode is given by [11]

$$f_{mn} = \frac{c}{2\sqrt{\varepsilon_r}}\left[\left(\frac{m}{W}\right)^2 + \left(\frac{n}{L}\right)^2\right]^{1/2} \tag{2.5}$$

where $W = 2R\phi_0 + t/\sqrt{\varepsilon_r}$ is the effective circumferential length and $L = Z_m + t/\sqrt{\varepsilon_r}$ is the effective axial length of the patch, 'ε_r' is the permittivity and *'t'* is the thickness of the cylindrical substrate. 'Z_m' is the axial length of the patch,'ϕ_0' is the angle from the center of the patch to the straight edge and *'R'* is the radius of curvature of the cylinder.

2.4 Wideband slotted conformal antenna

The conventional microstrip antenna has narrow bandwidth. One of popular techniques to enhance the bandwidth is done by cutting slots of half wavelength at the desired resonant frequency. The slots are embedded on the patch to improve impedance matching. The current distribution on the patch is changed due to presence of slots. By adding new slots into the patch, new resonant frequencies are created. The positions and dimensions of the slots should be properly optimized where the first two broadside radiation modes of the radiating patch excites nearer to each other to achieve a wider bandwidth. The microstrip slot antennas have different slot shapes such as rectangular, square, circular; and various feed shapes such as T, cross, fork-like, bow-tie, radial stub, pi, double-T, circular and rectangular [46–55]. The antennas used in these study employ square and triangular-patch feeds to excite the arc- and triangular-shape slots, respectively. These two combinations were chosen because of their wide impedance bandwidths and good radiation characteristics. Since a large slot is used in wide-slot antenna, a high level of the electromagnetic coupling to the feed line results. Therefore, varying the feed shape or slot shape will change the coupling property and thus control the impedance matching.

The size and geometry of the ground plane significantly affect the excitation mode and the operating bandwidth of the microstrip antenna. Defected ground structures may be achieved by cutting a slot of any arrangement on the ground plane. This defect disturbs the current distribution in the ground plane and enables control of excitation of radio waves in the substrate. The ground defect may be varied accordingly from simple configuration to more complex configuration to obtain the optimum performance. However defects in ground plane causes back radiation from ground plane.

Slots introduce capacitance, which counters the feed inductance and additional resonances are introduced. The additional resonance of the slot combines with the patch resonance which produces wideband response. The antenna used in this study employs a dumbbell shape slot on the three sides of patch in addition to partial ground plane. The use of circle on the one end of slot is the best case among the other geometries. It is because that the circle makes the fields on the slots more uniform than the other cases. Due to partial ground plane applied in the proposed work, the bandwidth is increased because of suppression of surface waves.

2.4.1 Design of slotted conformal antenna

For designing the antenna, flexible and thermally stable substrate like Rogers RT/duroid 5880 of permittivity (ε_r) 2.2 and thickness of 0.787mm with microstrip line feed for 50 Ω

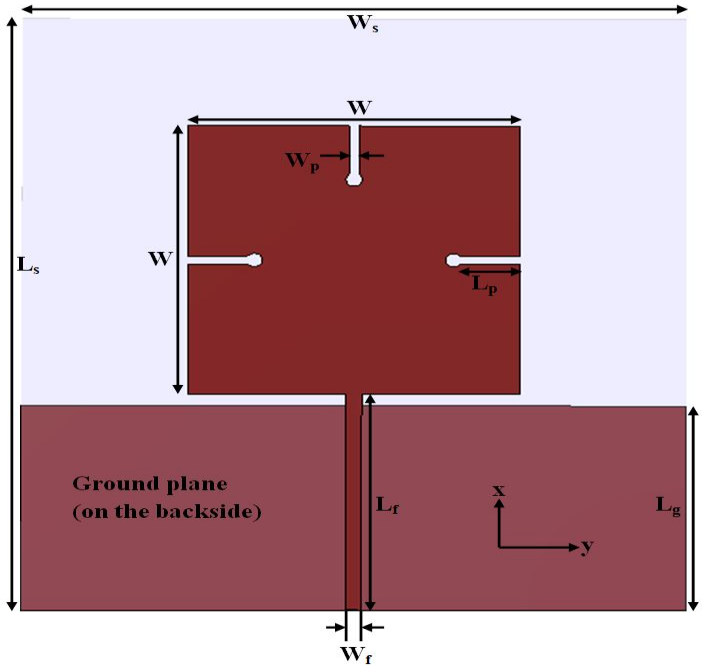

Figure 2.5 Geometry of planar antenna: L_s=110 mm, W_s=100 mm, W=50 mm, L_g=38 mm, L_f=40 mm, W_f=2.4 mm, L_p=9 mm, W_p=1.5 mm, Radius=1.25 mm.

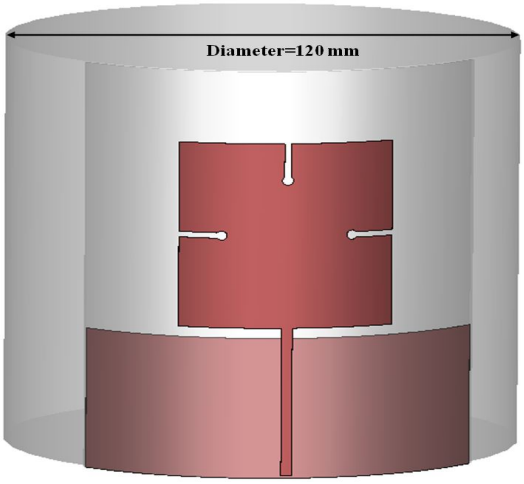

Figure 2.6 Conformal antenna model.

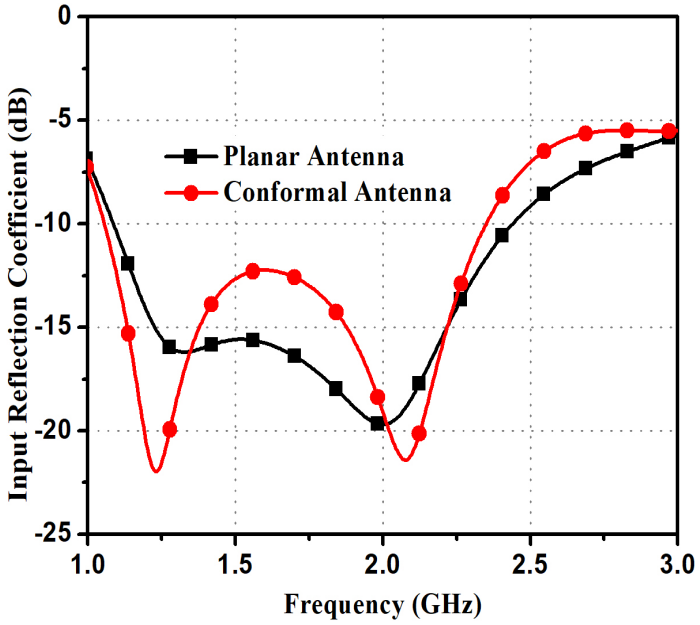

Figure 2.7 Return loss of planar and conformal antenna.

impedance matching is used. The dimension of substrate is 100×110×0.787 mm^3 and dimension of the patch is 50×50 mm^2. The geometry of proposed planar antenna is shown in Figure 2.5. The corresponding cylindrical conformal antenna with 60 mm radius of curvature is shown Figure 2.6.

The simulated return loss of the planar and proposed cylindrical conformal antenna with a 60 mm radius of curvature is compared in Figure 2.7. It shows that the return loss of the simulated antenna is obtained below -10 dB which indicates a good impedance matching condition.

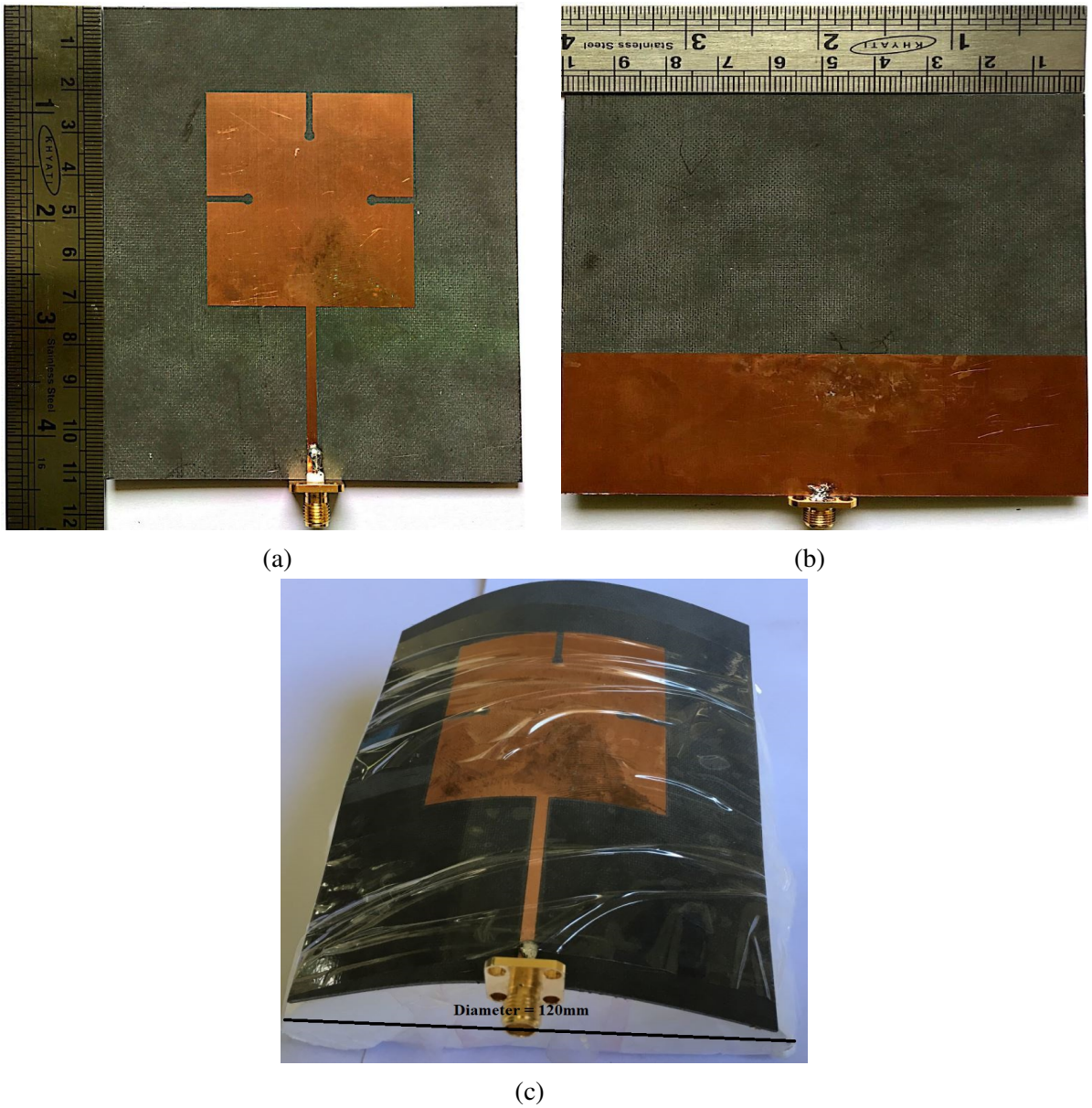

(a) (b)

(c)

Figure 2.8 Photograph of prototype fabricated antennas (a) front view of the proposed planar antenna (b) back view of the proposed planar antenna (c) front view of a proposed cylindrical conformal antenna with 60 mm radius of curvature.

There is a slight change in resonant frequency from planar to cylindrical conformal antenna. This is because of increase in the effective resonant length due to bending of the planar microstrip antenna structure due to which the resonant frequency of the cylindrical conformal antenna is shifted slightly towards left.

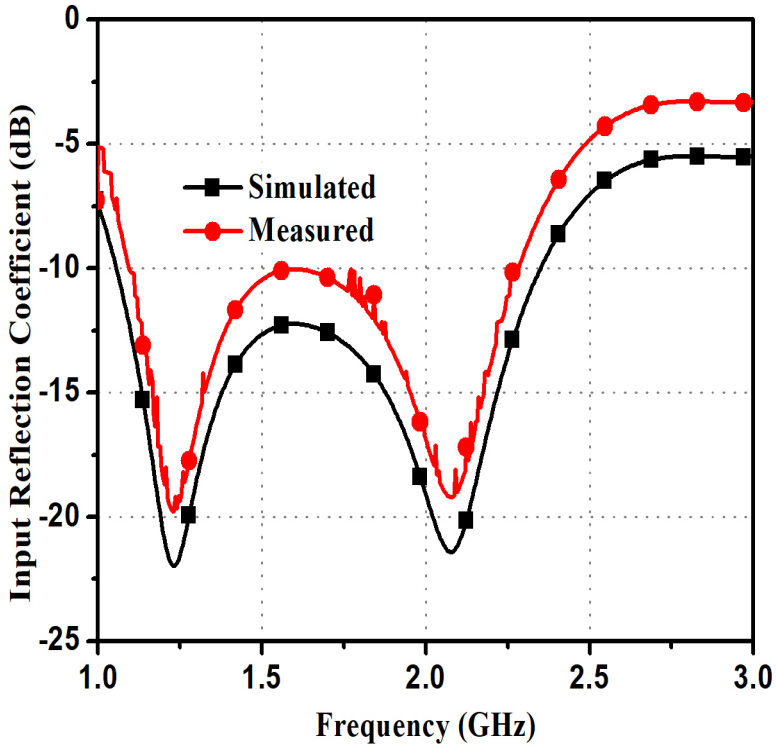

Figure 2.9 Input reflection coefficient of the proposed conformal antenna.

2.4.2 Results and discussion

The proposed antenna is designed and simulated using CST STUDIO SUITE 2016. A prototype planar antenna is fabricated on RT/duroid 5880 substrate with thickness of 0.787 mm. By using LPKF milling machine S100, the antenna is fabricated on a planar surface as shown in Figure 2.8(a) and 2.8(b) and it is rolled up to form a cylindrical shape on foam of radius of 60 mm as shown in Figure 2.8(c). The foam material is used as mechanical support for making 60 mm radius cylinder which has negligible radiation effect on the antenna. Both simulated and experimental input reflection coefficient (S_{11}) in dB of the proposed conformal antenna with 60 mm radius cylinder are demonstrated in Figure 2.9. The input reflection coefficient is measured utilizing HP vector network analyzer within the frequency range of 130 MHz to 13 GHz. It is investigated that the proposed cylindrical antenna achieves -10 dB impedance bandwidth of 1293 MHz, between the frequency range 1.056-2.349 GHz with 75.94% fractional bandwidth indicating wideband bandwidth.. It can also be investigated that the experimental reflection coefficient(dB) slightly deviates from the simulated results by using commercially available CST software may be due to tolerances in fabrication and SMA connector.

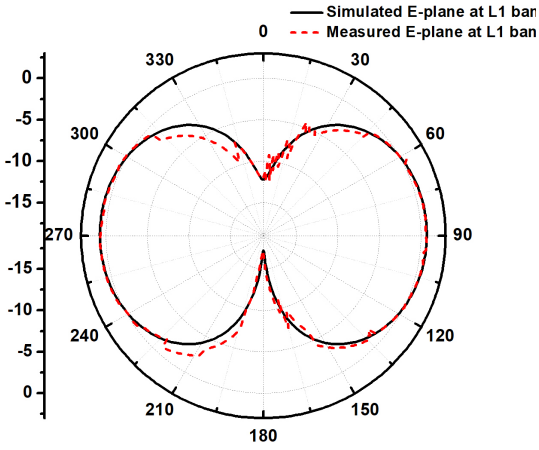

(a)

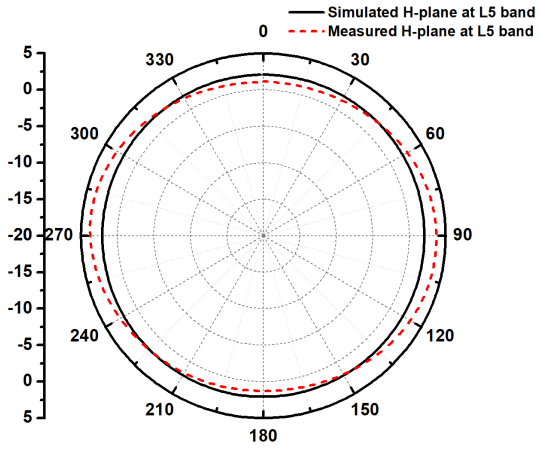

(b)

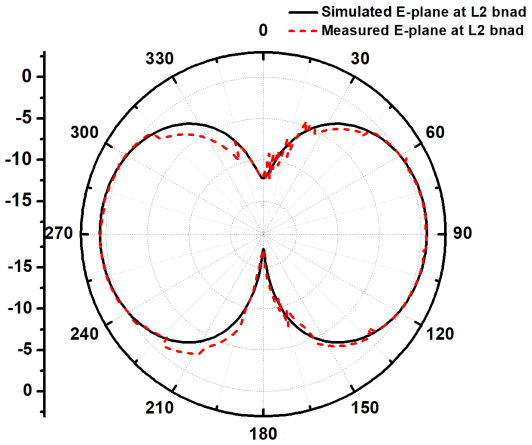

(c)

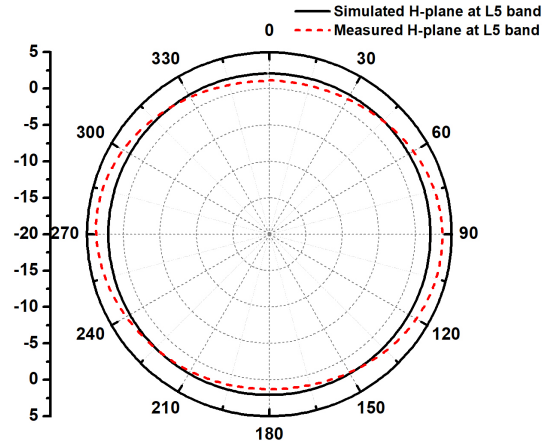

(d)

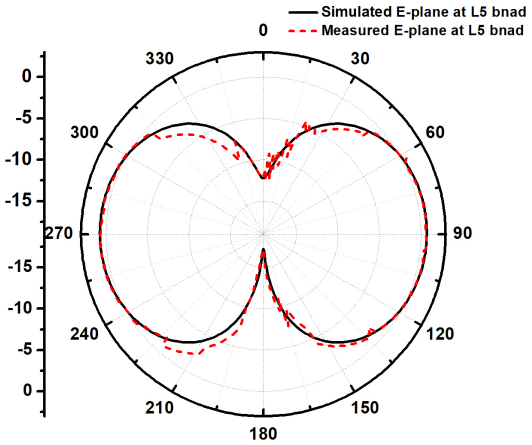

(e)

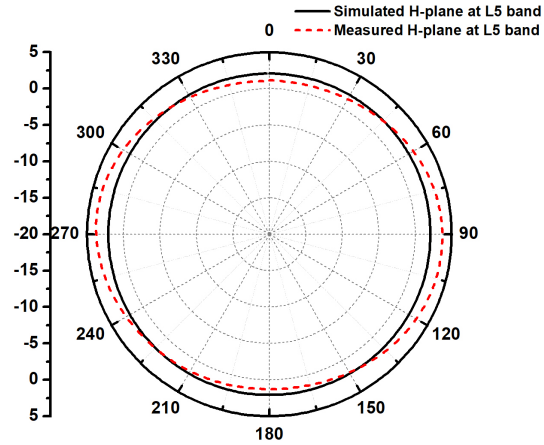

(f)

Figure 2.10 Radiation pattern:(a) E plane at 1.17645 GHz, (b) H plane at 1.17645 GHz, (c) E plane at 1.2276 GHz, (d) H plane at 1.2276 GHz, (e) E plane at 1.57542 GHz and (f) H plane at 1.57542 GHz

The simulated and measured far field radiation patterns at different GPS bands like L_1, L_2, and L_5, respectively are nearly omnidirectional patterns in the H-plane and figure of eight radiation patterns in the E-plane, which coincides well with the conventional antenna as shown in Figure 2.10.

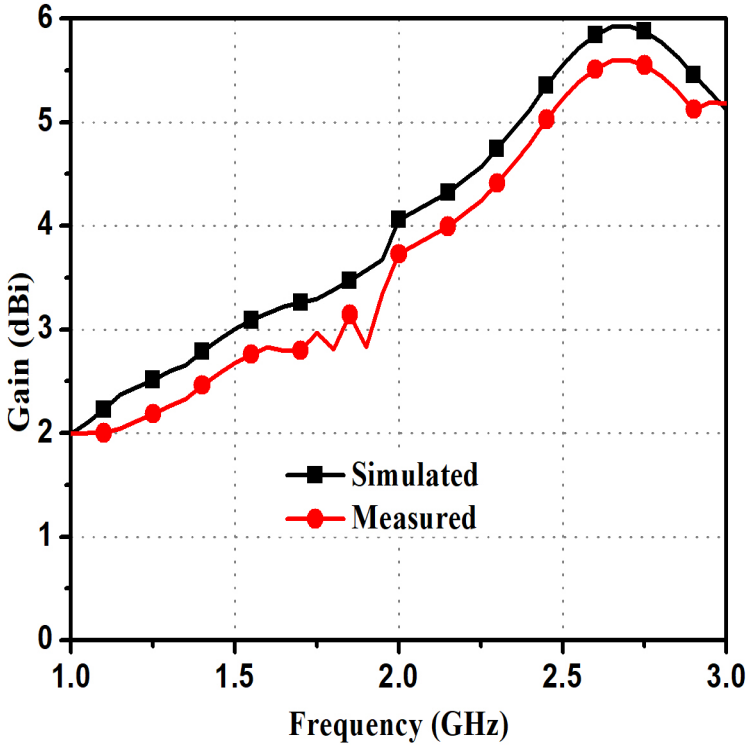

Figure 2.11 The gain of conformal antenna.

The peak gain of the cylindrical conformal antenna with 60 mm radius of curvature and the planar antenna are compared as shown in Figure 2.11. The variation in gain between conformal and planar antennas is due to the curvature of conformal antenna.

2.5 Printed cross-slot wideband conformal antenna

2.5.1 Design methodology of antenna and parametric study

For designing the antenna, thermally stable substrate like Rogers RT/duroid 5880 of permittivity ε_r 2.2 and thickness of 0.787 mm with microstrip line feed of 50 Ω impedance matching is used. The dimension of substrate is 100×110×0.787 mm^3 and dimension of the patch is

50×50 mm^2. In order to achieve wide operating bandwidth and omnidirectional coverage, partial ground concept is selected. The bandwidth is increased because of suppression of surface waves propagation. The geometry of the proposed planar antenna is shown in Figure 2.8. The planar antenna in Figure 2.12 is transformed to the conformal on a cylinder of radius 60 mm, which is shown in Figure 2.13.

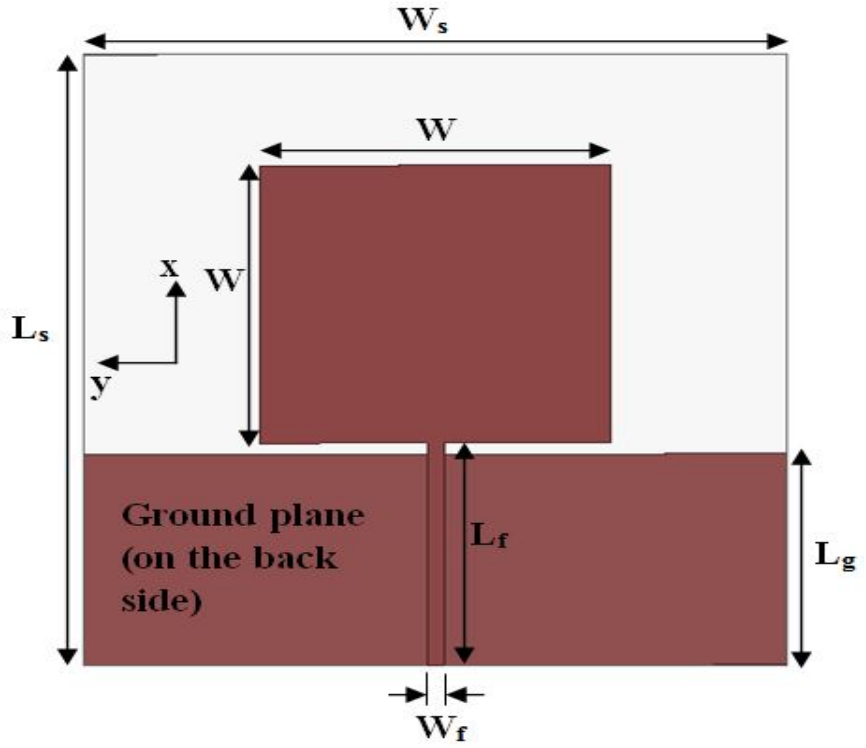

Figure 2.12 Geometry of planar antenna: L_s=110 mm, W_s=100 mm, W=50 mm, L_s=38 mm, L_f=40 mm, W_f=2.4 mm.

The effect of length of the feed-line on the impedance matching is observed. It can be referred that better impedance matching is achieved by increasing the length of feed-line. The optimized value for L_f in the proposed conformal antenna is 40 mm. The variation of bandwidth with L_f greater than 40 mm is represented in Figure 2.14.

Configuration of conformal antenna with horizontal dumbbell shaped slot is shown in Figure 2.15. A horizontal dumbbell shaped slot is introduced on the patch initially. The use of circle on the dumbbell shaped slot is the best case among the other geometries. The cylindrical conformal antenna with horizontal dumbbell shaped slot on 60 mm radius of curvature is shown in Figure 2.15. The effect of length of horizontal dumbbell shaped slot on the impedance matching is observed in Figure 2.16. The optimized dimension of L_h is 20 mm. If the length is increased, there is small change in impedance bandwidth.

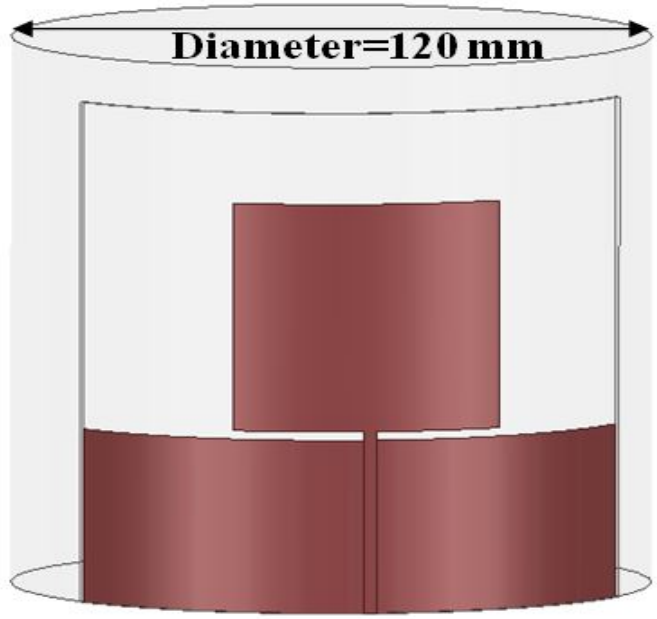

Figure 2.13 Configuration of conventional conformal antenna.

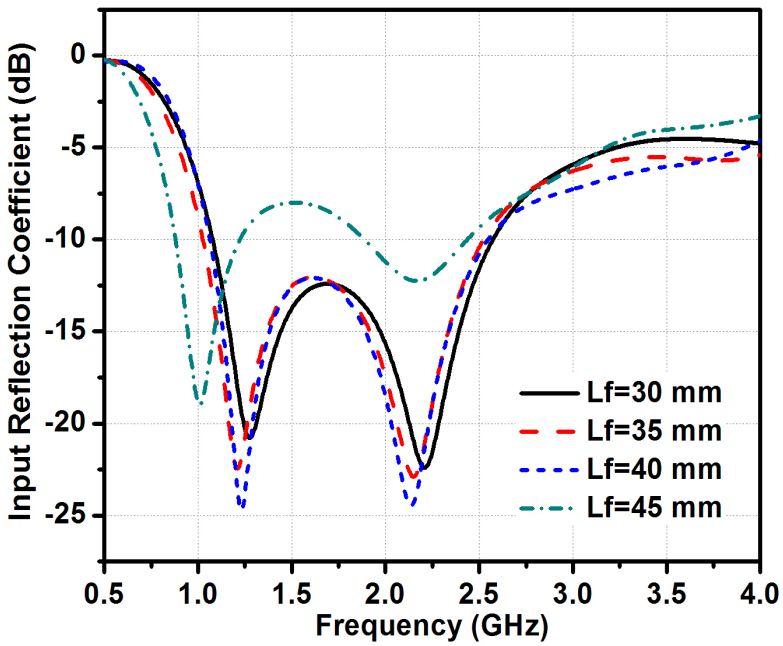

Figure 2.14 Input reflection coefficient (dB) of the conformal antenna for different L_f.

A dumbbell shaped cross slot on the patch is shown in Figure 2.17. Although there is not much difference in the impedance bandwidths for the designs in Figure 2.13 and 2.15, but better impedance matching for cross slot is obtained when compared with horizontal slot and without slot which is shown in Figure 2.18.

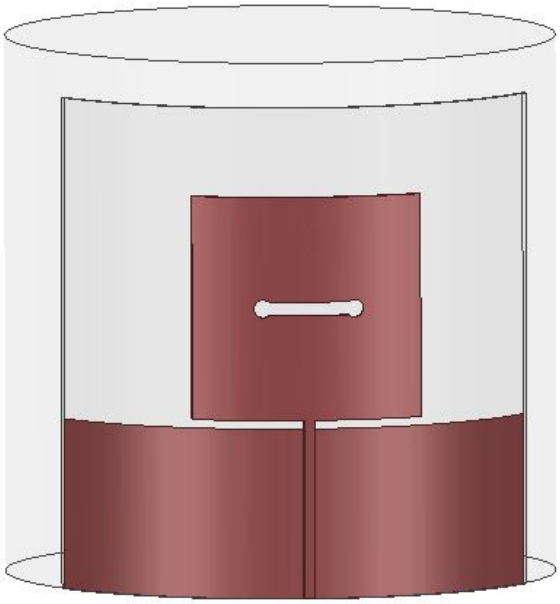

Figure 2.15 Configuration of conformal antenna with horizontal dumbbell shaped slot.

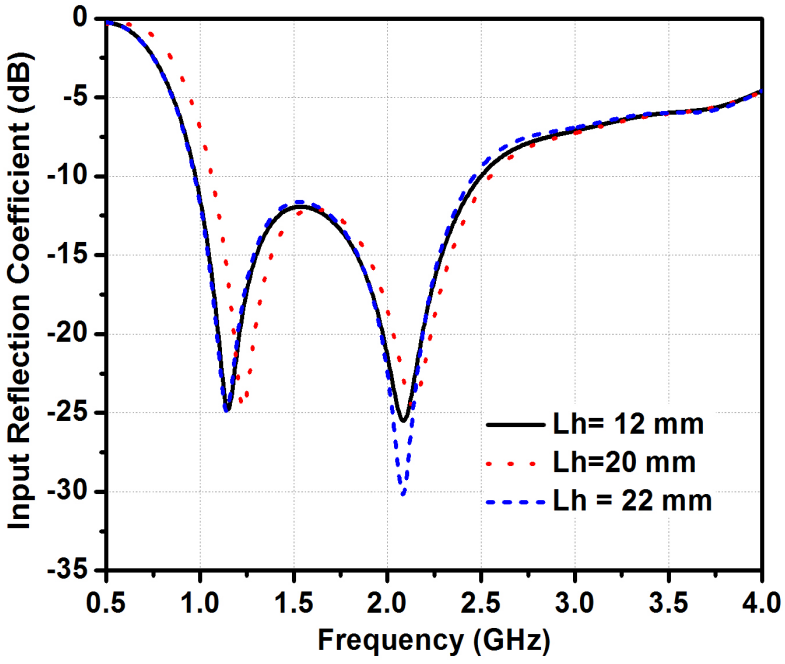

Figure 2.16 Input reflection coefficient (dB) of the conformal antenna for different L_h.

The simulated return loss of the planar and proposed cylindrical conformal antennas with a 60 mm radius of curvature are compared in Figure 2.18. It shows that the return loss of all antennas are obtained below -10 dB which indicates a good impedance matching condition. The proposed cylindrical antenna achieves -10 dB impedance bandwidth of 1434 MHz, between the frequency range 1.09-2.524 GHz with 79.28% fractional bandwidth indicating wide bandwidth.

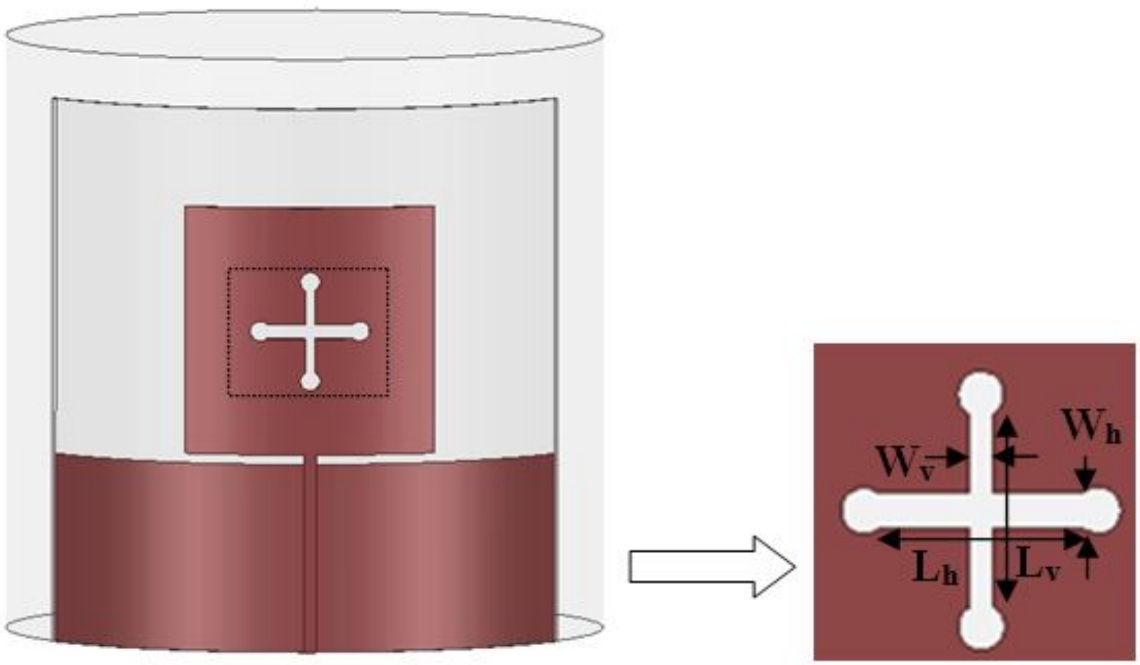

Figure 2.17 Top view of conformal antenna with cross-slot: L_h=20 mm, W_h=3 mm, L_v=20 mm, W_v=2 mm, Radius of circle = 2mm.

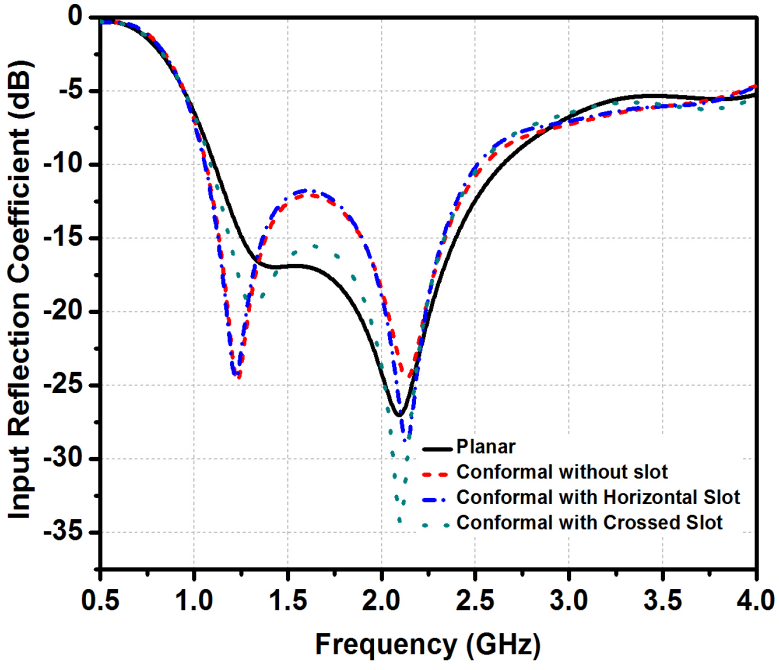

Figure 2.18 Input reflection coefficient (dB) of the conformal antenna.

A small variation in resonant frequency can be observed from planar to cylindrical conformal antenna in Figure 2.18 due to bending of the planar microstrip antenna structure. The resonant frequency of the cylindrical conformal antenna is shifted towards right. Also there

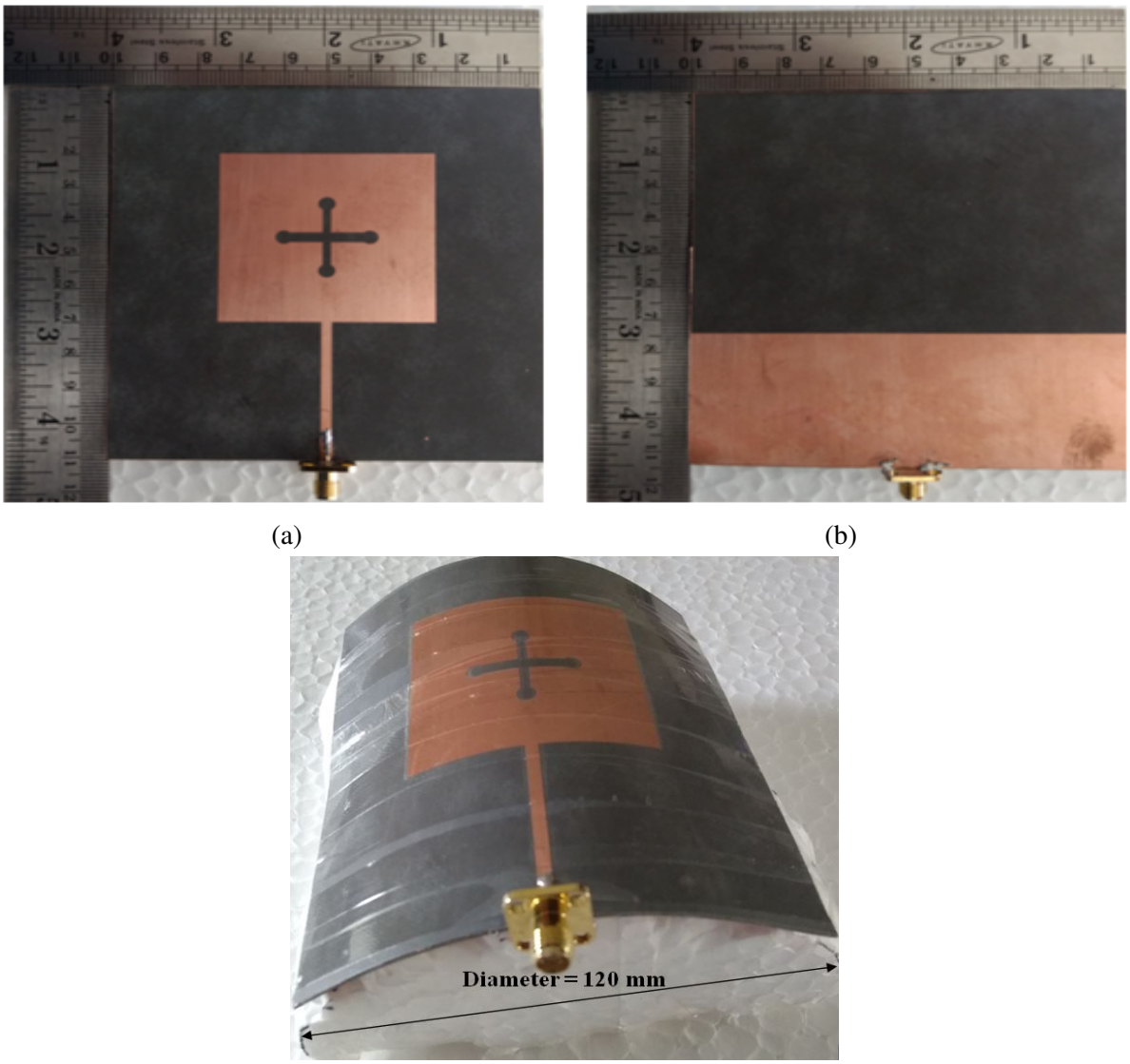

Figure 2.19 Photograph of prototype fabricated antennas (a) front view of the proposed planar antenna (b) back view of the proposed planar antenna (c) front view of a proposed cylindrical conformal antenna with 60 mm radius of curvature.

is a change in return loss between conformal antenna without any slot, with only horizontal dumbbell shape slot and cross dumbbell shaped slot. It indicates that the resonant frequency also depends on slot's length. The matching performance of antenna is improved incorporating modification in cross-slot structure.

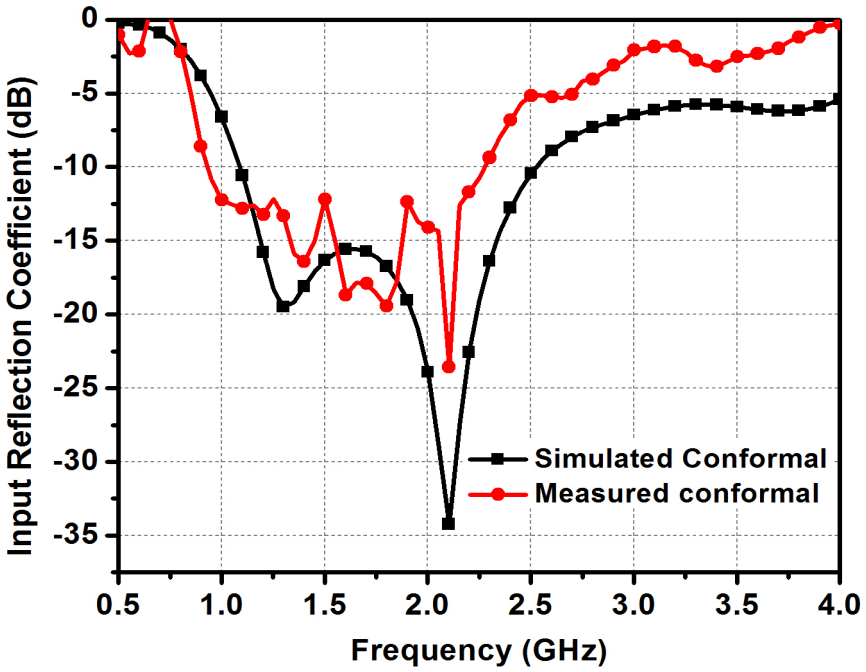

Figure 2.20 Input reflection coefficient of the proposed conformal antenna.

2.5.2 Results and discussion

A prototype of the proposed planar antenna is fabricated on RT/duroid 5880 substrate with thickness of 0.787 mm as shown in Figure 2.19(a) and 2.19(b) and it is transformed to form a cylindrical shape on foam of radius of 60 mm as shown in Figure. 2.19(c). The simulated and measured input reflection coefficient (S_{11}) in dB of the conformal antenna with 60 mm radius cylinder are shown in Figure 2.20. A wide bandwidth of 79.28%, operating from 1.09-2.524 GHz is obtained as shown in Figure 2.20.

The radiation patterns at 1.17645, 1.2276 and 1.57542 GHz in both E and H planes are illustrated in Figure 2.21. The two dimensional patterns of the antenna are obtained in an anechoic chamber. It is investigated that, the two dimensional patterns at various frequencies are similar, which is expected from a wideband antenna. From Figure 2.21 it can be referred that, the designed cylindrical conformal patch antenna has symmetrical radiation patterns. A figure of eight pattern and circular pattern are obtained in E-plane and H plane respectively.

The surface current distribution of the proposed conformal antenna at 1.575 GHz is shown Figure 2.22. A strong surface current distribution around the dumbbell shape of the cross slot can be observed.

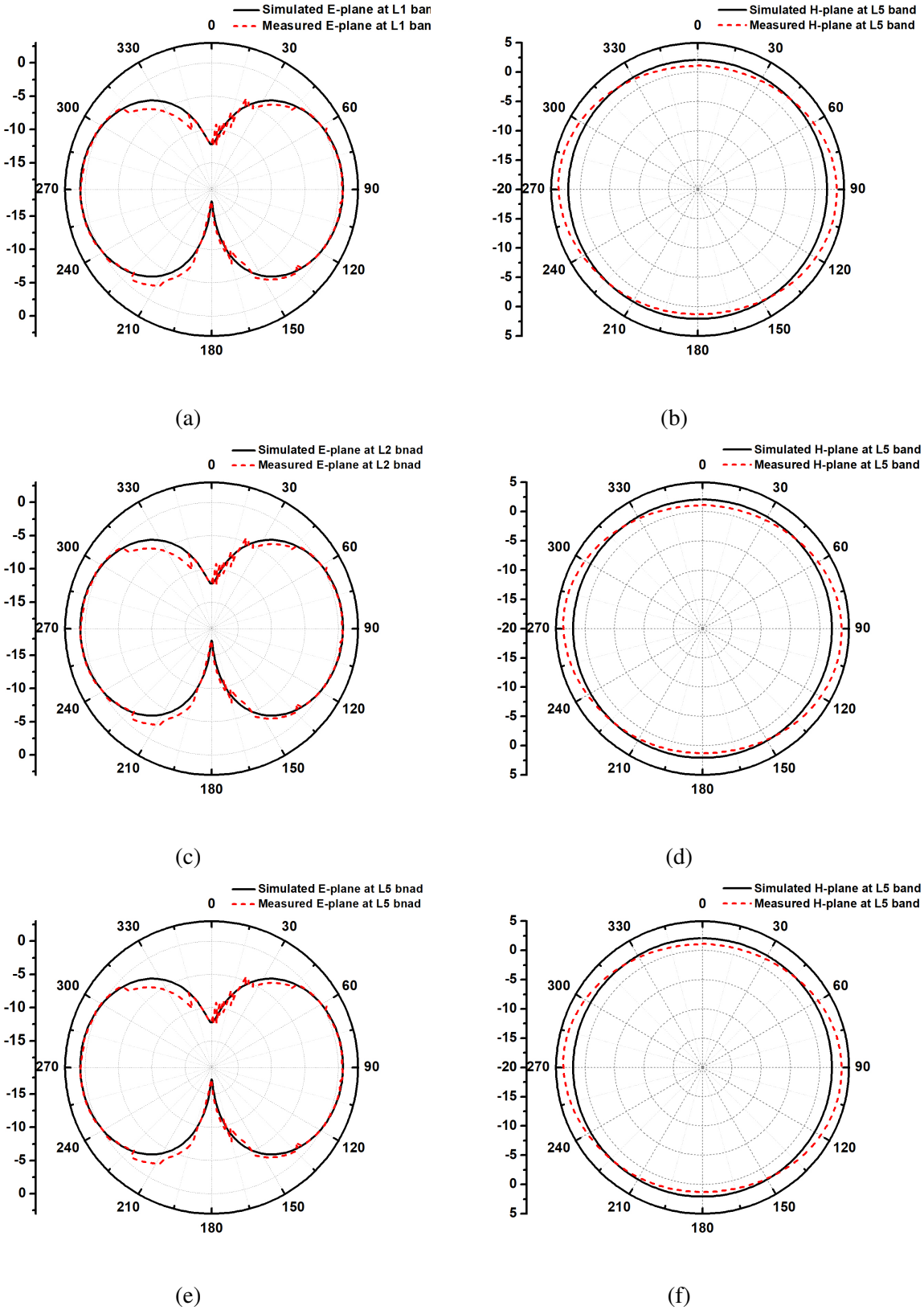

Figure 2.21 Radiation pattern:(a) E plane at 1.17645 GHz, (b) H plane at 1.17645 GHz, (c) E plane at 1.2276 GHz, (d) H plane at 1.2276 GHz, (e) E plane at 1.57542 GHz and (f) H plane at 1.57542 GHz

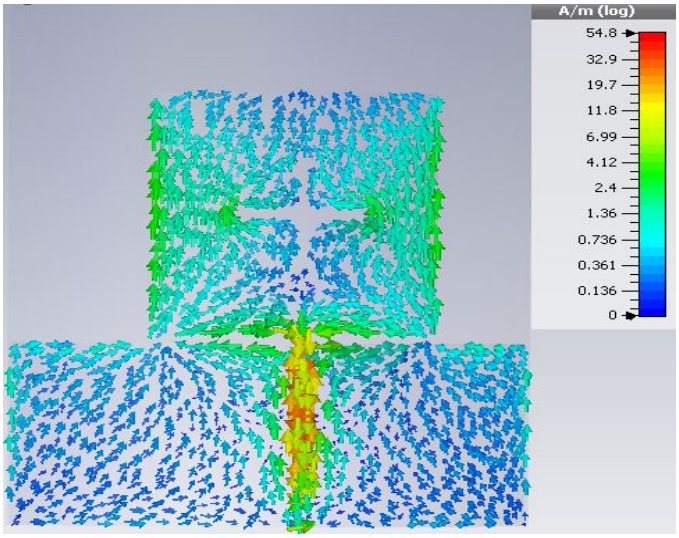

Figure 2.22 Surface current distribution of the proposed conformal antenna at 1.575 GHz.

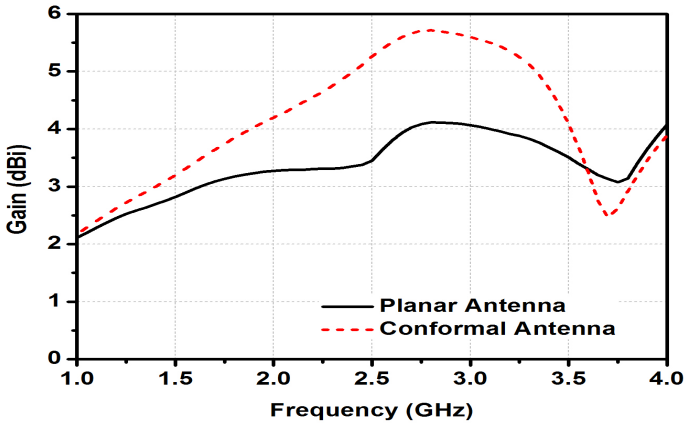

Figure 2.23 The simulated gain of the planar and conformal antenna.

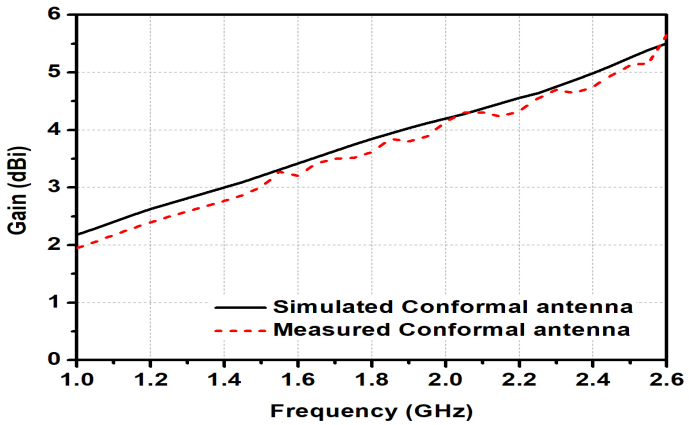

Figure 2.24 The gain of conformal antenna.

Table 2.1 Performance of the proposed conformal antenna compared with planar one existing in the literature.

Antenna	Perimeter (mm)	Frequency (GHz)	-10dB bandwidth	Gain (dBi)
Proposed work	420	L_1, L_2, L_3, L_4, L_5 band	79.28%	5.33
[58]	314.15	L_1	2.1%	-11
[59]	395.84	L_1	20 MHz	6.5
[60]	240	L_1	20 MHz	4

The gain of the cylindrical conformal antenna and planar antenna are compared in Figure 2.23. The antenna gain is varying from 2.37 to 5.33 dBi over the operating frequency band. The gain of conformal antenna is more than that of the planar antenna. The simulated and measured gain of the proposed cylindrical conformal antenna are compared in Figure 2.24.

The overall performance of the proposed cylindrical conformal antenna is compared with those of previously reported planar antennas at GPS frequency in [58-60] and given in Table 2.1. In spite of the fact that the proposed cylindrical conformal antenna has large size, yet it gives competitively wide bandwidths. Moreover, the antenna gain is larger than the gain of antennas existing in the literature [58],[60].

2.6 Bow-tie shaped wideband conformal antenna with wide-slot

2.6.1 Antenna design and parametric study

2.6.1.1 Design of conventional cylindrical conformal bow-tie antenna

As compared to a printed dipole and linear wire antenna, the bow-tie antenna has broadband characteristics with simple geometry. Bow-tie antennas are used to achieve compact size [68]. Figure 2.25a shows the front view and Figure 2.25b depicts the back view structure of the conventional bow-tie printed antenna.

The design of bow-tie antenna is similar to rectangular patch antenna. The resonant frequency in the dominant mode TM_{10} can be calculated as shown below [68, 69]

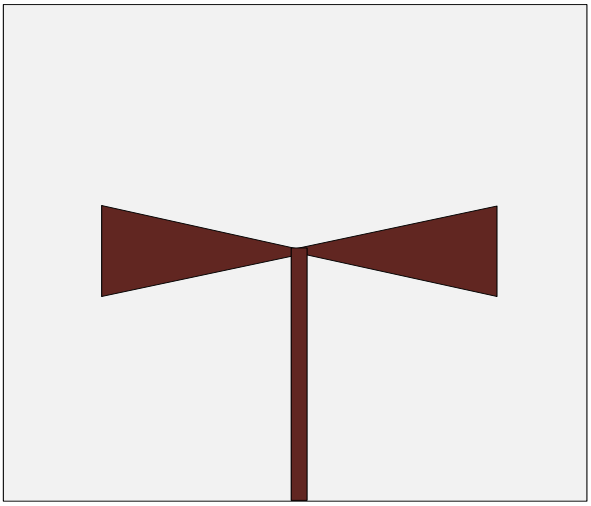

(a)

(b)

Figure 2.25 Structure of conventional bow-tie antenna without ground slot: (a) front view, (b) back view.

$$f_r = \frac{c}{2\sqrt{\varepsilon_r L}}\left(\frac{1.152}{R_t}\right). \tag{2.6}$$

$$R_t = \frac{L}{2}\frac{(W + 2\Delta l) + (W_c + 2\Delta l)}{(W + 2\Delta l) + (S + 2\Delta l)}. \tag{2.7}$$

$$\Delta l = h\frac{0.412(\varepsilon_e + 0.3) + \left(\frac{W}{h} + 0.262\right)}{(\varepsilon_e - 0.258) + \left(\frac{W}{h} + 0.813\right)}. \tag{2.8}$$

$$\varepsilon_e = \left(\frac{\varepsilon_r + 1}{2}\right) + \left(\frac{\varepsilon_r - 1}{2}\right)\left(1 + \frac{12h}{W_i}\right)^{-1/2}. \tag{2.9}$$

$$\varepsilon_e = \left(\frac{W + W_c}{2}\right). \tag{2.10}$$

where
L/2 is the side length of the bow-tie patch
W is the height of the bow-tie patch
c is the velocity of Electromagnetic wave
ε_r is the relative permittivity
ε_e is the effective permittivity
S is the length of the bow-tie patch
f_r is the resonant frequency of the bow-tie antenna
h is the thickness of the substrate
W_i is the height at the center of the bow-tie patch

The substrate RT/duroid 5880 is chosen as it is flexible and has heat stabilization. The low dielectric constant of 2.2 of substrate is considered to meet the wide bandwidth specification. The simulation of the antenna is done using commercially available computer simulation technology (CST) microwave studio.

The antenna used in the proposed work utilizes a microstrip line feed with characteristic impedance of 50 Ω to excite the bow-tie patch. The 10 dB impedance bandwidth of bow-tie antenna can be enhanced by applying slot in the ground plane.

2.6.1.2 Design of cylindrical conformal bow-tie antenna with wide slot in ground

A similar bow-tie shaped slot is also placed on the ground plane. The combination of the bow-tie slot on the ground and radiating patch is selected on account of its good radiation characteristics and wide impedance bandwidth. As wide slot is utilized in the design, a large coupling results with the feed line. So, the coupling can be changed by varying the slot shape or feed shape to achieve impedance matching.

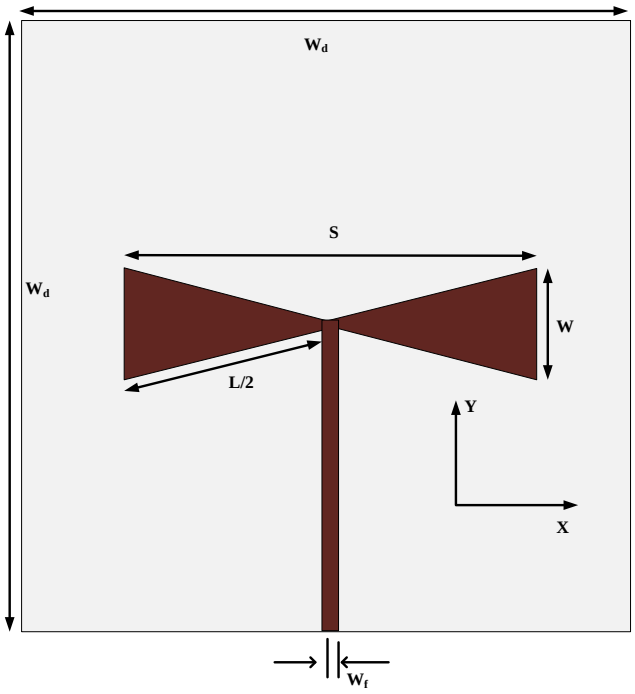

(a)

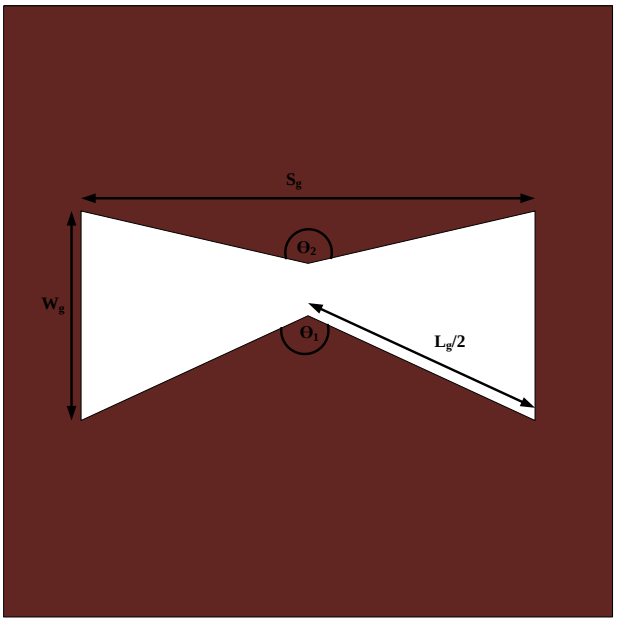

(b)

Figure 2.26 Geometry of conventional bow-tie antenna with wide-slot on ground: (a) front view, (b) back view.

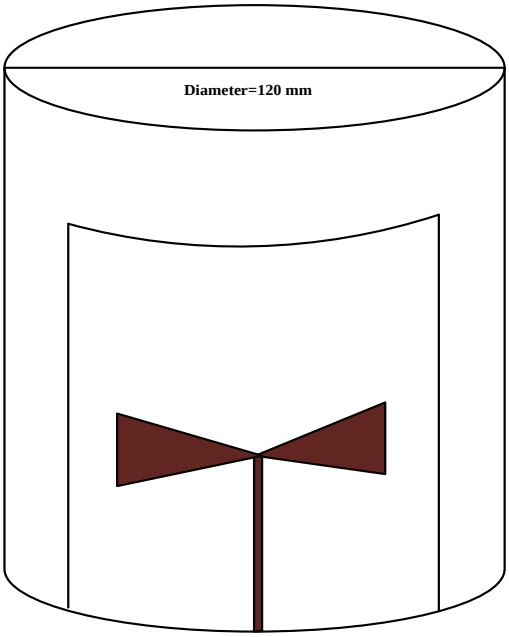

Figure 2.27 Configuration of conventional conformal bow-tie antenna.

Table 2.2 Optimized dimension of the proposed antenna.

Parameters	**Value**	**Parameter**	**Value**
W_d	120 mm	W_s	1.1 mm
S	80 mm	S_g	93 mm
W	22 mm	W_g	40 mm
L/2	41 mm	$L_g/2$	47.5 mm
L_f	60 mm	θ_1	135.56 drgree
W_f	1.5 mm	θ_2	156.46 degree
L_s	12.7 mm	Radius of circle in dumbbell shape slit	1 mm

The geometry of front view and back view of the proposed wide-slot planar antenna is demonstrated in Figure 2.26a and 2.26b respectively. The dimensions of the proposed bow-tie antenna are illustrated in Table 2.2. The planar bow-tie antenna is transformed to the conformal on a cylinder of radius 60 mm, which is shown in Figure 2.27.

The effect of length of the feed-line on the impedance matching is observed. It can be referred that better impedance matching is achieved by increasing the length of feed-line. The optimized value for L_f in the proposed conformal antenna is 60 mm. However, if the length is increased further, the size of the antenna will be increased. The simulated reflection coefficient (dB) of the proposed conformal antenna with feed-line lengths of 30, 40, 50, and 60 mm is shown in Figure 2.28a.

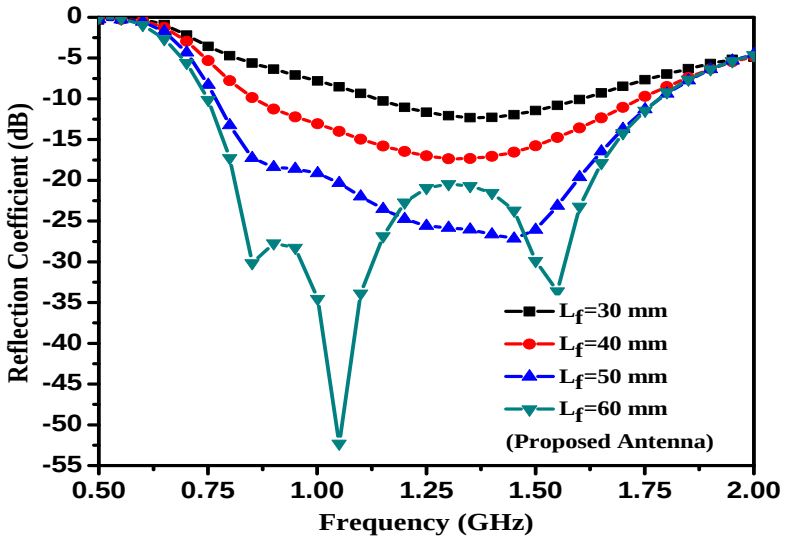

(a)

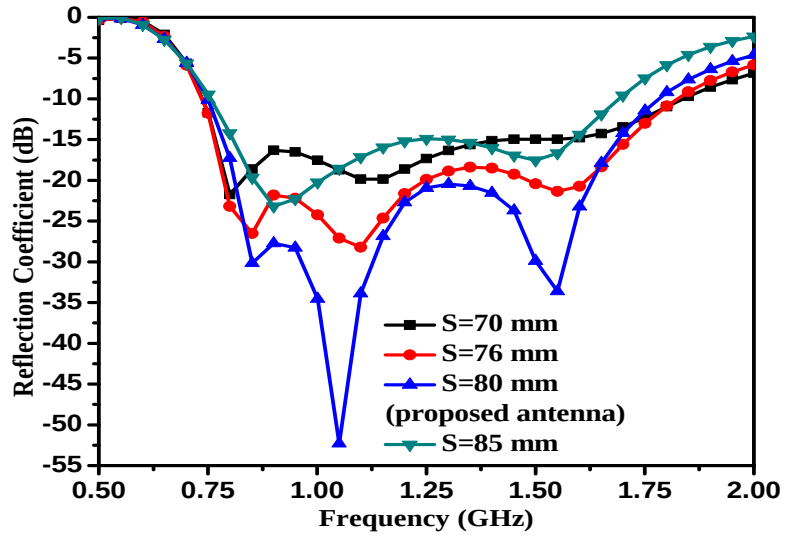

(b)

Figure 2.28 Reflection coefficient of the proposed conformal antenna: (a) for different L_f. (b) for different S.

The effect of the dimensions of the patch on the impedance matching is also investigated. The impedance matching can be obtained by increasing length of bow-tie dimension 'S' from 70 to 85 mm. The optimized value for S in the proposed antenna is 80 mm. With further increase in the value of 'S', the return loss is increased. The reflection coefficient (dB) of the designed antenna with a dimension of a patch of 'S' as 70, 76, 80 and 85 mm is shown in Figure 2.28b.

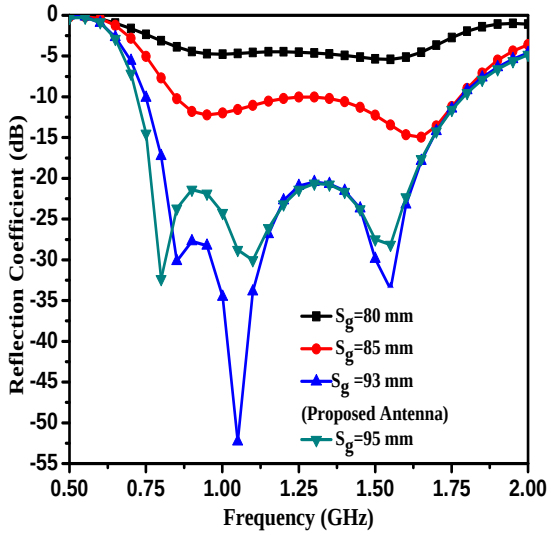

(a)

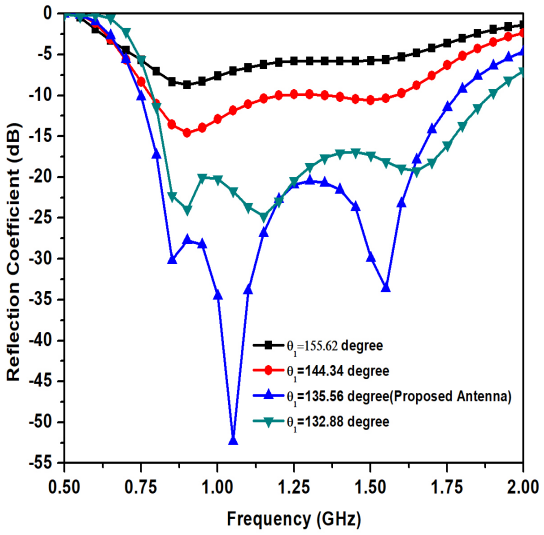

(b)

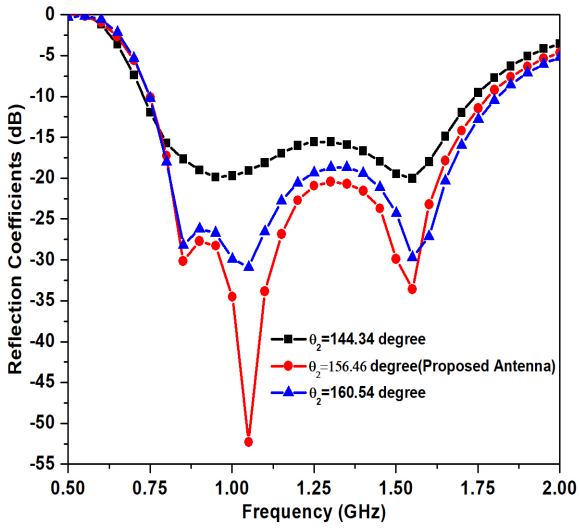

(c)

Figure 2.29 Simulated reflection coefficient of the proposed conformal antenna: (a) for different S_g, (b) for different θ_1 and (c) for different θ_2.

So as to obtain a large coupling, a wide slot is introduced in the ground. The effect of the angle of the slot θ_1, θ_2 and length of slot S_g on the reflection coefficients of the antenna are shown in Figure 2.29a, 2.29b, and 2.29c. As shown in these figures, there is a good impedance matching for θ_1=135.56 degree, θ_2=156.46 degree and S_g=93 mm.

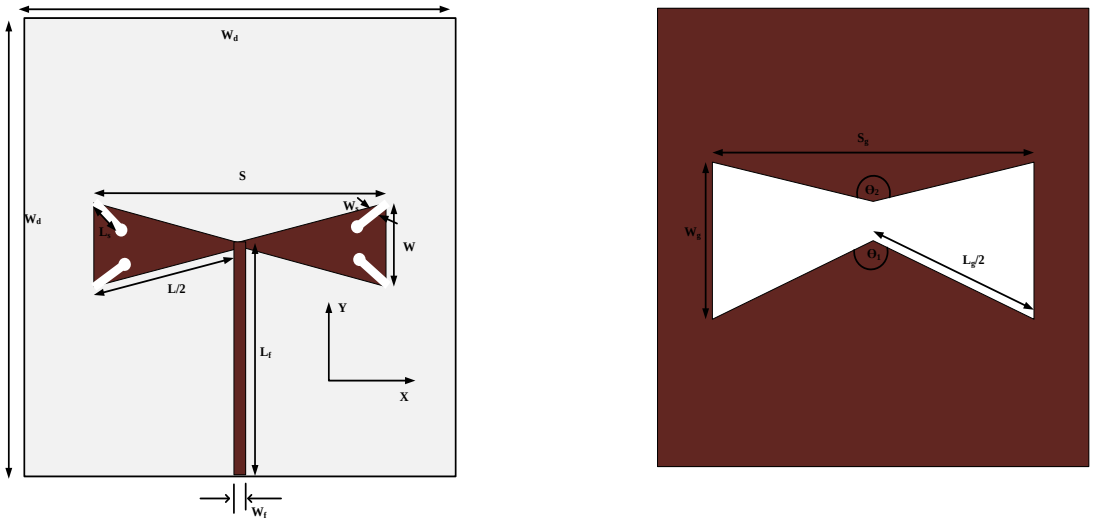

(a) (b)

Figure 2.30 Geometry of the proposed bow-tie antenna: (a) front view and (b) back view.

2.6.1.3 Design of proposed cylindrical conformal bow-tie antenna with dumbbell shaped slit loading on patch

According to [1-3], the feed inductance counters capacitance introduced by slits and slots in the patch. In addition, additional resonances caused by slot combines with the patch resonance which makes the antenna to have a wideband response. Patch antennas with slits can have different shapes like circular, square and rectangular. A dumbbell-shaped slit introduced on the four corners of the patch without or with modifying ground plane as shown in Figure 2.30a and 2.30b. The use of the circle on the one end of the slit is the best case among the other geometries. It is because that the circle makes the fields on the slits more uniform than the other cases. The proposed planar antenna in Figure 2.30 is transformed to the conformal antenna on 60 mm radius of cylinder which is shown in Figure 2.31.

The effect of slits on the patch is explored in Figure 2.32. The impedance matching is improved by introducing different slits like rectangular or dumbbell on the patch. In case of dumbbell-shaped slit, the impedance matching is better than a rectangular antenna due to presence of slits on patch.

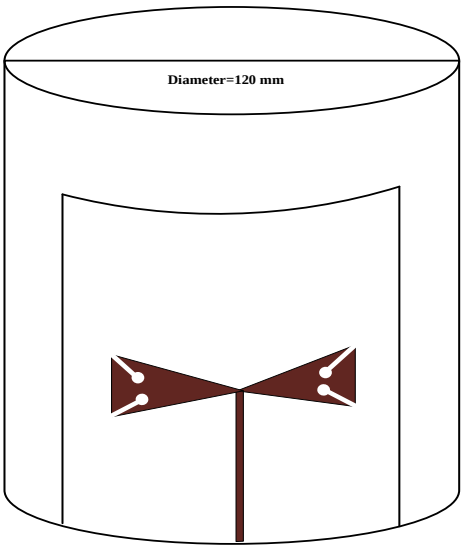

Figure 2.31 Configuration of proposed cylindrical conformal antenna with 60 mm radius of curvature.

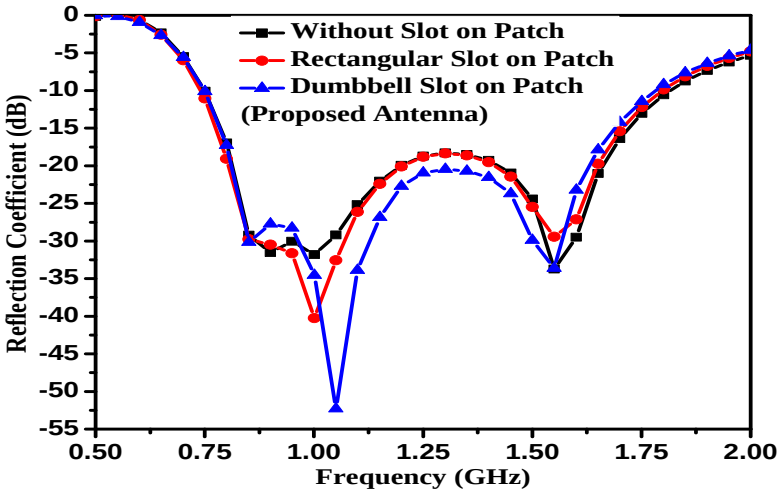

Figure 2.32 Reflection coefficient of the proposed conformal antenna with the effect of slits on the patch.

2.6.2 Results and discussions

A prototype planar antenna is fabricated on RT/duroid 5880 substrate with thickness of 0.787 mm. By using LPKF milling machine S100, the antenna is fabricated on a planar surface as shown in Figure 2.33a and 2.33b, and it is rolled up to form a cylindrical shape on the foam of radius of 60 mm as shown in Figure 2.33c. The foam material is used as mechanical support for making 60 mm radius of the cylinder which has negligible radiation effect on the antenna.

Both simulated and measured reflection coefficient (S_{11}) in dB of the proposed conformal antenna with 60 mm radius cylinder are demonstrated in Figure 2.34. At the frequencies

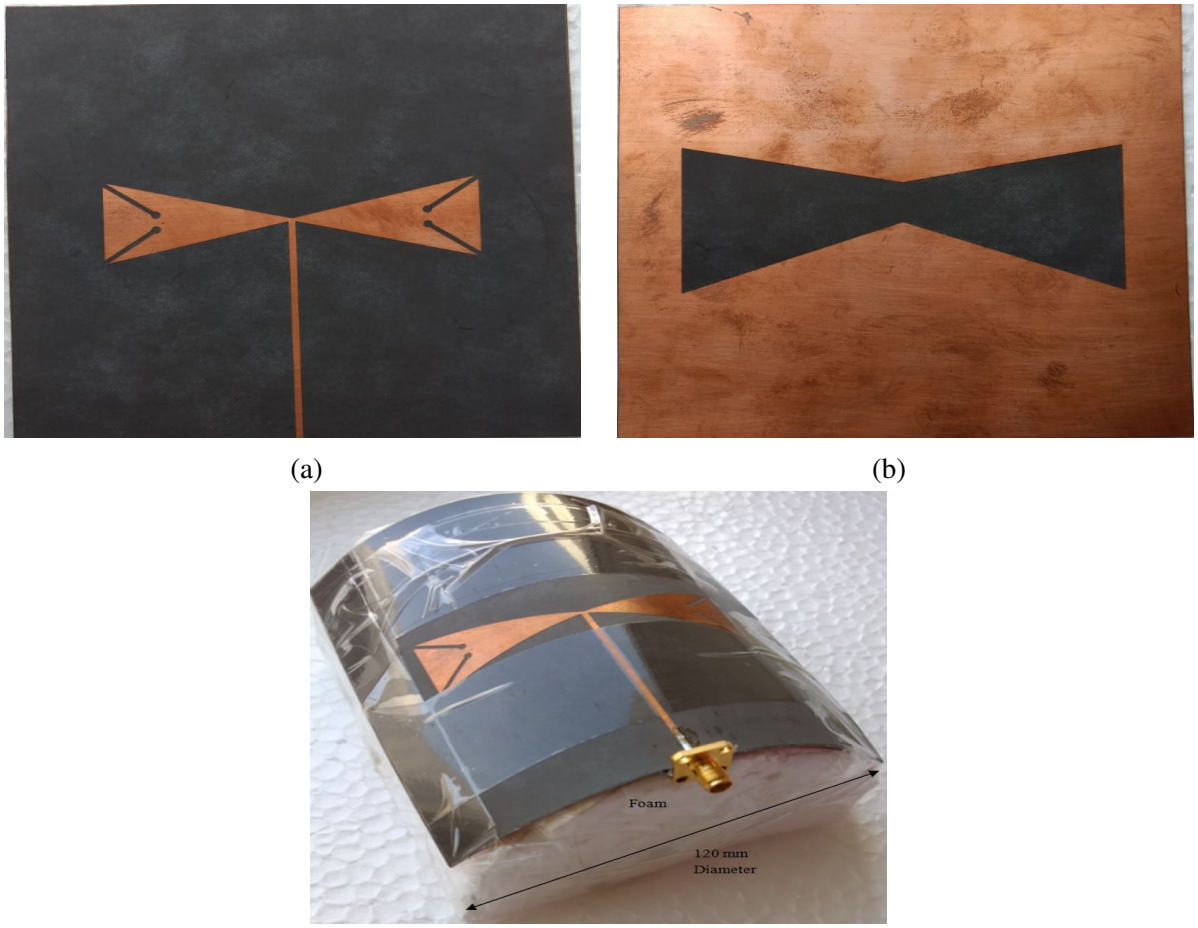

Figure 2.33 Photograph of prototype fabricated antennas: (a) front view of the proposed planar antenna, (b) back view of the proposed planar antenna and (c) top view of a proposed cylindrical conformal antenna with 60 mm radius of curvature.

between -10 dB reflection coefficient values, reflection coefficient is near to -40 dB, which indicates a good impedance matching in the operating frequency range. The simulated reflection coefficient is obtained using CST STUDIO SUITE 2016 by considering discrete port with 50 Ω impedance. A four hole round shaped pin with female type SMA connector which is working in the range DC to 18 GHz is connected to the fabricated antenna. The antenna is measured utilizing HP vector network analyzer within the frequency range of 130 MHz to 13 GHz. It is investigated that the proposed, designed cylindrical conformal patch antenna has a wide -10 dB reflection coefficient fractional bandwidth of 81.4% , operating from 0.75 to 1.78 GHz. It can also be investigated that the measured reflection coefficient(dB) agrees with the impedance bandwidth achieved by using commercially available CST software.

The radiation patterns at 1.17645, 1.2276 and 1.5754 GHz in both E and H planes are illustrated in Figure 2.35a to 2.35f respectively. The two dimensional patterns of the antenna

are obtained in an anechoic chamber. To measure the radiation pattern, standard horn antenna is used at the transmitter and conformal antenna is connected to receiver. The conformal antenna radiation pattern is measured in receiving mode. It is investigated that the radiation patterns at various frequencies are similar, which is required for a wideband antenna. It can be referred that, the proposed designed cylindrical conformal patch antenna has symmetrical radiation patterns as shown in Figure 2.35. In E plane, a figure of eight like pattern and circular pattern in H-plane are obtained.

The surface current distribution at 1.17 GHz and 1.575 GHz are shown in Figure 2.36a and 2.36b respectively. The strongest current distribution is around the end of the dumbbell shaped slits. The slits on the radiating patch can cause increase of the excited surface current paths. Similarly the field distribution of the proposed conformal antenna at 1.17 and 1.575 GHz are given in Figure 2.37a and 2.37b respectively. The simulated and measured gain with respect to frequency are presented in Figure 2.38. The gain of the proposed antenna is measured by gain transfer method. The gain transfer method requires an antenna with known gain (called standard antenna). In the measurement, the standard horn antenna is used whose gain is known. Compared to the low frequency region, the gain is effectively increased at high frequency. Hence, the antenna gain is varying from 3.5 to 4.78 dBi over the operating frequency band.

The overall performance of the proposed cylindrical conformal antenna is compared with those of previously reported planar antennas at GPS frequency in [58-61] and other frequencies

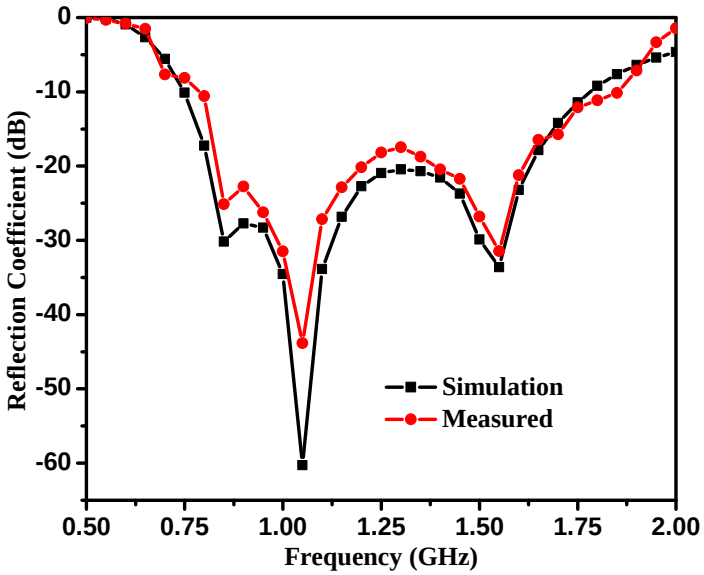

Figure 2.34 Reflection coefficient of the proposed conformal antenna with the effect of slits on the patch.

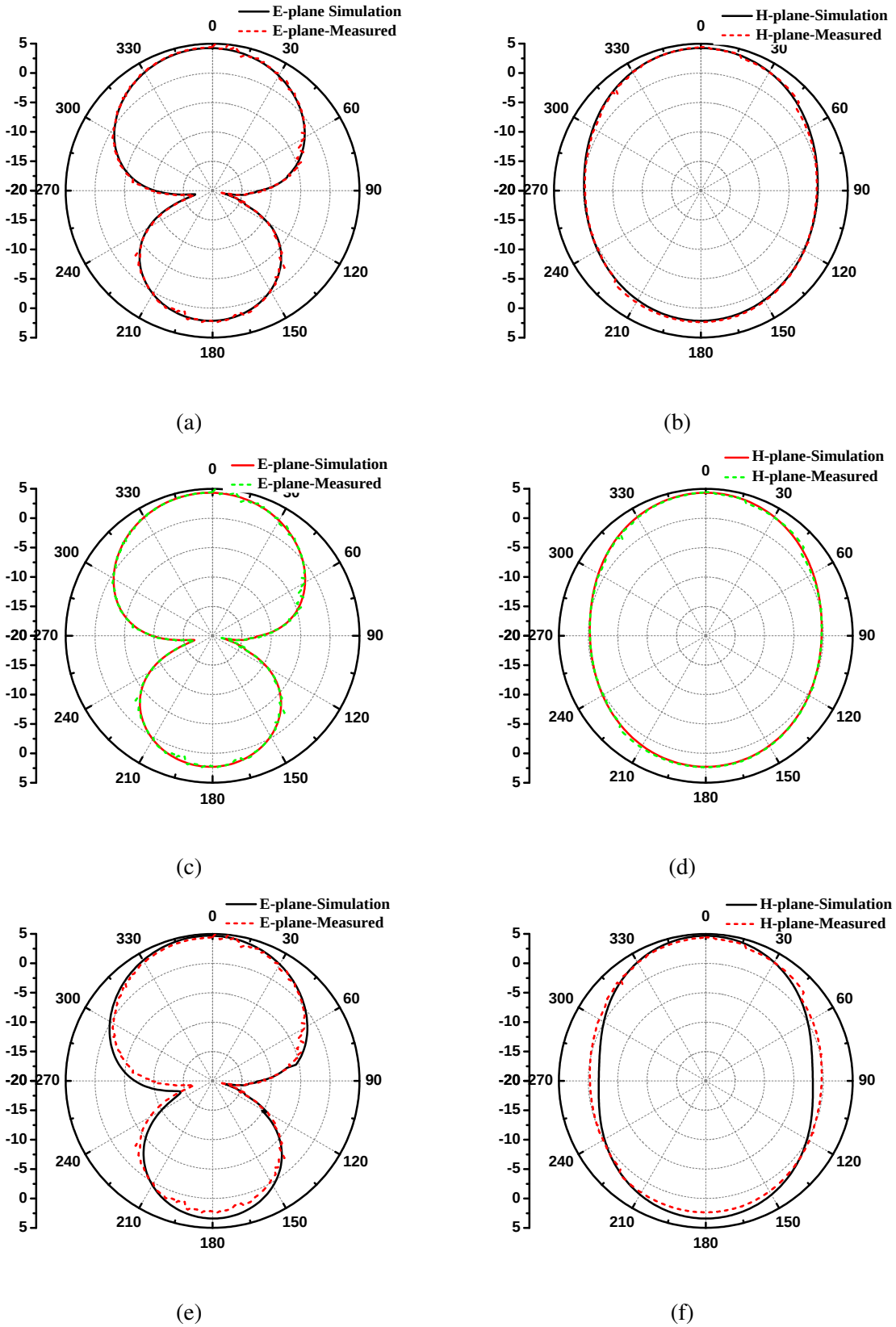

(a) (b)

(c) (d)

(e) (f)

Figure 2.35 Radiation pattern:(a) E plane at 1.17645 GHz, (b) H plane at 1.17645 GHz, (c) E plane at 1.2276 GHz, (d) H plane at 1.2276 GHz, (e) E plane at 1.57542 GHz and (f) H plane at 1.57542 GHz

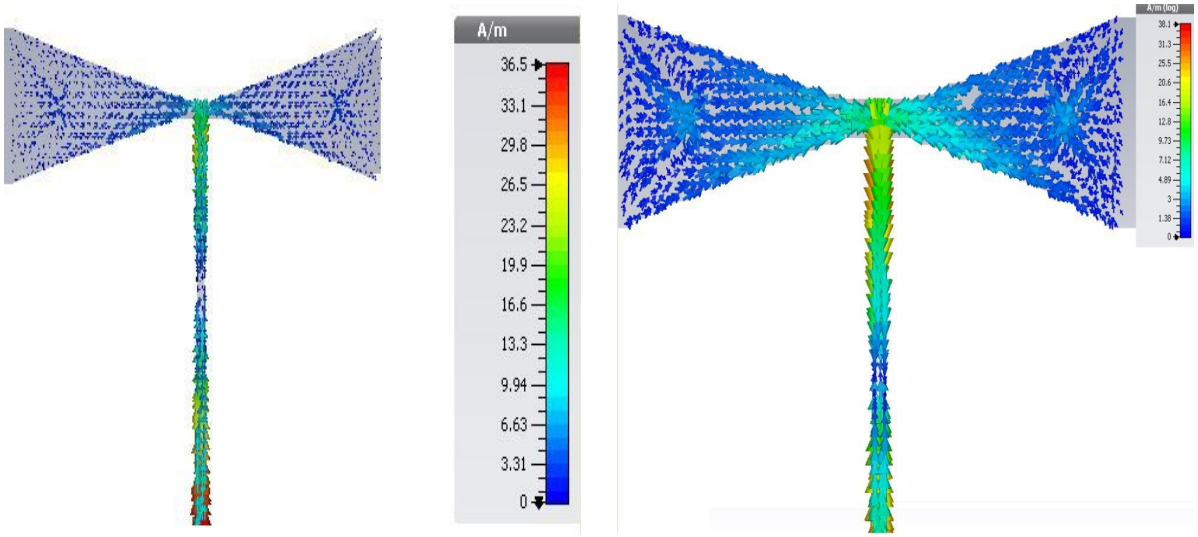

(a) (b)

Figure 2.36 Current distribution of proposed conformal antenna at: (a) 1.17 GHz (b) 1.575 GHz.

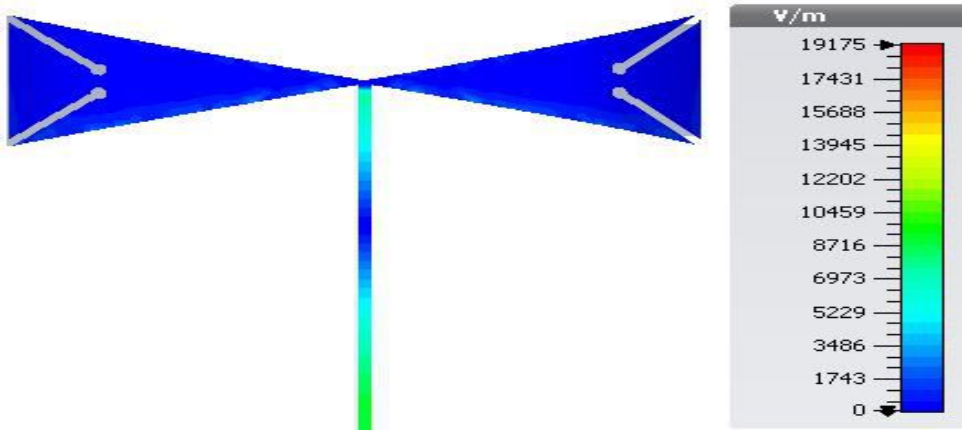

(a)

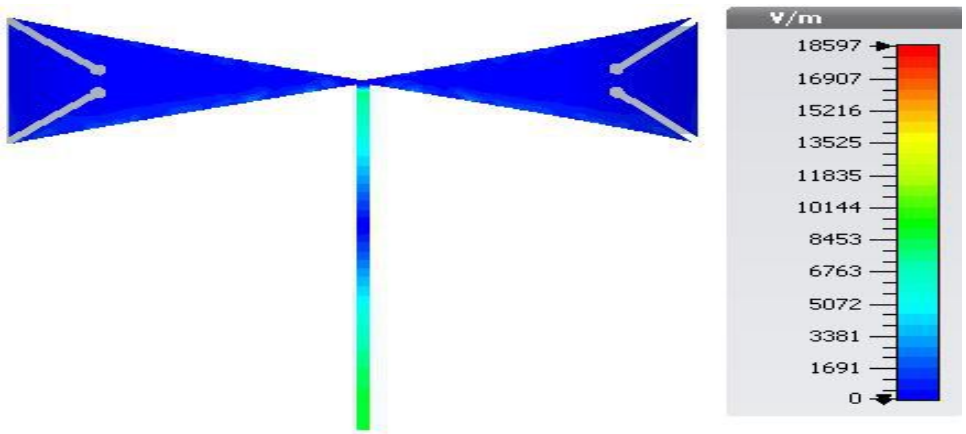

(b)

Figure 2.37 Field distribution of proposed conformal antenna at: (a) 1.17 GHz (b) 1.575 GHz.

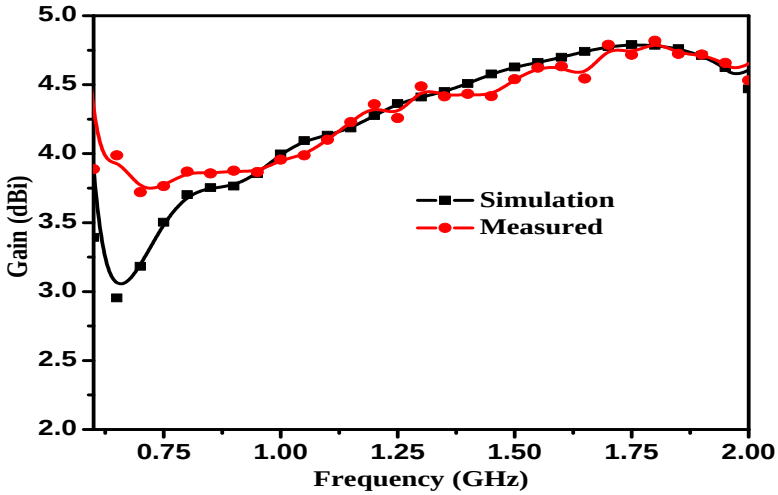

Figure 2.38 Simulated and measured proposed conformal antenna gain.

Table 2.3 Performance of the proposed conformal antenna compared with planar one existing in the literature.

Antenna	**Perimeter (mm)**	**Frequency (GHz)**	**-10dB bandwidth**	**Gain (dBi)**
Proposed work	480	L_1,L_2, L_3,L_4,L_5 band	81.4%	4.78
[58]	314.15	L_1	2.1%	-11
[59]	395.84	L_1	20 MHz	6.5
[60]	240	L_1	20 MHz	4
[61]	360	L_1	27 MHz	5.4
[68]	264	0.737	15 MHz	-
[69]	120.86	2.66	168 MHz	7.83

in [68-69] and given in Table 2.3. In spite of the fact that the proposed cylindrical conformal antenna is large in size, yet it gives comparatively wide bandwidths. Moreover, the peak gain is also larger than the antennas existing in the literature [58] and [60].

2.7 Conclusion

A bow-tie shaped wideband conformal antenna with wide-slot, fabricated on a cylinder of 60 mm radius of curvature, can be used for GPS and Galileo frequency applications. The performance of the antenna is validated through simulation and measurement results. The operating bandwidth of the proposed conformal antenna obtained as 81.4% which includes the bandwidth necessary for GPS applications. A good agreement is seen between the measurement and sim-

ulation results. Furthermore, the proposed antenna demonstrates stable radiation characteristics with a gain of about 3.5 to 4.78 dBi in the whole operating frequency range of 0.75 to 1.78 GHz. In view of the achieved characteristics, the proposed bow-tie patch with wide slot, loaded on the ground cylindrical conformal antenna can be considered as a suitable candidate in non planar surface like missile application such as anti-tank guided missile(ATGM). Similarly the designed antenna can be used as conformal array for gain enhancement which can be used for many commercial purposes.

Chapter 3

Cylindrical Conformal Fractal Antenna for GPS Application

3.1 Introduction

As space constraints on the vehicle are always a limitations for antenna design, research methods are developed to minimize the size of the patch antenna. This is a very challenging task but useful for many applications such as handset internal antennas, radio frequency front-end antennas and antennas for GPS applications. Moreover, miniaturization will reduce system requirements and must be applied in the antenna design. Fractal geometry is the promising technique by which the electrical length of the antenna is increased with a gradual decrease in size of the antenna. Different fractal geometries are available like Koch fractal, Minkowski fractal and Sierpensiki gasket in published literature.

Some antennas are designed using fractal concept on flat surface at S, C and X bands [70-74]. H. L. Dholakiya and D. L. Pujara proposed a microstrip antenna with a circular shaped fractal slot to improve the bandwidth for 2 to 6 GHz with operating bandwidth of 52% [70]. A. Karmakar et al. proposed a complementary stacked patch antenna with fractal shaped defect for wideband characteristics for 1.8 to 6.4 GHz with fractional bandwidth of 89.1% on flat surface [71]. In some of the published literature [72, 73, 74] the bandwidth information is not available. Some of the antennas are designed on the FR4 substrate in [9-12]. The dielectric loss tangent of FR4 is 0.02 whereas Rogers RT/duroid is 0.0009 which indicates that the losses of FR4 are

more compared with Rogers RT/duroid 5880. Also FR4 is not flexible like Rogers RT/duroid 5880, hence RT duroid is selected in the proposed work.

In this chapter, novel high performance and compact cylindrical conformal antennas based on fractal structure are proposed for GPS application.The proposed cylindrical conformal antenna exhibits broad bandwidth by incorporating partial ground concept. The planar, as well as the proposed cylindrical conformal antennas are designed, simulated and validated.

3.2 Fractal structures

For designing a compact antenna, fractal geometry is applied in design of antennas as the area occupied by the conventional antenna can be increased by the fractal structure. The advantages of fractal concept is increase in electrical length of the antenna which reduces the resonant frequency of operation. Fractals are self symmetrical structures. Some of the configurations are listed below.

3.2.1 Koch curve

The Koch curve, the simplest fractal, is generated by dividing the straight line into three parts. The middle part of the straight line bends into the triangular shape as shown in Figure 3.1, with 60^0 flare angle. The same process can be repeated for the fractal geometry up to finite number of iterations.Total length of the Koch Edge in the nth iteration is $L = (4/3)^n$. Thus, after *'n'* iterations, the total number of the Koch Edges will be 4^n.

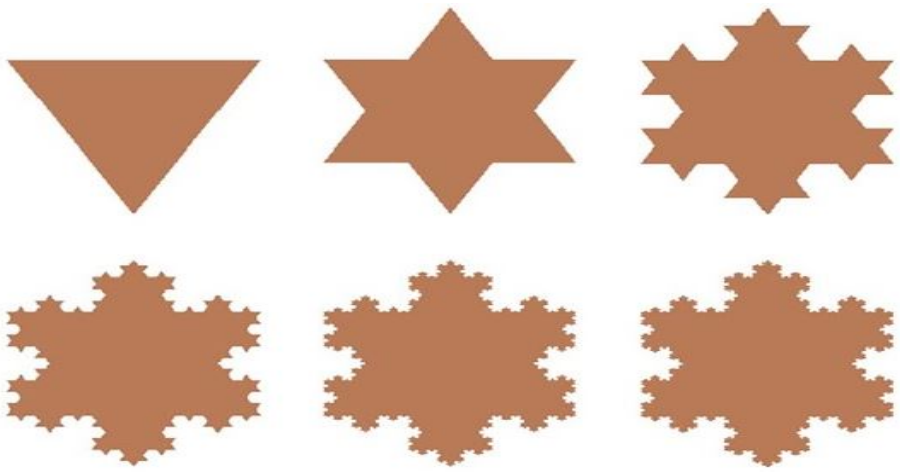

Figure 3.1 Koch fractal iteration structure.

3.2.2 Minkowski geometry

The geometrical shape of Minkowski curve is designed by taking straight line (initiator) as shown in Figure 3.2. This recursive process is repeated up to 2nd iteration. It is somehow similar to Koch curves where equilateral triangles are used but in Minkowski geometry, rectangles are used. The iteration factor (IF) can be calculated from indentation length (IL) and indentation width (IW) as $IF = \frac{IW}{IL}$.

3.2.3 Sierpinski gasket

The widely used fractal geometry for antenna applications is Sierpinski gasket. The self-similar current distribution on this antenna introduces multi-band characteristics. Two different approaches like multiple-copy and decomposition can be used to generate the Sierpinski gasket antenna with the help of self-similarity and space filling properties, as shown in the Figure 3.3. The Sierpinski gasket shape is generated by removing inverted equilateral triangle from the main triangle. This process can be repeated till n^{th} iteration.At n^{th} iteration, the number of triangles being removed, $N = \sum_{i=0}^{i=n-1} 3^i$

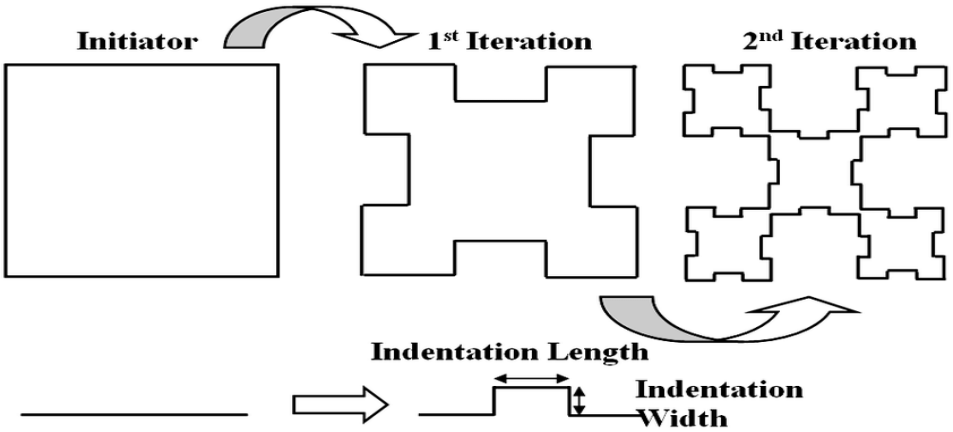

Figure 3.2 Minkowski fractal iteration structure.

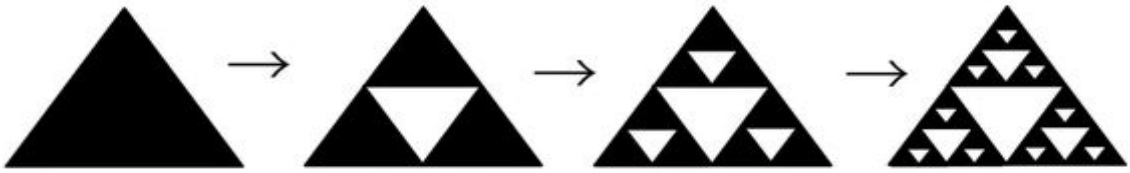

Figure 3.3 Sierpinski gasket fractal iteration structure.

3.2.4 Sierpinski carpet

The Sierpinski carpet geometry is generated by using square structures. The square of one-third size is subtracted from main square and this process is repeated number of times to attain the desired geometry. The Sierpinski carpet fractal antenna with four iterations is shown in Figure 3.4.

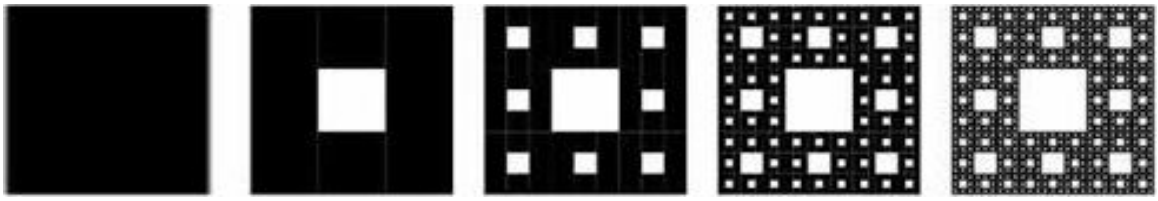

Figure 3.4 Sierpinski carpet fractal iteration structure.

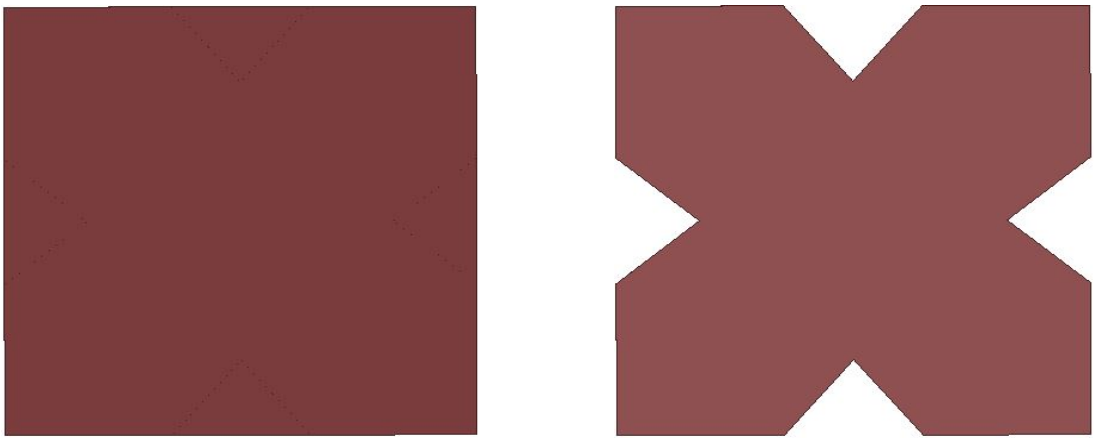

(a) (b)

Figure 3.5 Scheme of the Koch fractal iteration structure. (a) 0^{th} iteration; (b) 1^{st} iteration.

3.3 Cylindrical conformal antenna with Koch fractal

3.3.1 Design of a Koch fractal conformal antenna

A square patch antenna is designed at the resonant frequency. Koch fractal is applied along the boundary of the designed antenna. The scheme of the 0^{th} and 1^{st} iteration of Koch fractal curve is shown in Figure 3.5.

The geometry of both planar and cylindrical conformal antenna are shown in Figure 3.6. The optimized dimensions are W_1=100 mm,W_2=55.5 mm,W_3 =20 mm, W_4=12.69 mm. A

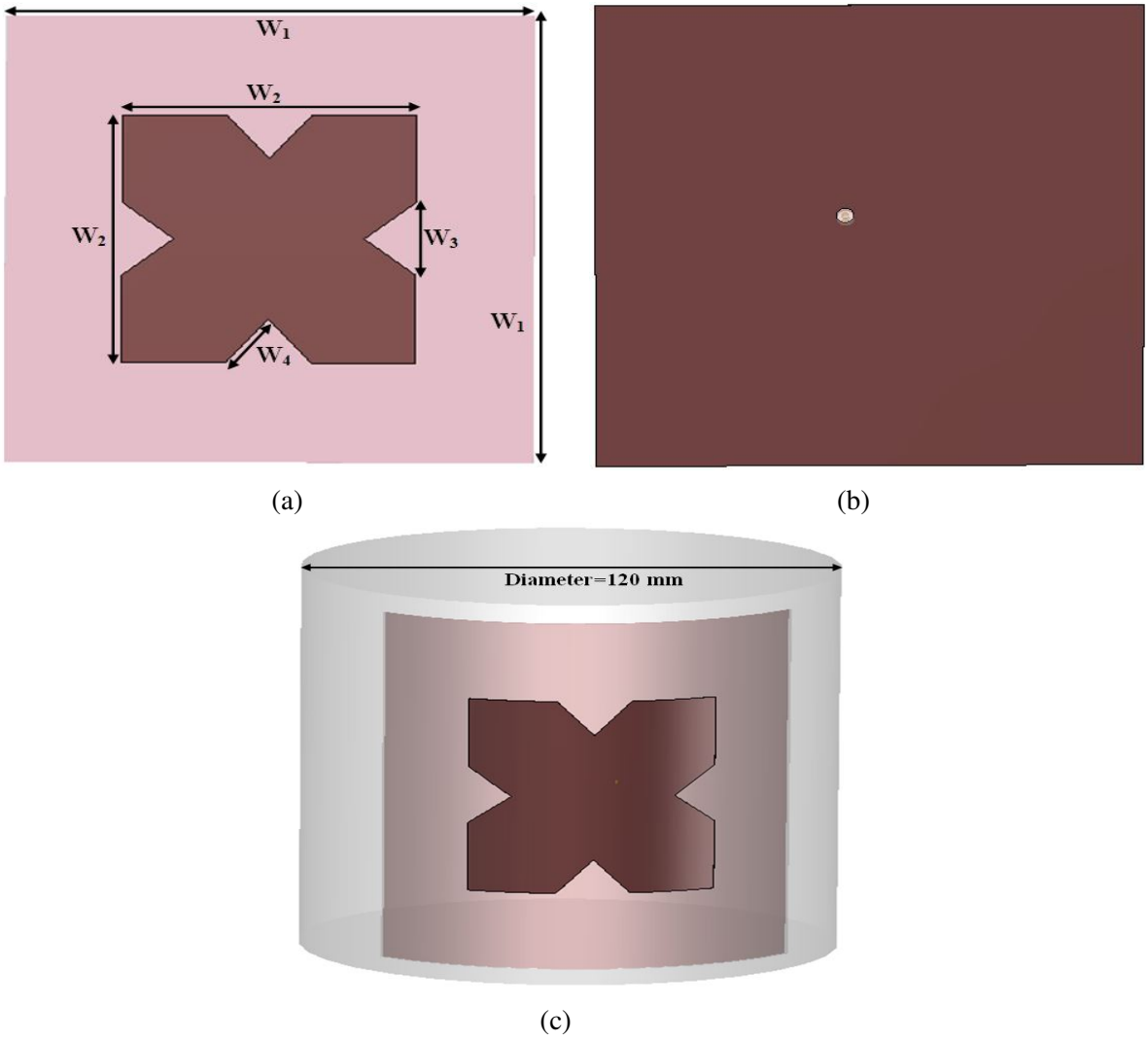

Figure 3.6 Simulated model (a) front view of Planar antenna. (b) bottom View of planar antenna (c) conformal antenna with a 60mm radius of curvature.

planar antenna with Koch fractal designed at 1.67 GHz is presented in this section. Flexible substrate like Rogers RT/duroid 5880 of permittivity(ε_r) 2.2 and thickness of 0.787 mm with coaxial probe feed is used to design the proposed antenna. The dimension of the substrate is 100×100×0.787 mm^3 and dimension of the patch is 55.5×55.5 mm^2. To obtain compact antenna, four sides of the square patch are replaced by Koch fractal curve with optimized indentation angle of 104^0. The planar antenna is transformed to cylindrical conformal antenna with a 60 mm radius of curvature.

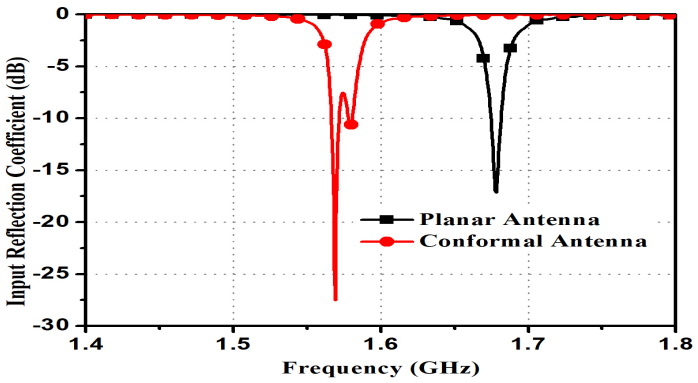

Figure 3.7 Return loss of conformal and planar antenna.

3.3.2 Simulation results

The simulated return loss for the planar antenna as well as a cylindrical conformal antenna with a 60 mm radius of curvature achieves 10 dB impedance bandwidth of 20 MHz (1.56-1.58 GHz), indicating a good impedance matching condition as illustrated in Figure 3.7.

The resonant frequency of the planar antenna is 1.67 GHz whereas, for the proposed cylindrical conformal antenna is 1.575 GHz. The resonant frequency of the cylindrical conformal antenna is decreased as the effective resonant length is increased due to bending of the planar microstrip antenna structure.

The radiation pattern of the conformal antenna with 60 mm radius at 1.575 GHz is represented in Figure 3.8. Since the entire surface of cylindrical conformal antenna is not parallel to the principal axes which causes change in radiation pattern. Therefore, the conformal antenna radiates energy around the cylindrical surface.

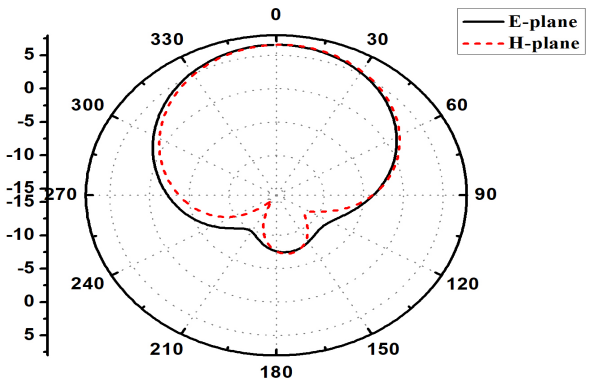

Figure 3.8 Radiation pattern of conformal antenna.

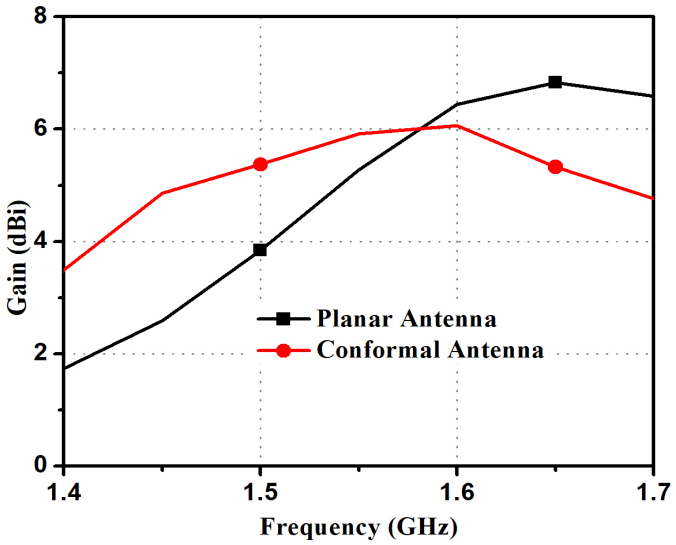

Figure 3.9 Gain of simulated antenna.

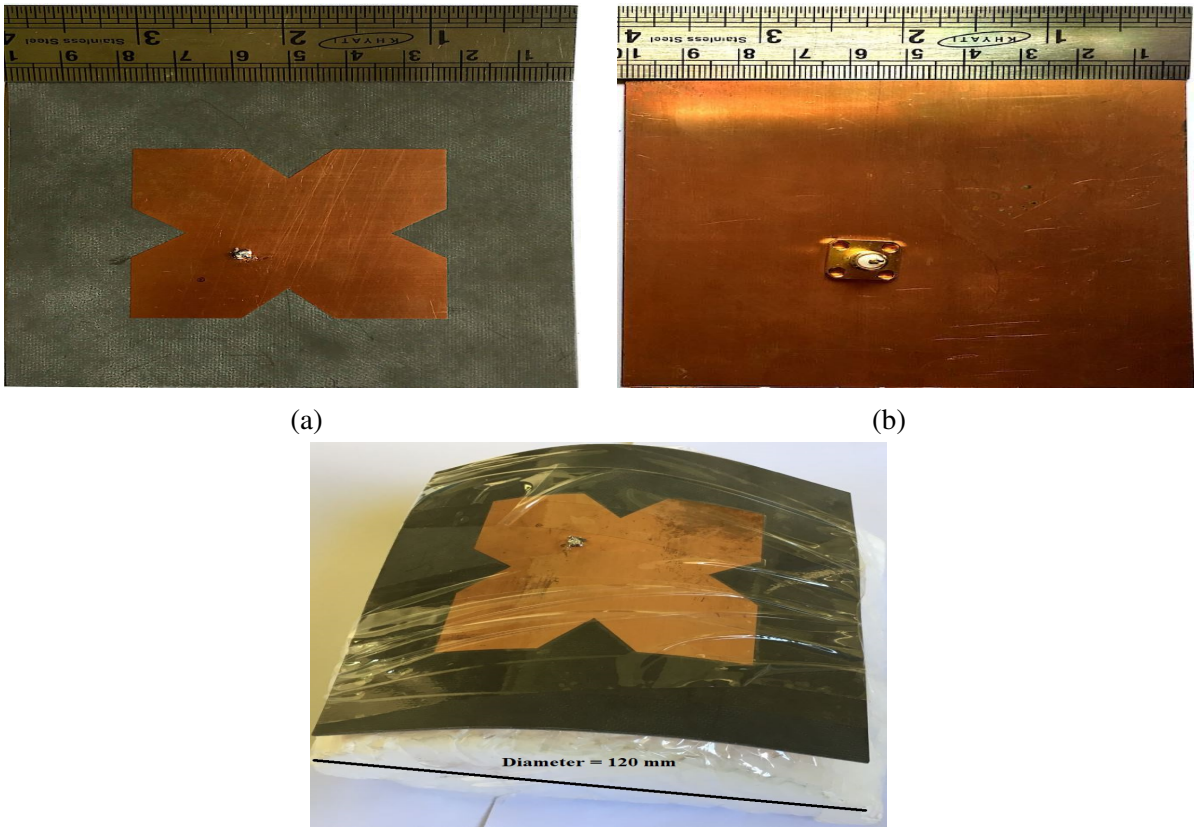

(a) (b)

(c)

Figure 3.10 Photographs of fabricated antenna (a) top view of planar antenna (b) bottom view of planar antenna (c) top view of proposed conformal antenna with 60 mm radius of curvature.

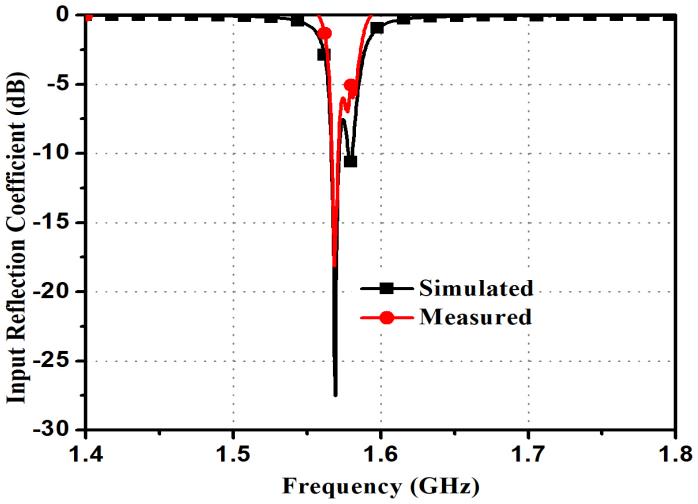

Figure 3.11 The magnitude of the reflection coefficient of conformal antenna.

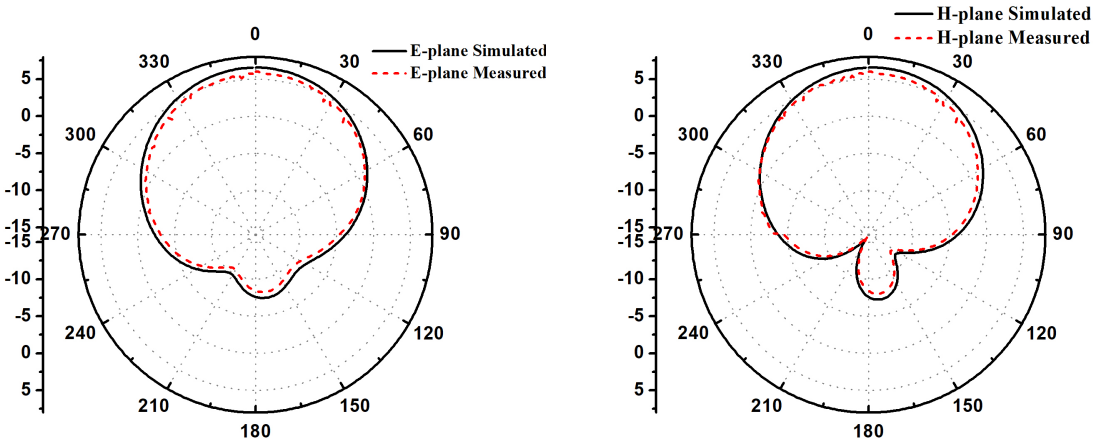

(a) (b)

Figure 3.12 The radiation patterns of conformal antenna (a) E-plane pattern at 1.5 GHz (b) H-plane pattern at 1.5 GHz.

3.3.3 Results and discussions

The Koch fractal based planar antenna is fabricated on RT/duroid 5880 substrate of size 100×100 mm^2 and it is rolled up to form a cylindrical shape on foam of radius of 60 mm as shown in Figure 3.10. By using an HP N5230A vector network analyzer, the magnitude of the reflection coefficient for cylindrical conformal antenna is measured . The comparison between simulated and measured results of the reflection coefficient of the proposed conformal antenna is represented in Figure 3.11. The -10 dB impedance bandwidth is obtained as 20 MHz, in the frequency range 1.56-1.58 GHz.

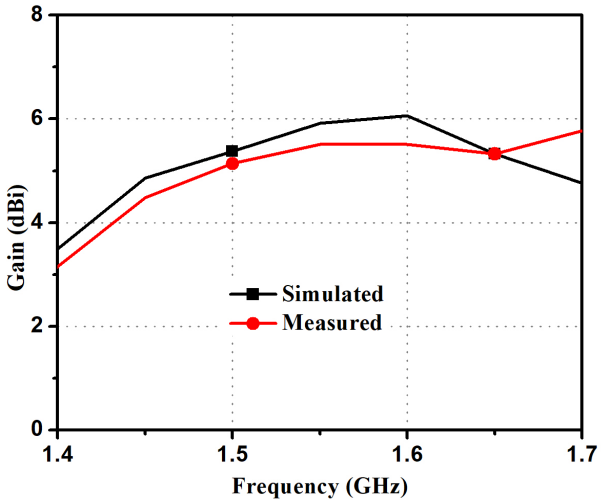

Figure 3.13 The gain plot of conformal antenna.

The two dimensional radiation patterns for cylindrical conformal antenna at 1.575 GHz frequency is performed in an anechoic chamber. The comparison between simulated and measured E-plane and H-plane radiation patterns are illustrated in Figure 3.12. The proposed cylindrical conformal antenna has a measured peak gain of 5.9 dBi at centre frequency of 1.575 GHz as shown in Figure 3.13.

The simulated peak gain of the conformal antenna and the planar antenna are compared as shown in Figure 3.9. The curvature of the cylindrical antennas causes variation in gain also.

3.4 Design of Minkowski fractal conformal antenna

3.4.1 Antenna design

A square patch antenna fed by an inset microstrip line feed is considered, as shown in Figure 3.14. The microstrip line feed is fed at the edge, whereas the inset feed is fed away from the edge to reduce the impedance. The impedance at the edge is large as current is zero, feed impedance matching can be established by properly selecting the width and depth of inset feed. A square patch antenna is designed for GPS frequency and dimensions are slightly optimized to achieve a better performance. A self-symmetrical structure is used to maximize the electrical length and for reducing the size of antenna.

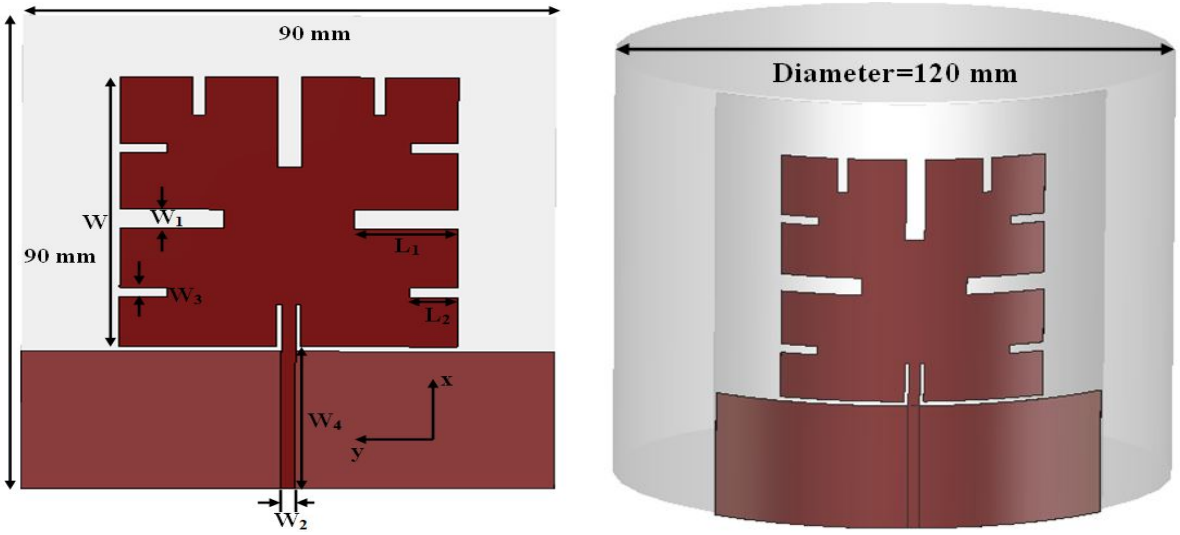

(a) (b)

Figure 3.14 The top views of (a) planar antenna (b) conformal antenna with 60 mm radius of curvature.

The Minkoski fractal structure is modified in two stages as shown in Figure 3.15 and 3.16 respectively. The optimized indentation factor of 1^{st} and 2^{nd} stages are 0.2 and 0.25 respectively. In order to achieve wide operating bandwidth and omnidirectional coverage, partial ground concept is selected. The dimensions of the proposed antenna are as follows: W=57 mm, L_1=20 mm, W_1=4 mm, L_2=39 mm, W_2=2.4 mm, L_3=8 mm, W_3=2 mm, W_4=30 mm. The size of partial ground is 29 mm×90 mm.The substrate size is selected as 90 mm×100 mm. The microstrip line is designed for 50 Ω. The cylindrical conformal antenna of 60 mm radius curvature is obtained by the transformation of the planar antenna.

3.4.2 Simulation results

The substrate is chosen to be Rogers RT/duroid 5880, which has soft property and can be easily bend to make into conformal. The electrical parameters of the material of relative permittivity (ε_r) of 2.2, dielectric loss tangent (tan δ) of 0.0009 and a substrate thickness of 'h' as 0.787 mm are selected. The proposed conformal, as well as a planar antenna are designed and simulated using CST studio suite-2016. Minkowski fractal first and second iterations are simulated for both planar and conformal with 60 mm radius surfaces. Although back radiation occurs due to truncation of ground, bandwidth is increased because of suppression of surface wave propagation.

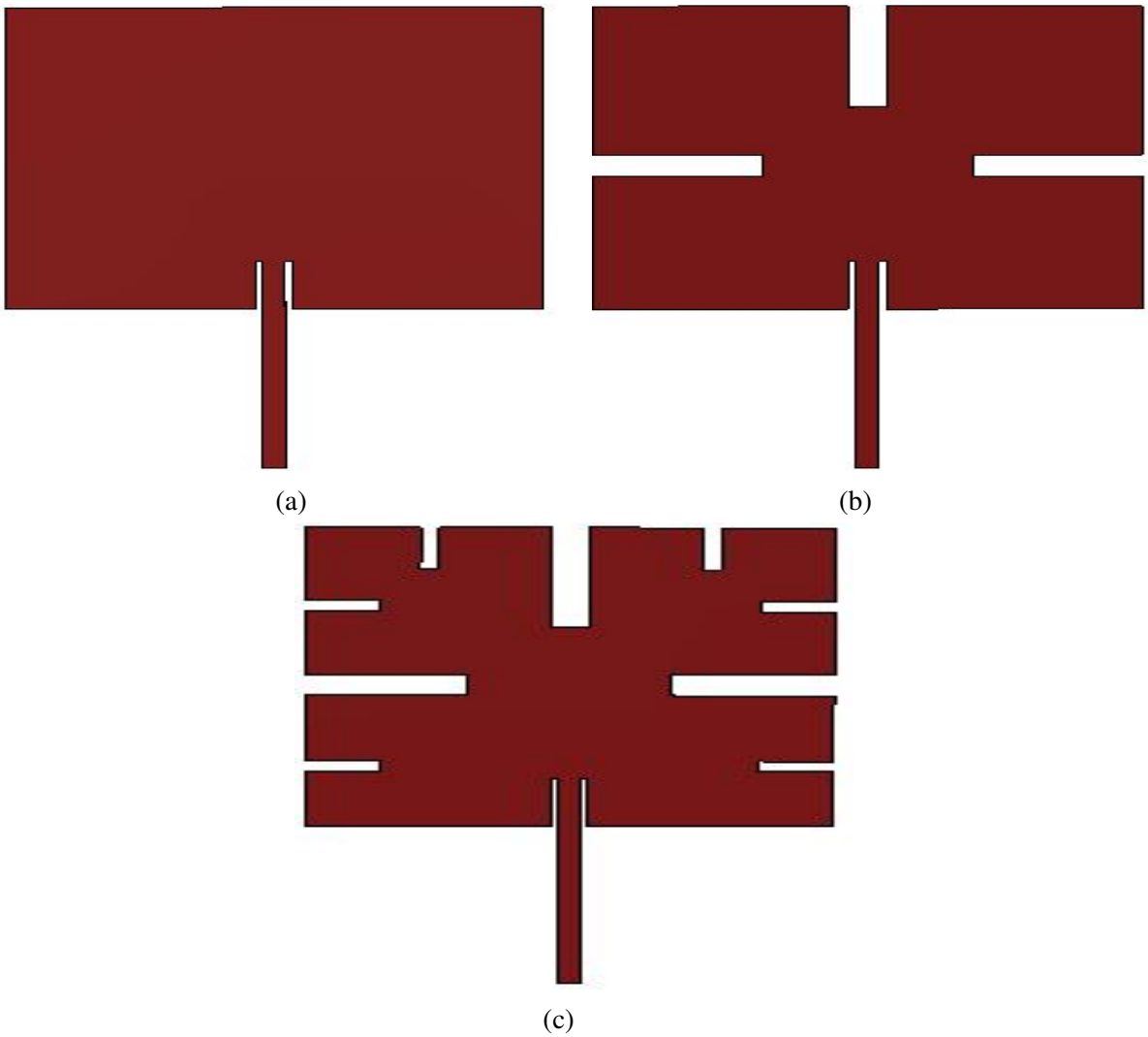

Figure 3.15 The Scheme of Minkowski fractal iteration of planar structure (a) Initiator(0^{th} iteration) (b) 1^{st} iteration (c) 2^{nd} iteration.

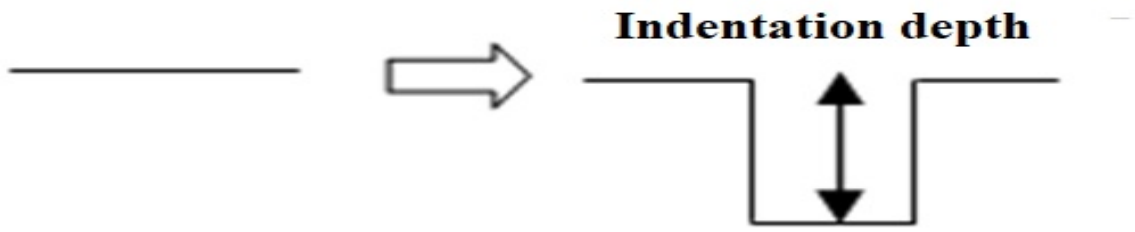

Figure 3.16 Minkowski fractal generator.

The magnitude of the reflection coefficient of simulated antenna for second iteration is compared in Figure 3.17. The operating frequency range of 0^{th} iteration, 1^{st} iteration and 2^{nd} iteration of Minkowski fractal planar antenna are 1.35-1.70 GHz,1.17-1.68 GHz, and 1.15-1.66 GHz respectively. The results demonstrate that by modifying the design of minkoskwi fractal,

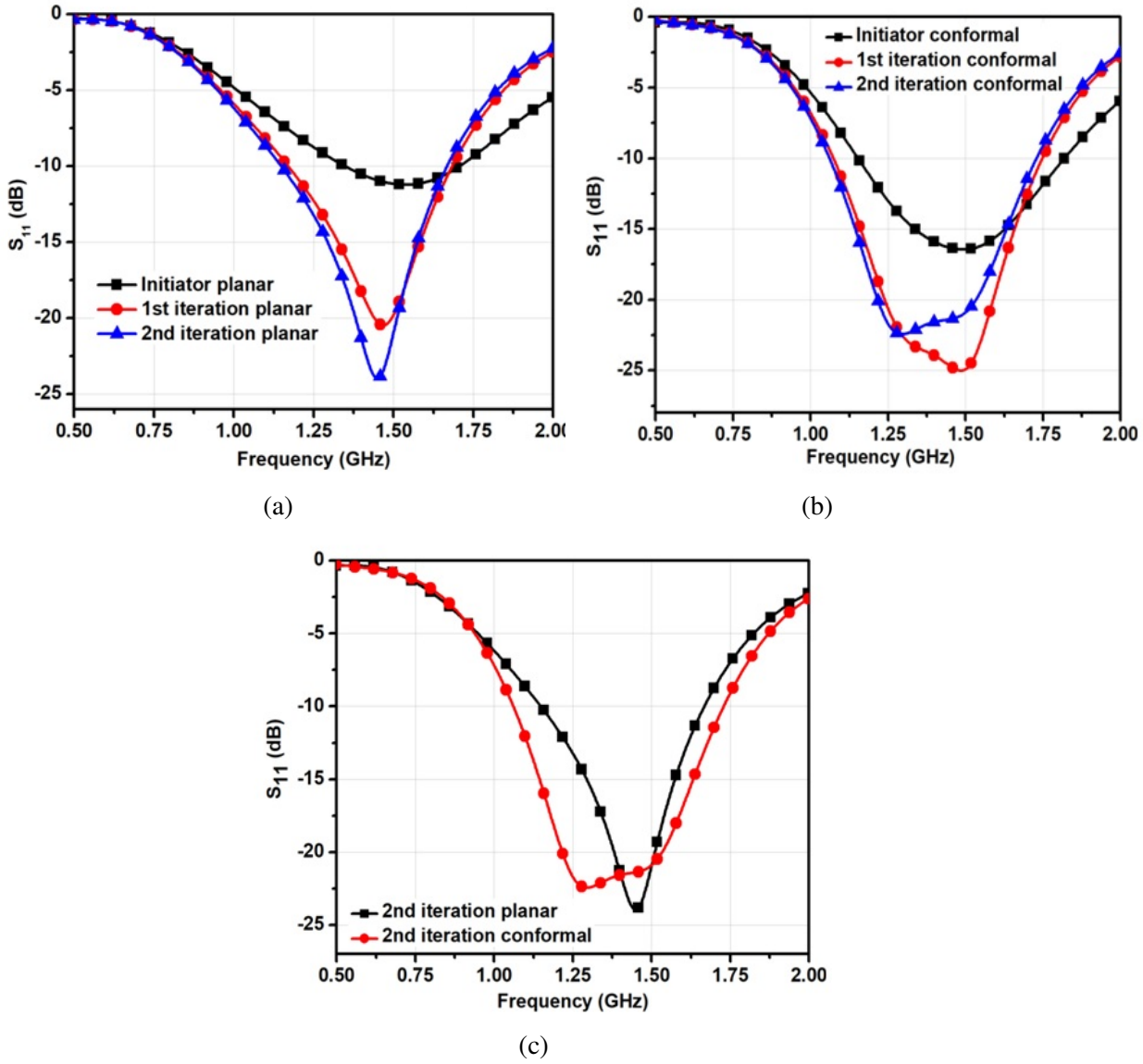

Figure 3.17 The simulated magnitude of the reflection coefficient.

the effective electrical length for current distributions is also increasing for which the operating frequency is shifted from right to left.

From the magnitude of the simulated reflection coefficient plot of conformal antenna, the operating frequency range of 0^{th} stage, 1^{st} stage and 2^{nd} stage of Minkowski fractal conformal antenna are 1.15-1.8 GHz, 1.09-1.7 GHz, and 1.07-1.68 GHz respectively. That means by increasing the number of iterations, the effective electrical length for current distributions is also increased for which the operating frequency is shifted from right to left as in planar structure. Also the magnitude of the reflection coefficient between planar and conformal antenna are compared in Figure 3.17. The increase in the effective resonant length due to bending structure of the antenna, resulted in shift of operating frequency.

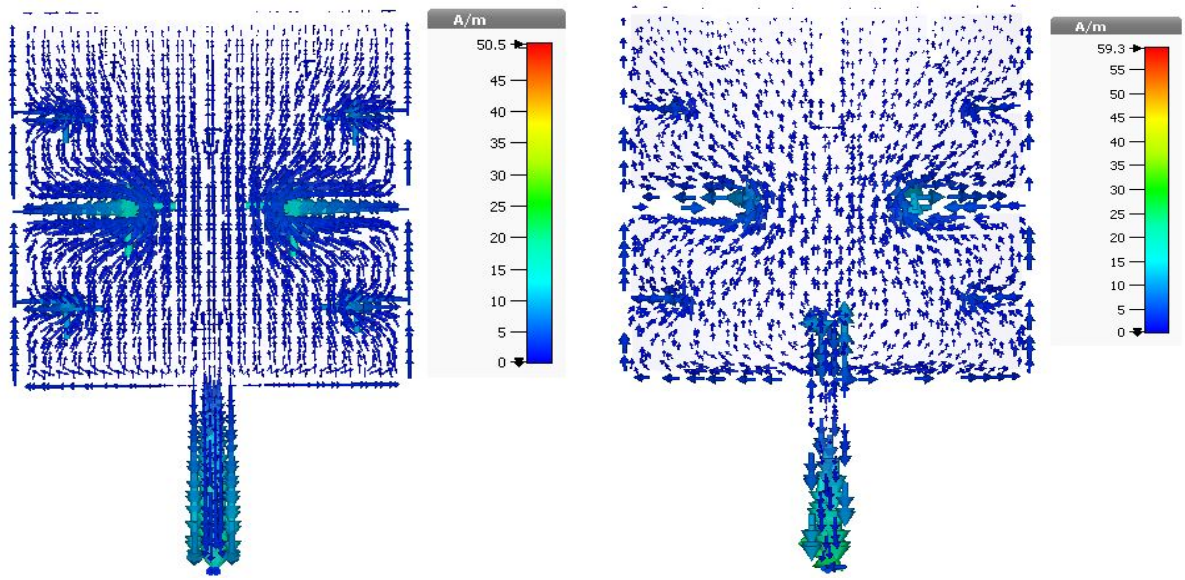

(a) (b)

Figure 3.18 The simulated field distribution at 1.575GHz (a) 2^{nd} iteration of planar antenna (b) 2^{nd} iteration of conformal antenna with 60mm radius.

To observe the radiated field distributions, the simulated field patterns for 2^{nd} iteration planar as well as conformal antennas are shown in Figure 3.18. The fields are dense near two sides of fractal slots. Also, the field distributions of conformal antenna is less dense as compared with planar structure.

3.4.3 Results and discussions

To validate the proposed antenna, 2^{nd} stage Minkowski fractal planar antenna as well as cylindrical conformal with 60 mm radius are fabricated on RT/duroid 5880 substrate of volume 57×57×0.787 mm^3 and measurements are performed. The prototype fabricated antennas are shown in Figure 3.19. Foam material is used as a cylindrical base for cylindrical conformal antenna as it has no effect on antenna radiation. The magnitude of the reflection coefficient for both planar and corresponding cylindrical conformal antennas are measured using an HP N5230A vector network analyzer.The magnitude of the measured reflection coefficient of the proposed antennas is illustrated in Figure 3.20. The measured impedance bandwidth (-10 dB) from 1.09 to 1.7 GHz and agrees well with the simulated results with a fractional bandwidth of 43.72%.

The radiation patterns for both planar and cylindrical conformal at different frequencies are done in an anechoic chamber. Both the planar and conformal antenna have a partial ground

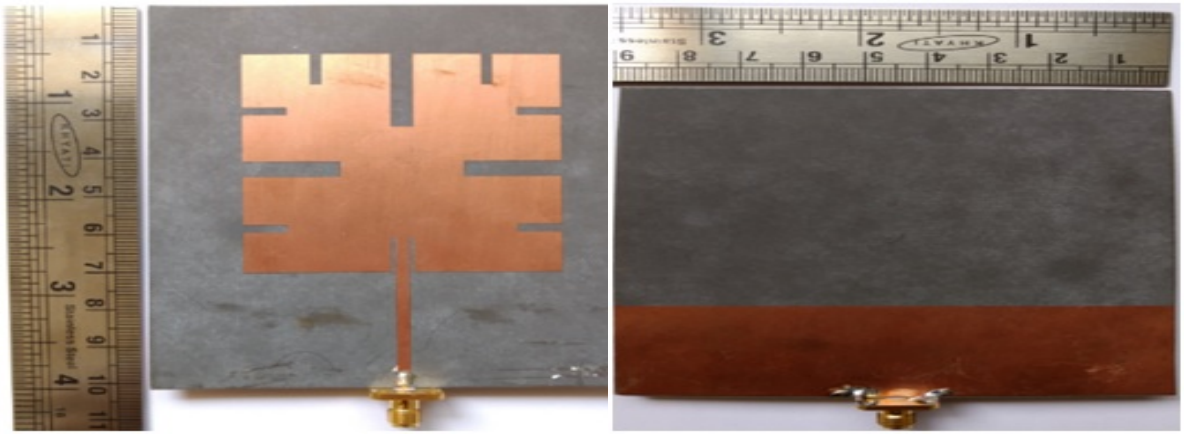

(a) (b)

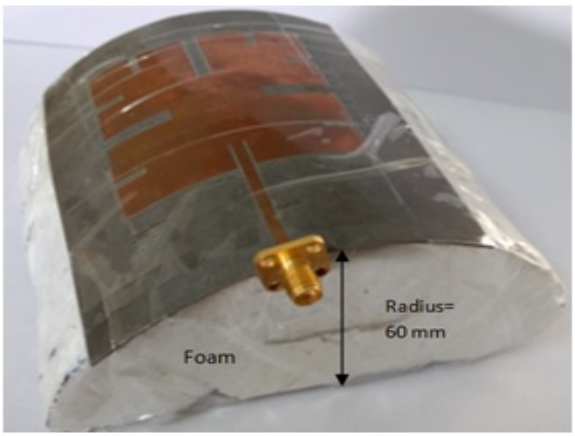

(c)

Figure 3.19 Photographs of fabricated antenna (a) top view of planar antenna (b) bottom view of planar antenna (c) top view of proposed conformal antenna with 60 mm radius of curvature.

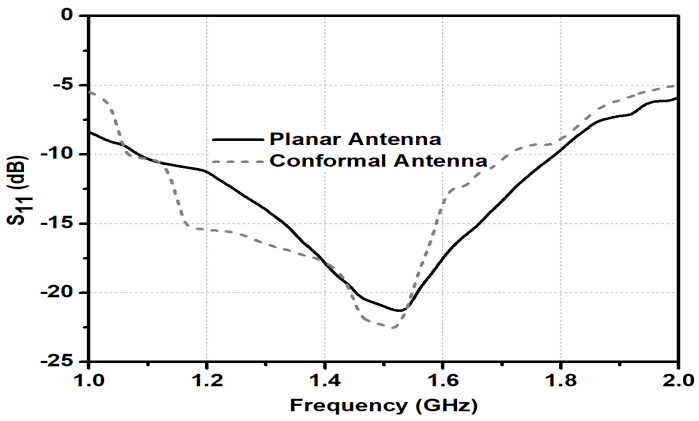

Figure 3.20 The measured magnitude of the reflection coefficient of planar and conformal antenna.

plane. The E-plane radiation pattern is plotted along xz plane and H-plane pattern is plotted along yz plane which is obtained as circle as illustrated in Figure 3.21. By the gain transfer

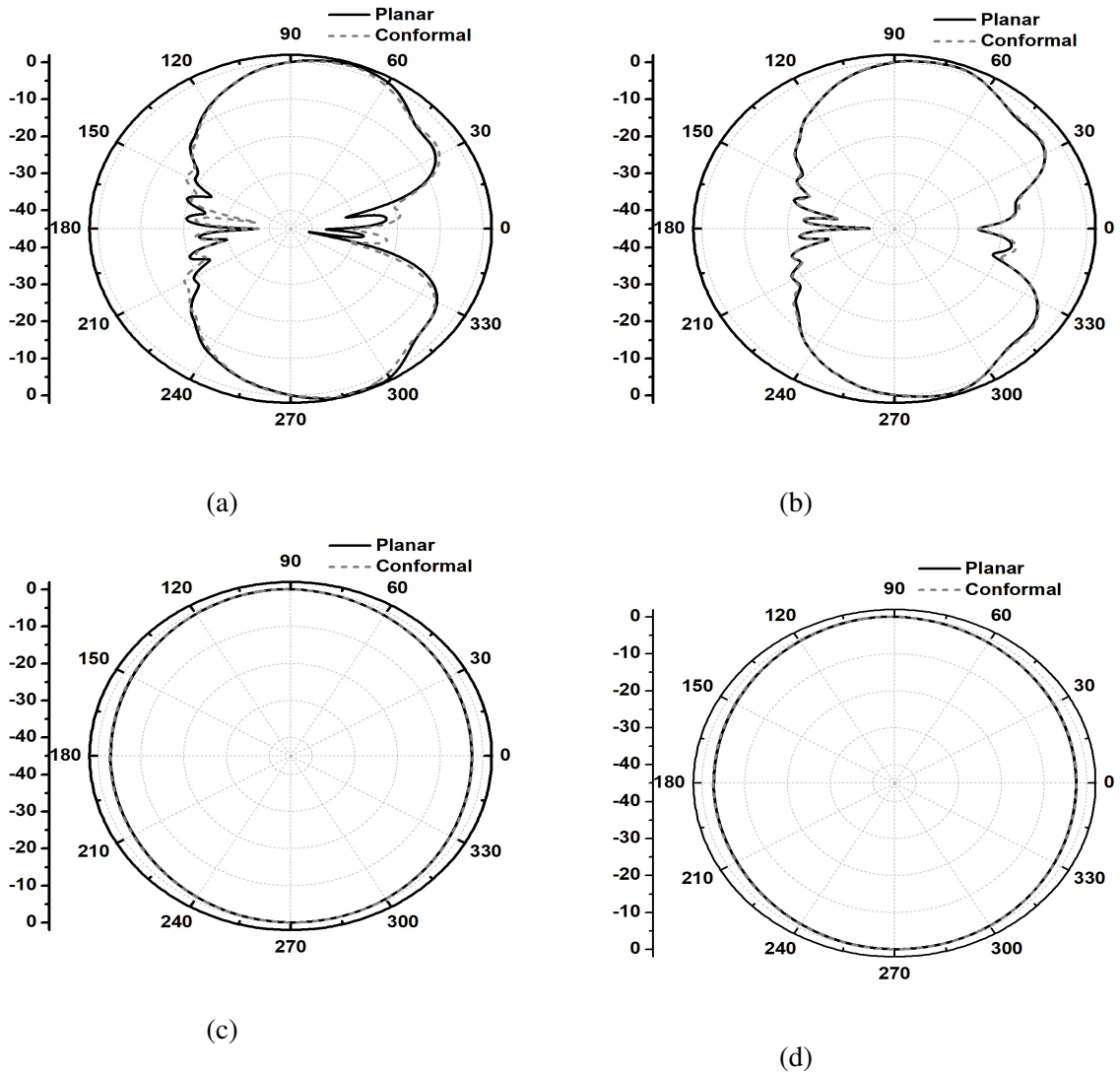

Figure 3.21 The measured radiation patterns of planar and conformal antenna (a) E-plane pattern at 1.5 GHz (b) E-plane pattern at 1.57 GHz (c) H-plane pattern at 1.5 GHz (d) H-plane pattern at 1.57 GHz.

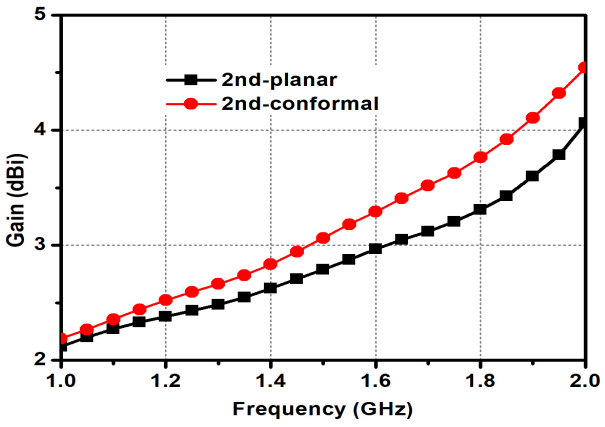

Figure 3.22 The measured gain plot of planar and conformal antenna.

Table 3.1 Comparison of the proposed cylindrical antenna with planar antenna existing in literature.

Antenna	**Perimeter (mm)**	**Frequency (GHz)**	**-10dB bandwidth**	**Gain (dBi)**
Proposed work	480	L_1,L_2, L_3,L_4,L_5 band	620 MHz (43.72 %)	3.5
[58]	314.15	1.575	2.1%	-11
[59]	395.84	1.575	20 MHz	6.5
[60]	240	L_1	20 MHz	4

method, the gain of the proposed antenna is measured. The peak gain ranges from 2.3 to 3.5 dBi in the operating frequency band (1.09 to 1.7 GHz) is shown in Figure 3.22. The proposed cylindrical conformal antenna is compared with existing planar antennas at GPS frequency as listed in Table 3.1.

3.5 Conclusion

This chapter presents the design of fractal based planar as well as a conformal antenna with a 60 mm radius of curvature. The designed cylindrical conformal antenna with Koch fractal is operating at 1.575 GHz with a bandwidth of 20 MHz.The proposed conformal antenna with Minkowski fractal is compared with the existing references of the planar antenna at GPS frequency. It offers a good wideband fractional bandwidth requirements at the standard GPS and Galileo frequency application which can be used for many applications.

Chapter 4

Conformal Wideband Antenna with Parasitic Elements and Metamaterial for WiMAX Application

4.1 Introduction

In wireless system, WiMAX (Worldwide Interoperability for Microwave Access) is a broadcast communications which is used for wireless data transfer over long distances in a variety of ways. It has potential application in military communications. But, the antenna mounting platform in wireless system is not planar in few cases. Hence, it is recommended to design the antenna conformal to the device to make it invisible to the human eye. The concept of conformal antennas are proposed to integrate the antenna into the outer metallic layers of aircrafts, high-speed trains or other vehicles, with the purpose of reducing the aerodynamic drag, small radar cross section, less fuel consumption and gas emissions [11]. So it is a challenging task to design a conformal antenna. J. Bregains et.al proposed a WiMAX conformal broad-beam antenna at 3.5 GHz with bandwidth up to 5.1% to get maximum gain up to 6.95 dBi [75].

Although in some communication system like mobile devices, base stations as well as radio broadcasting and aircraft communications, omnidirectional antennas are used, but such type of antennas are having low gain [76]. For long distance communication, there is a requirement of wideband directional high gain antenna.

For gain enhancement, different techniques are reported in the published literature. The use of parasitic elements in antenna for gain enhancement is a well-known technique. A gain enhancement of 4.4 dBi is achieved at 2.96 GHz by using a triangular shaped parasitic element which is reported in [39]. Design of a printed log-periodic dipole array antenna with gain enhancement of 2 dBi in the high frequency range of 21-40 GHz is attempted in [40]. Gain enhancement of antenna by using superstrate technique are presented in [41, 77]. However, use of superstrate increases the weight of antenna which is not suitable for conformal application due to difficulties in bending.

In the past few years, metamaterials are developed by researchers due to some uncommon electromagnetic (EM) properties which do not exist in nature. EM wave absorbers [78], invisible cloaking [79], improved emissions [80], EM tunneling [81] and clear imaging [82] are developed by arrangement of metamaterial unit cells. The zero or low index metamaterial (ZIM or LIM) are investigated for beam focusing and can be used for gain enhancement of the antenna over large frequency range.

The gain enhancement of printed antenna is also attempted utilizing zero index metamaterial as superstrate in [42],[83, 84, 85, 86, 87, 88, 89, 90]. However, use of zero index metamaterial as superstrate makes the patch antenna systems heavy in weight. So superstrate type of antenna is not suitable especially for conformal antenna due to difficulty in bending. Although a microstrip antenna with high gain and directivity using negative permeability metamaterial for dual frequency band like 5.2 and 6.75 GHz is proposed, but it has larger dimension of 50×54 mm^2 in [91]. A 3-D metamaterial structure is used to reduce mutual coupling of a two element patch antenna array operating in 2.35-2.45 GHz in [92]. A reduction of 18dB mutual coupling is achieved with a bandwidth of 100 MHz. A new method to reduce the mutual coupling of a microstrip patch antenna array operating at 5.3 GHz by using modified split ring resonator (MSRR) metamaterial structures is presented in [93]. The mutual coupling is reduced by 23 dB for the antenna size of 72×40 mm^2. B. Hazarika et al. proposed a multi-layered dual-band on-body conformal integrated antenna for WBAN communication with 9.8% bandwidth only in [94]. The conventional microstrip patch antenna has less bandwidth [2]. The low index metamaterial (LIM) layers can be used to enhance the gain of an antenna. But gain improvement in the entire operating frequency range still remains a challenge.

A planar vivaldi antenna with inhomogeneous planar zero index metamaterial for gain enhancement is reported in [95]. But, the size of the antenna is large with $140\times80\times0.5$ mm^3 dimensions. A bow-tie dipole array antenna with average gain of 4 dBi in between 5.98 to 10.12 GHz is designed in [96].

In this chapter, a cylindrical conformal wideband antenna consisting of three novel fork shaped dipole elements operating in between 3.1 and 3.88 GHz is proposed. The enhancement of the directive behavior of a conformal antenna using parasitic element and periodic metamaterial unit cells is established. For gain enhancement as well as narrow beamwidth, triangular shaped parasitic elements and low index metamaterial unit cells are integrated with antenna. The design and simulation of the proposed conformal antenna is performed using Ansys Electronics Desktop.

4.2 Metamaterial

Metamaterial (MTM) word has been taken from the Greek word meta, it means beyond material which is having homogeneous electromagnetic structures. So, metamaterial has unusual properties not available in nature [97]. The microwave metamaterials are fabricated on printed circuit boards with a metallic structure called unit cell MTM and repeating them in all directions. Such unit cell MTMs are mainly designed with printed resonator or non-resonator metallic structures. Two types of metamaterial structures exist in microwave regime, namely periodic and non-periodic MTM structure. Periodic and non-periodic unit cell MTM structures are considered as equivalent to homogeneous and inhomogeneous medium, respectively. The unit cell MTM is designed by calculating sub-wavelength values at the operating frequency band. So, it can be described using the effective medium theory. An effective homogeneous structure average cell size *'p'* should be much smaller than the guided wavelength 'λ_g'. But the exact cell size is determined based on effective homogeneity limit or effective-homogeneity condition which corresponds to a rule of thumb effectiveness condition. So, microwave engineers often use, $p=\lambda_g/4$, lumped components ($p<\lambda_g/4$) and quasi-lumped components ($\lambda_g/4<p<\lambda_g/2$) and distributed components ($p>\lambda_g/2$) [98]. In case of lumped components, the phase variation of the signal from the input to the output of the component is negligible and the component may be considered as a localized or small size element. In case of distributed component, phase variation along the component cannot be ignored, because the component must be considered as a transmission line section. Thus, MTM has a distributed structure which constitutes lumped elements.

If the condition of effective-homogeneity is satisfied, the structure behaves as a real material with unusual characteristics that can manipulate electromagnetic waves which depend on the nature of the unit cell. The constitutive parameters are the permittivity (ε) and the permeability (μ), which are related to the refractive index n by

$$n = \sqrt{\varepsilon_r \mu_r} \tag{4.1}$$

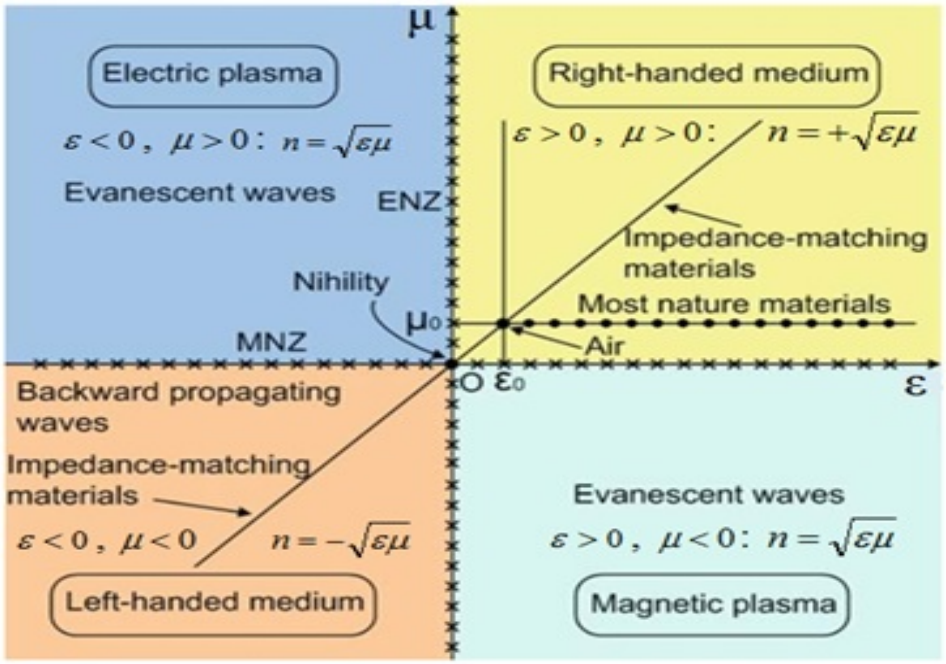

Figure 4.1 All possible properties of isotropic materials in the ε-μ domain.

where ε_r and μ_r are the relative permittivity and permeability. Four possible signs and properties of isotropic materials in the ε –μ diagram are illustrated in Figure 4.1. In the first quadrant ($\varepsilon > 0$ and $\mu > 0$) represents right-handed materials (RHM), which support the forward propagating waves. From the Maxwell's equations, the electric field E, the magnetic field H, and the wave vector k form a right-handed system. The second quadrant ($\varepsilon < 0$ and $\mu > 0$) denotes electric plasma, which support evanescent waves. The third quadrant ($\varepsilon < 0$ and $\mu < 0$) is the well-known left-handed materials (LHM), which is supporting a backward propagating wave. In LHM, the electric field E, the magnetic field H, and the wave vector k form a left-handed system. The fourth quadrant ($\varepsilon > 0$ and $\mu < 0$) represents magnetic plasma, which supports evanescent waves. In electromagnetics, an evanescent field, or evanescent wave, is an oscillating electric and/or magnetic field that does not propagate as an electromagnetic wave, but whose energy is spatially concentrated in the vicinity of the source (oscillating charges and currents). Due to the precise shape, geometry, size, orientation and arrangement of MTM, their smart properties can change characteristics of electromagnetic waves: by blocking, absorbing, enhancing, or bending waves, to achieve benefits that go beyond the ordinary or conventional materials. By using these properties, an antenna can be designed with different characteristic to suit specific requirements. The selection of MTM properties is also a necessary part to improve the performance of the antenna. MTM antenna can be designed using left handed (LH)

and right handed (RH) materials. The phase velocity (v_p), propagation constant (β) and group velocity (v_g) are less than zero for LH material and are greater than zero for RH material. LH material can only provide backward wave radiation. So, RH material is useful for directivity enhancement of the antenna. Fast-wave i.e. $v_p > c$ (speed of light in air) is supporting leaky-wave antenna structure. In case of $v_p < c$, there will be no radiation in the leaky wave antenna and this condition is suitable for end fire radiation in air i.e. surface wave antenna. In case of surface wave antenna, the directivity can be enhanced by using zero index metamaterial (ZIM) principle. Ideally, the refractive index (n) of ZIM is considered as zero and phase velocity become infinity which is impossible in real life. Hence, materials with near zero or low index metamaterial (LIM) are consdered like a lens with beam focusing property. These type of metamaterials belong to LH material in first quadrant of the $\varepsilon - \mu$ diagram. In order to design high gain antenna, it is necessary to focus the radiated beam in the direction of radiation.

4.3 Design and characteristics of low index metamaterial

Double 'S' shaped metamaterial unit cell is proposed in this work. The proposed unit cell gives a longer current path as compared to parallel-line and S-shaped structures. The proposed metamaterial unit cell is designed and placed side by side on substrate like RT/duroid 5880 of thickness 0.787 mm as shown in Figure 4.2(a). The dimensions of the metamaterial unit cell

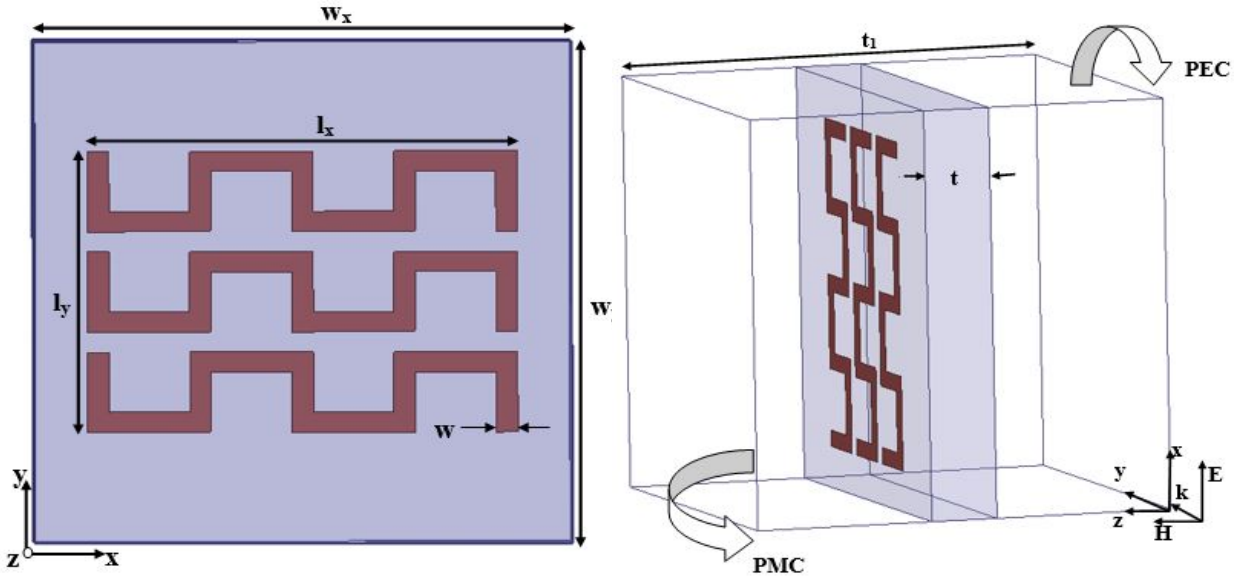

(a) (b)

Figure 4.2 (a) The configuration of the proposed metamaterial unit cell (b) The simulated model under waveguide medium. The size of parameters are W_x=W_y=5 mm, l_y=2.8 mm, l_x=4 mm, t=0.787 mm, w=0.2 mm and t_1=5 mm.

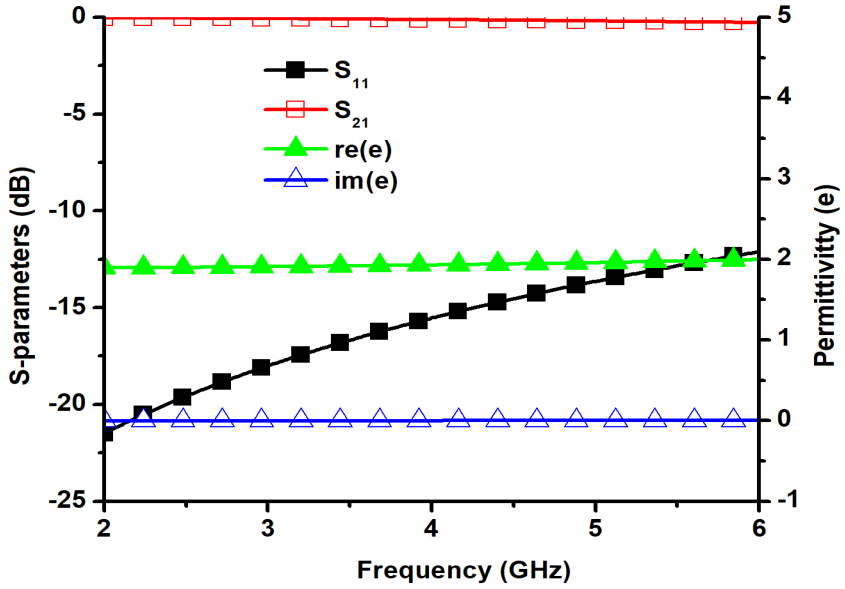

Figure 4.3 Characteristics of the proposed metamaterial unit cell.

are 'l_x' and 'l_y' along x direction and y direction respectively. The simulation is performed with perfect electric conductor (PEC) and perfect magnetic conductor (PMC) boundary condition so that electric field is directed along x- direction and wave propagates along y- direction as demonstrated in Figure 4.2(b). The metamaterial unit cell is simulated using ANSYS Electronics Desktop. The unit cell is characterized by using effective medium theory. The simulated scattering parameters and permittivity are shown in Figure 4.3 and effective refractive index can be retrieved using the technique reported in [99, 100].The effective parameters of the proposed metamaterial unit cell such as refractive index (n), wave impedance (Z), permittivity (ε_x) and permeability (μ_z) are calculated from the [99]

$$\text{Refractive Index}(n) = \frac{1}{kd} cos^{-1}\left(\frac{1 - {S_{11}}^2 + {S_{21}}^2}{2S_{21}}\right) \tag{4.2}$$

$$\text{Normalized Impedance}(Z) = \sqrt{\left(\frac{(1 + S_{11})^2 + {S_{21}}^2}{(1 - S_{11})^2 + {S_{21}}^2}\right)} \tag{4.3}$$

$$\text{Permittivity}(\varepsilon_x) = n/Z \tag{4.4}$$

$$\text{Permeability}(\mu_z) = n \times Z \tag{4.5}$$

Where d is the thickness and k is the wave-number of the incident wave.

According to [101], metamaterials are defined as artificial effectively homogeneous electromagnetic structures with unusual properties not readily available in nature. An effectively homogenous structure is a structure whose average cell size is much smaller than guided wave length. The parameter of the material like permittivity and permeability depend on the unit cell structure and its periodic arrangement. The parameters can take positive and negative signs which lie in the four quadrants of the μ - ε diagram. If both the parameters are positive, they lie in the first quadrant and propagation takes place through the material. The metamaterial considered in the proposed work falls in the first quadrant, where the parameters are different from the substrate value. It can be referred that the refractive index is about 1.4 over a frequency range 2-6 GHz which is low as compared with refractive refractive index of antenna which is 1.48 as given in Figure 4.4. So these type of metamaterials can be considered as low index metamaterial (LIM). By changing the l_x and l_y parameters, the refractive index is tuned to 1.4 for the entire frequency range of operations. Thus, LIM are efficient to focus wave into a narrow beam. LIM need to be placed along the direction of radiated field. The effective parameters of unit cell and antenna are listed in Table 4.1.

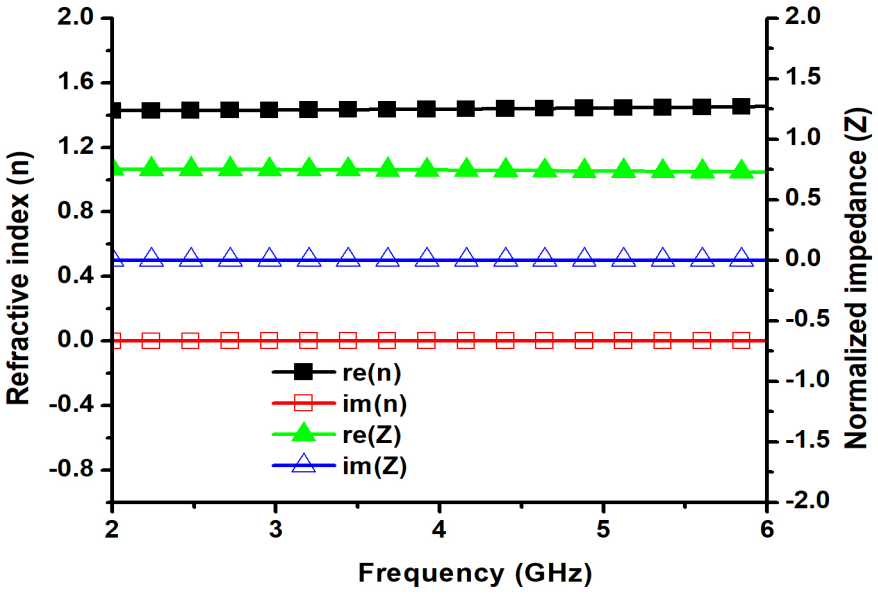

Figure 4.4 The effective parameters of the metamaterial unit cell.

Table 4.1 Comparison of effective parameters of antenna and MTM unit cell.

Parameters	**Antenna**	**MTM unit cell**
Refractive index (n)	1.48	1.4
Permittivity (ε)	2.2	1.89
Permeability (μ)	1	1

Table 4.2 Optimized value of parameters.

Parameters	**Size (mm)**	**Parameters**	**Size (mm)**
L	50	R_2	4.5
W	45	r_2	2.95
a	6.5	R_3	3.5
b	11.35	r_3	2
c	10.13	W_1	2.3
R_1	5.7	W_2	2.7
r_1	4	L_g	14

4.4 Antenna design and parametric study

4.4.1 Design of directional conformal antenna with fork shaped dipoles

The basic antenna designed for WiMAX application consists of three dipole elements. Each dipole element is designed with semi-annular ring structure along with a rectangular strip which results in fork shaped structure. The antenna is designed to concentrate the current along the circumference of the semi-annular ring. Single fork shaped structure element has omnidirectional radiation. For directional radiation, an antenna with three dipole elements is proposed. A 50 Ω microstrip line is used to feed the antenna. A transition from the microstrip line to a parallel strip line is done for ease of measurement and feeding. Three fork shaped elements with different dimensions are connected to the parallel strip line as shown in Figure 4.5(a).The outer radii of three elements are R_1, R_2, and R_3 whereas inner radii are r_1, r_2 and r_3. The radii of three elements R_1, R_2, and R_3 are related as $R_1/R_2=R_2/R_3=R$. By tuning parameters R, L_g, and W_2, a better return loss can be obtained. The design of the dipole element is varied as log periodic structure [102]. Therefore, based on the concept of log-periodic antenna, the proposed antenna is comprising of three fork shaped dipole elements instead of wire dipole for bandwidth enhancement. The optimized dimensions are given in Table 4.2.

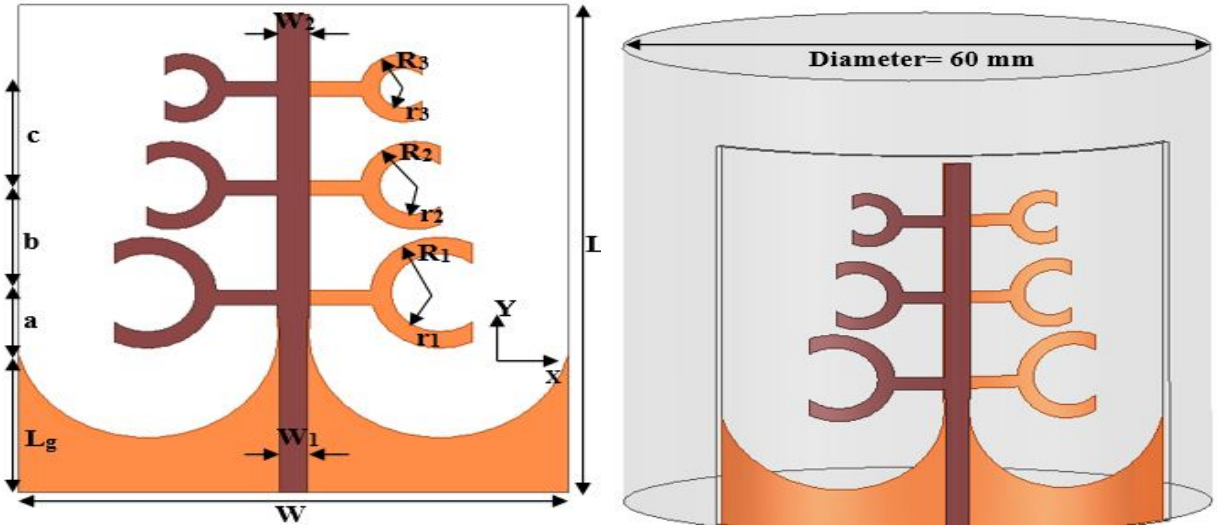

(a) (b)

Figure 4.5 Geometry of basic antenna (a) planar antenna (b) cylindrical conformal antenna.

Wide bandwidth with endfire radiation is achieved with three fork-shaped elements as patch on one side and three similar fork-shaped elements as ground plane on opposite side of the substrate. The transition between feed line and parallel strip line is attempted by tapering the ground plane like half circles to the width of the parallel strip line. The ground plane can also be considered as a reflector to deliver directional radiation patterns. The planar basic antenna is transformed to the conformal antenna on a cylinder of radius 30 mm, which is depicted in Figure 4.5(b). The overall size of the antenna is printed on a substrate of 45×50 mm^2.

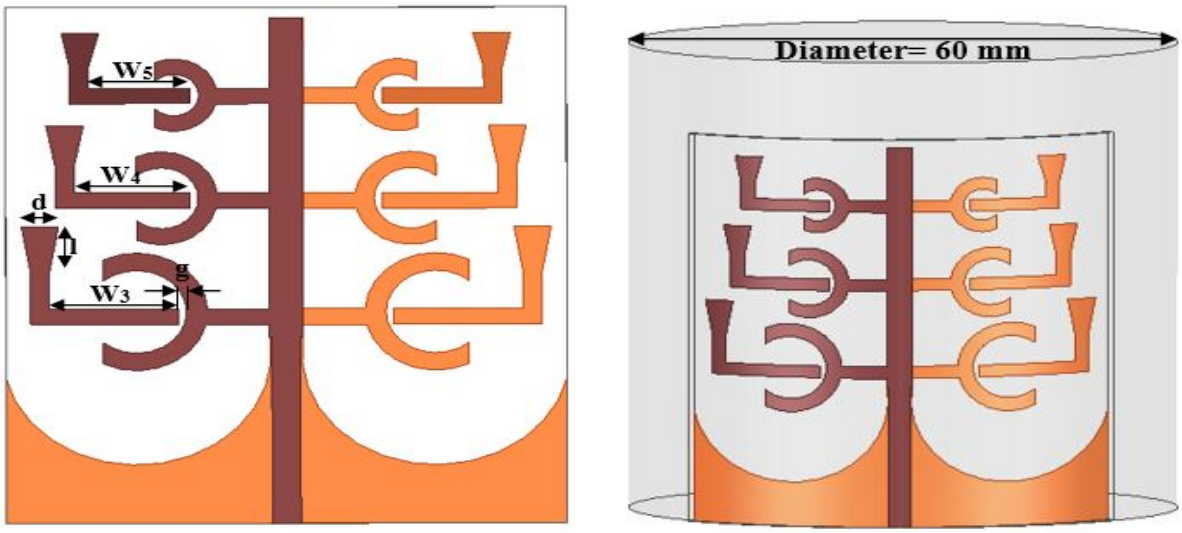

(a) (b)

Figure 4.6 Geometry of basic antenna (a) planar antenna (b) cylindrical conformal antenna.

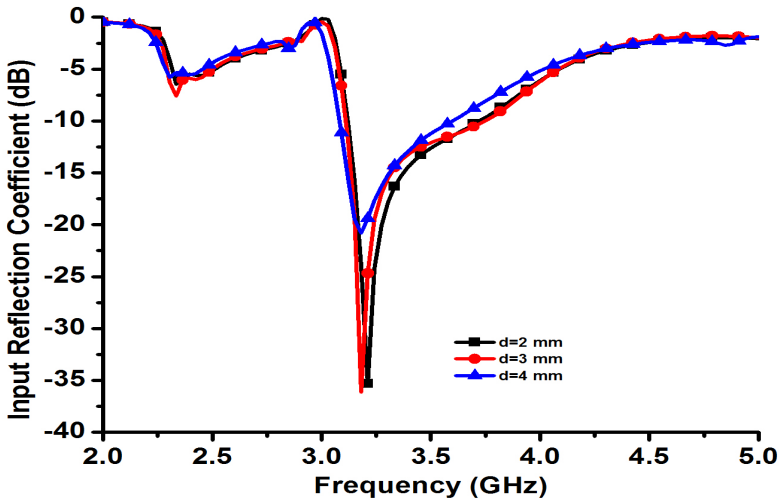

Figure 4.7 Simulated input reflection coefficient of the conformal antenna loaded with triangular shaped parasitic elements with the variations of parameter d.

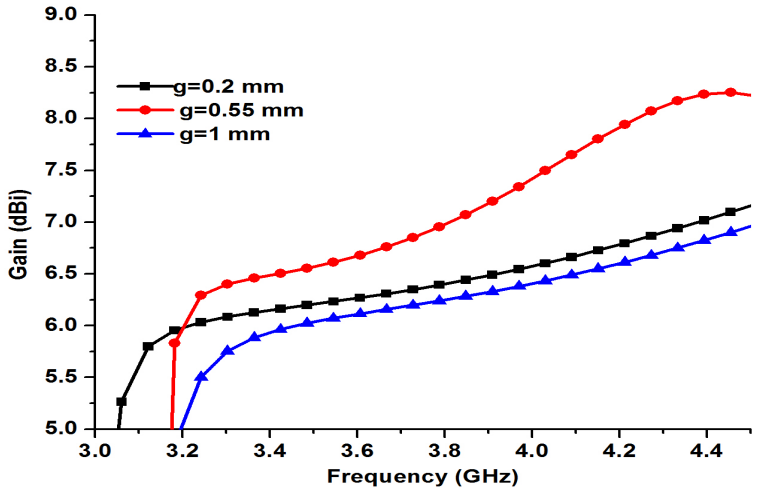

Figure 4.8 Simulated gain with variations of the parameter 'g' of the antenna loaded with triangular shaped parasitic elements.

4.4.2 Design of conformal antenna loaded with triangular shaped parasitic elements

To enhance the conformal antenna's directional properties, three printed triangular shaped metallic parasitic elements are incorporated on both sides of substrate in the unfilled space of fork shaped element as shown in Figure 4.6. The effect of the width of parasitic element 'd' on input reflection coefficients is illustrated in Figure 4.7. As a result the optimized value of'd' is obtained as 3 mm. The empty space 'g' between fork and triangular shaped element plays a sig-

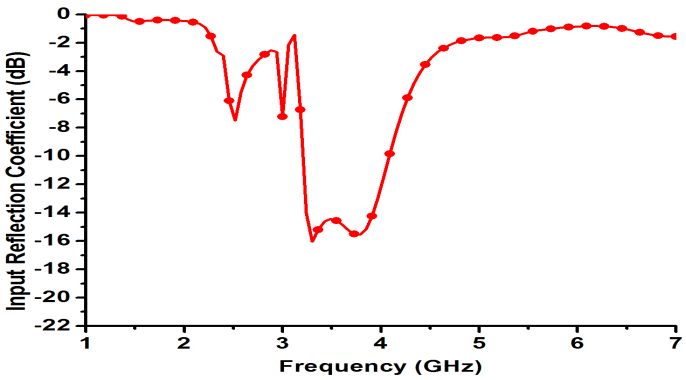

Figure 4.9 Simulated input reflection coefficient of the proposed conformal antenna loaded with triangular shaped parasitic elements.

nificant role for directional radiation. To investigate the coupling effect of parasitic elements, the distance between parasitic element and fork shaped element is varied, while maintaining other dimensions as constant. The results are represented in Figure 4.8 and the optimum value of 'g' is selected as 0.55 mm for the triangular shaped parasitic element. The parasitic elements have vertical lengths of l= 3.5 mm with different horizontal lengths of W_3 = 10.4 mm, W_4 = 9.3 mm and W_5 = 8.15 mm for the first, second and third elements respectively. The addition of the triangular shaped element does not make the antenna loose its wideband operation and also the direction of its maximum radiation. The parasitic element can be further optimized to improve the directional properties of the proposed conformal antenna. The simulated input reflection coefficient of the proposed optimized conformal antenna is shown in Figure 4.9. The comparison

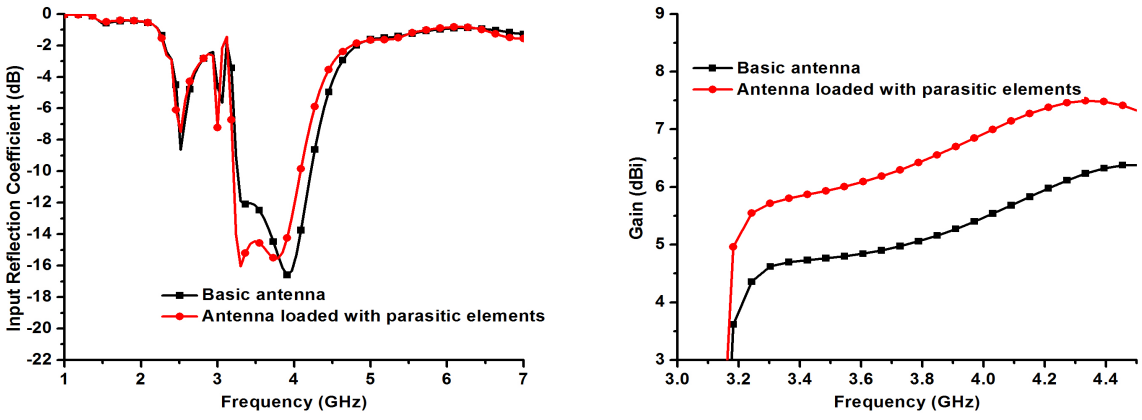

(a) (b)

Figure 4.10 Simulated results comparison of the conformal antenna (a) input reflection coefficient (b) gain.

of input reflection coefficients, gain of basic antenna and antenna loaded with triangular shaped parasitic elements are shown in Figure 4.10.

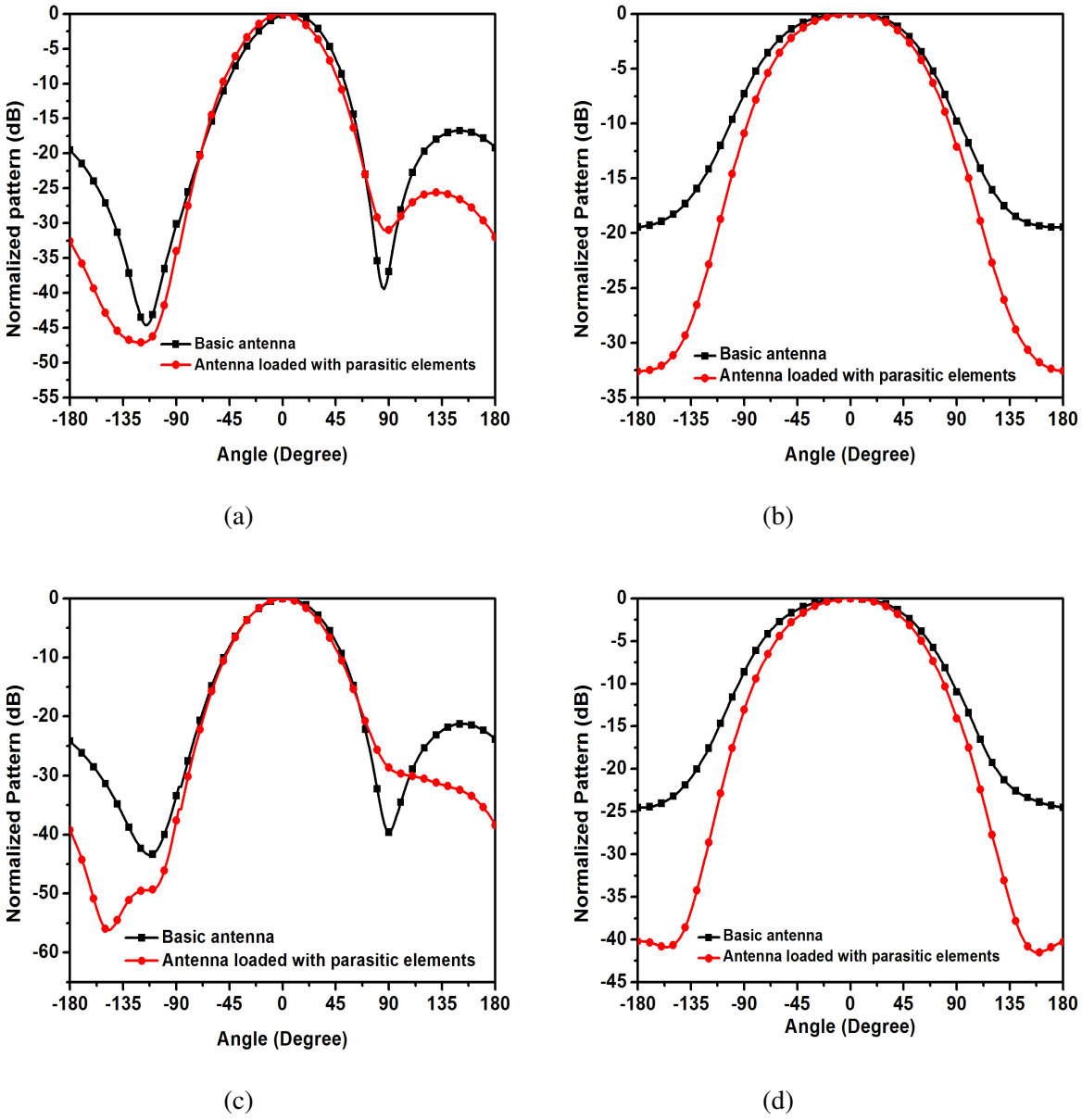

Figure 4.11 Simulated radiation pattern comparison of the conformal antenna (a) E-plane at 3.3 GHz (b) H-plane at 3.3 GHz (c) E-plane at 3.5 GHz (d) H-plane at 3.5 GHz.

The normalized radiation patterns of the basic and antenna loaded with triangular shaped parasitic elements at 3.3 GHz and 3.5 GHz are shown in Figure 4.11. The antenna loaded with parasitic elements demonstrated a decrease in beamwidth with respect to basic antenna, thus verifying the theory of directional radiation. The half power beamwidth (HPBW) of basic antenna in H-plane (yz plane) is around 123^0 which decreases to 108^0, while in E-plane (xy plane) it decreases from 57^0 to 55^0 at 3.3 GHz after loading with parasitic elements. Similarly

at 3.5 GHz, the HPBW of basic antenna is around 117^0 which diminishes to 100^0 in H-plane, though in E-plane it decreases from $58^0$to 54^0.

4.4.3 Design of proposed conformal antenna integrated with triangular shaped parasitic elements and low index metamaterial (LIM)

In the proposed antenna, metamaterials are used to enhance the gain of the antenna by placing them along the direction of radiation. For which the given substrate length is extended up to 15 mm in the triangular shaped parasitic element integrated conformal antenna. To investigate the impact of metamaterial unit cell, it is placed side by side in the both sides of extended substrate in an array of 3×6 numbers as shown in Figure 4.12. The unit cells are placed side by side in such a way that they are excited by the endfire radiation of the fork shaped array and triangular shaped parasitic elements. The optimized values of the parameters for the placement of an array of 3×6 metamaterial unit cells are L_m=10.4 mm, W_m=29 mm and m=3.5 mm. The proposed conformal antenna have impedance bandwidth near to 780 MHz (3.1-3.88 GHz) as shown in Figure 4.13.

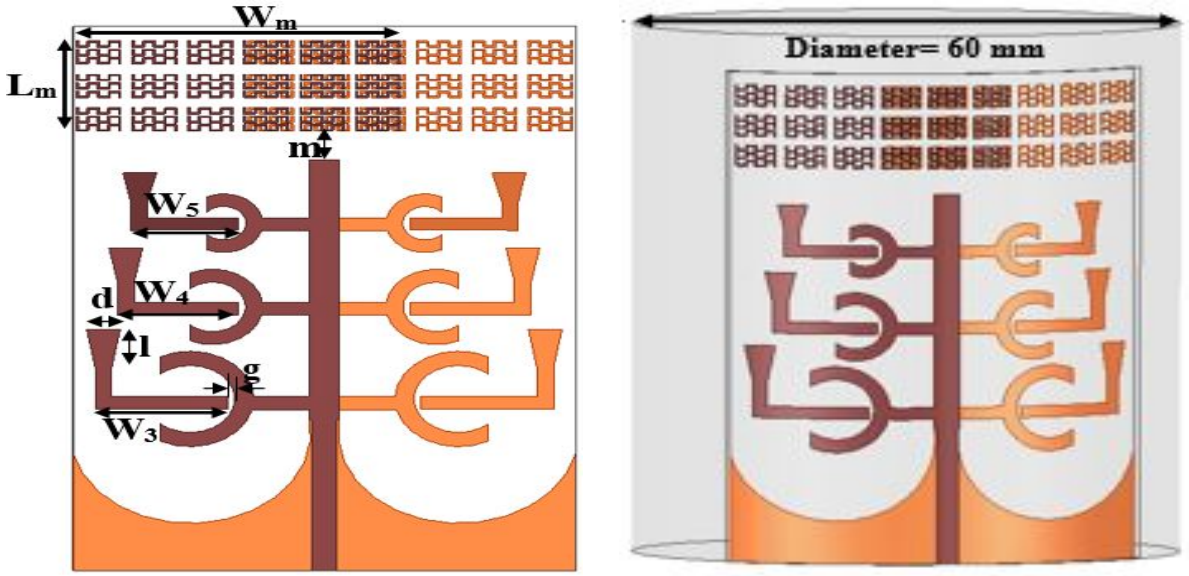

(a) (b)

Figure 4.12 Configuration of the proposed antenna integrated with triangular shaped parasitic elements and metamaterial unit cells (a) planar antenna (b) cylindrical conformal antenna.

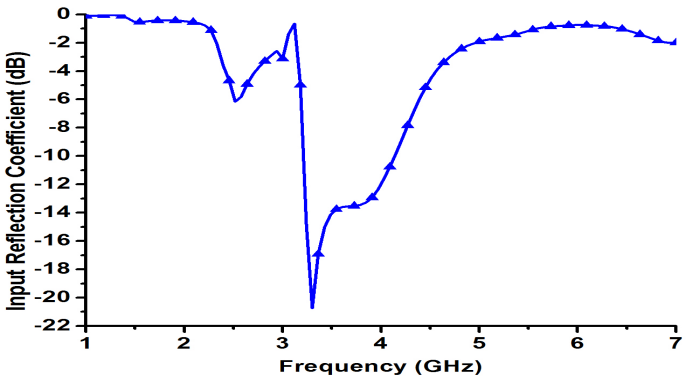

Figure 4.13 The simulated input reflection coefficient of the proposed conformal antenna integrated with triangular shaped parasitic elements and metamaterial unit cells.

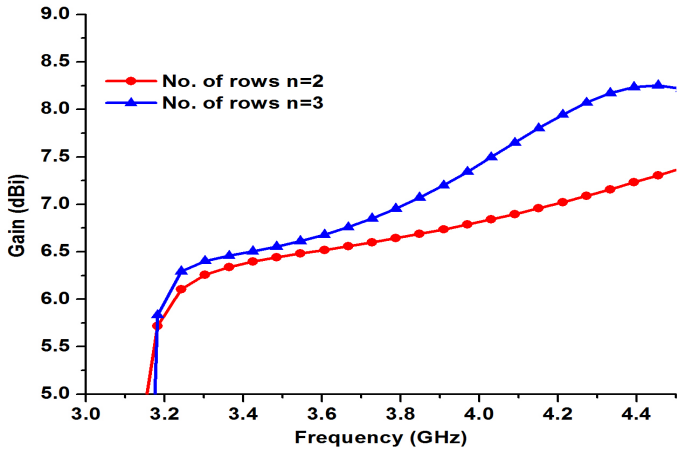

Figure 4.14 The simulated gain with variations of number of rows in the periodic metamaterial unit cells 'n' of the proposed conformal antenna integrated with triangular shaped parasitic elements and metamaterial unit cells.

To examine the effect of number of rows 'n' of unit cells in the antenna, a simulation is done to evaluate the variation of gain with respect to number of rows which is shown in Figure 4.14. It is noticed that by increasing the number of rows the gain is enhanced proportionately.

To observe the effect of different bending angle in the cylindrical conformal antenna, parametric study is performed to compare the variation of input reflection coefficient, gain and normalized radiation pattern with respect to bending angles of 45^0, 90^0 and 180^0 which is shown in Figure 4.15 and 4.16. It is noticed that by increasing the bending angle the input reflection coefficient is slightly shifted towards lower band as in Figure 4.15(a), due to increase of the effective resonant length as antenna is bent. It can be investigated that, the gain values are decreased as shown in Figure 4.15(b).

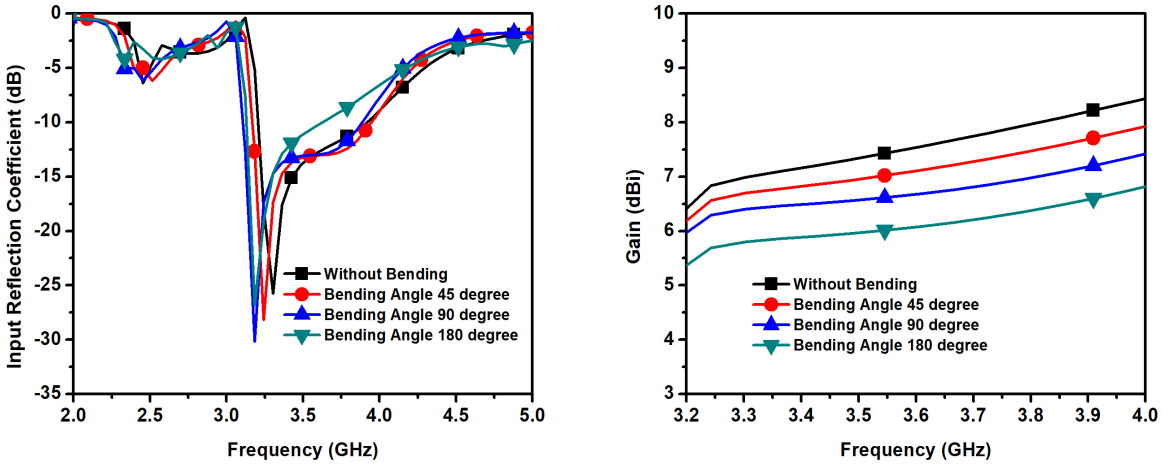

(a) (b)

Figure 4.15 The simulated results comparison of the conformal antenna with different bending angle (a) input reflection coefficient (b) gain.

The comparison of the simulated radiation pattern of the conformal antenna at 3.3 and 3.5 GHz with different bending angle is shown in Figure 4.16. For conformal configurations with different bending angles, the pattern changes are expected since surface of the antenna is curved.

The simulated input reflection coefficients of all the designed cylindrical conformal antennas on 30 mm radius of curvature are compared in Figure 4.17(a). It is seen that by integrating parasitic elements and metamaterial unit cells, a small change in resonant frequency is observed but better impedance matching is achieved with respect to basic antenna. The enhancement of antenna gain by integrating parasitic elements and low index metamaterial can be observed from Figure 4.17(b). It is seen that the basic antenna has a gain of 4.7 dBi after incorporation of parasitic elements and low index metamaterial gain has increased to 6.5 dBi at 3.5 GHz. Thus the presence of triangular shaped parasitic elements and low index metamaterial unit-cells enhances the average gain by 1.8 dBi at 3.5 GHz.

The refractive index and phase velocity (v_{ph}) are inversely proportional to each other. In basic antenna, the EM wave is propagating with constant phase velocity and refractive index of antenna substrate is $n_{ant} = \sqrt{\varepsilon_r} = 1.48$. But, the refractive index of the metamaterial obtained from Figure 4.4 and is around 1.4 over frequency range of 2 to 6 GHz which is less than that of antenna (n_{ant}). Subsequently, in the metamaterial region, the phase velocity is greater than the antenna substrate. Therefore, the radiated beam of the basic antenna will be more directive with narrow beamwidth, when EM wave propagates in the metamaterial region as shown in Figure

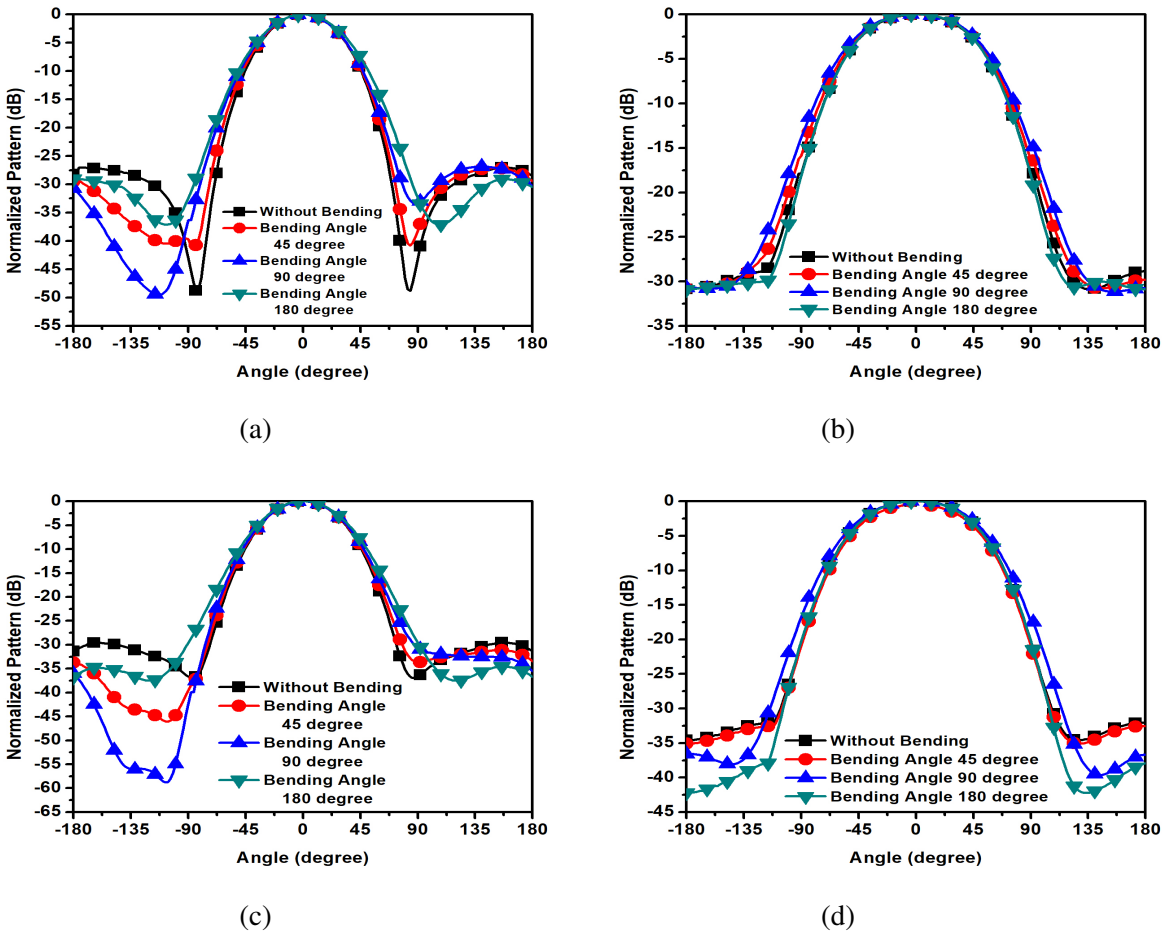

Figure 4.16 The simulated radiation pattern comparison of the conformal antenna with different bending angle (a) E-plane at 3.3 GHz (b) H-plane at 3.3 GHz (c) E-plane at 3.5 GHz (d) H-plane at 3.5 GHz.

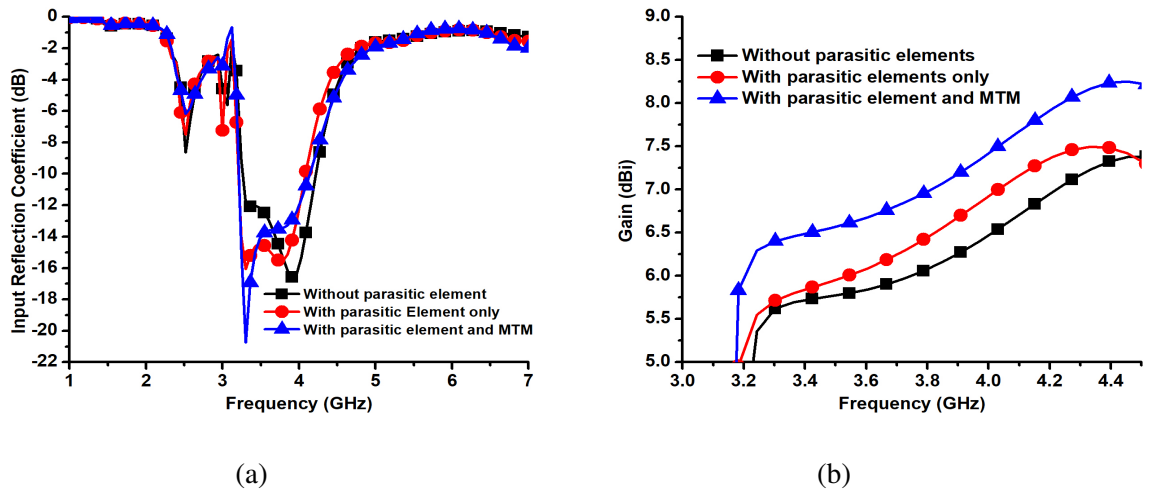

Figure 4.17 The simulated results comparison of the conformal antenna (a) input reflection coefficient (b) gain.

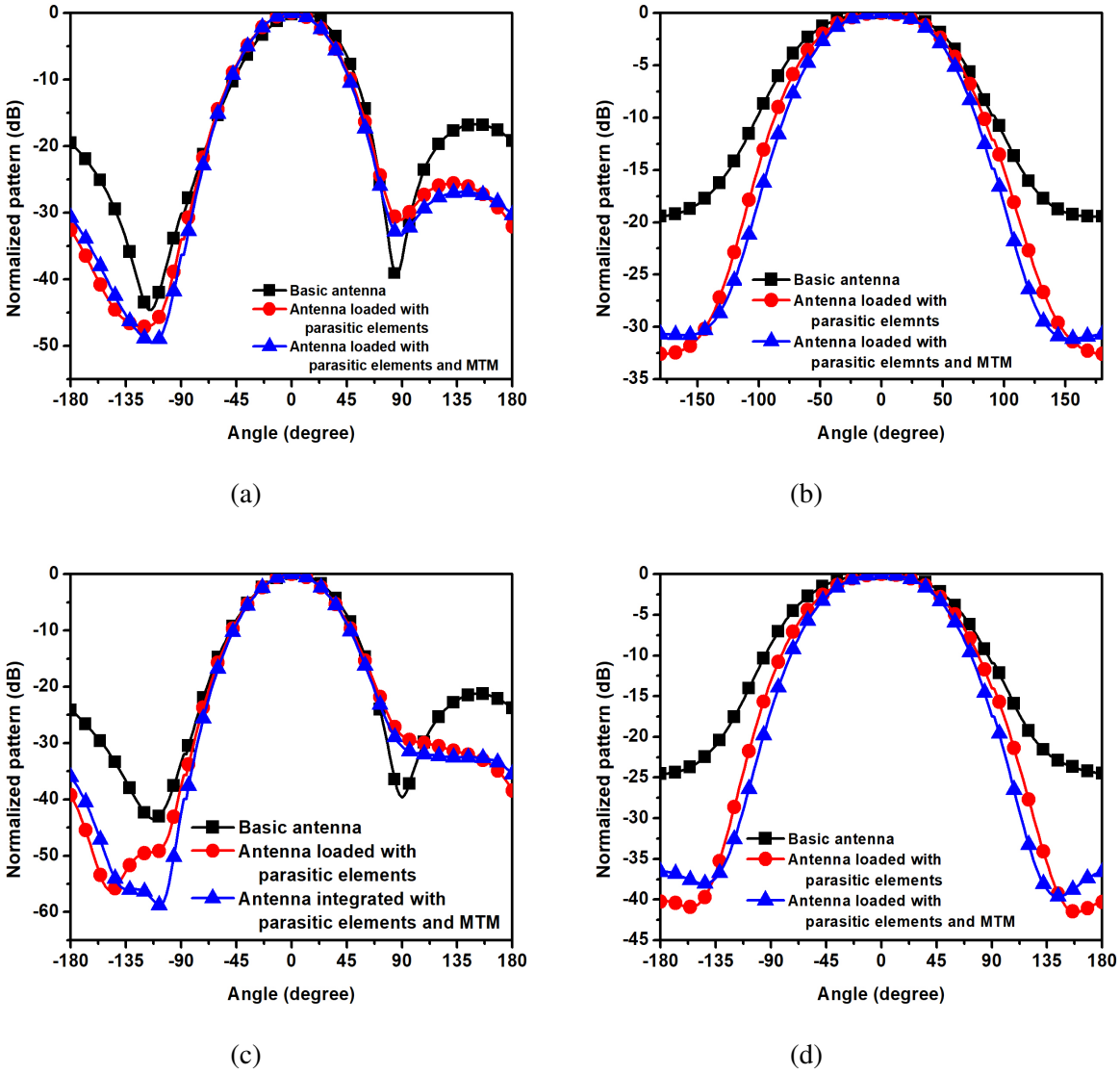

Figure 4.18 The simulated radiation pattern comparison of the conformal antenna (a) E-plane at 3.3 GHz (b) H-plane at 3.3 GHz (c) E-plane at 3.5 GHz (d) H-plane at 3.5 GHz.

4.12. In this way the proposed metamaterial behaves like a beam focusing lens. The normalized radiation patterns of the basic conformal antenna and antenna integrated with parasitic elements and metamaterial unit cells are compared at 3.3 GHz and 3.5 GHz in Figure 4.18. The antenna integrated with parasitic elements and LIM demonstrates a decrease in beamwidth. The half power beamwidth (HPBW) of basic conformal antenna in H-plane (yz plane) is around 123^0 which decreases to 99^0, while in E-plane (xy plane) it decreases from 57^0 to 54^0 after employing parasitic elements and LIM cells at 3.3 GHz. Similarly at 3.5 GHz, the HPBW of basic antenna is around 117^0 which diminishes to 92^0 in H-plane, though in E-plane it decreases from 58^0 to 53^0 subsequently by utilizing parasitic elements and LIM cells.

4.5 Experimental results

The prototype of the basic antenna, antenna loaded with triangular shaped parasitic elements and antenna integrated with triangular shaped parasitic elements and low index metamaterial are fabricated on planar surface of substrate like RT/duroid 5880 with 0.787 mm thickness by using LPKF milling machine S100 and rolled up to form a cylindrical shape on the foam of radius of 30 mm radius as shown Figure 4.19, 4.20 and 4.21. For mechanical support, the foam material is used which has negligible radiation effect on the antenna.

A four-hole round pin with female type SMA connector working in the range DC to 18 GHz is connected to the fabricated antennas. The input reflection coefficient for conformal fabricated antennas are measured by using HP vector network analyzer within the frequency range of 130 MHz to 13 GHz and plotted in the frequency range between 1 to 7 GHz which is illustrated in Figure 4.22(a). By the gain transfer method, the gain of the proposed antenna is measured. The gain transfer method requires an antenna with known gain.

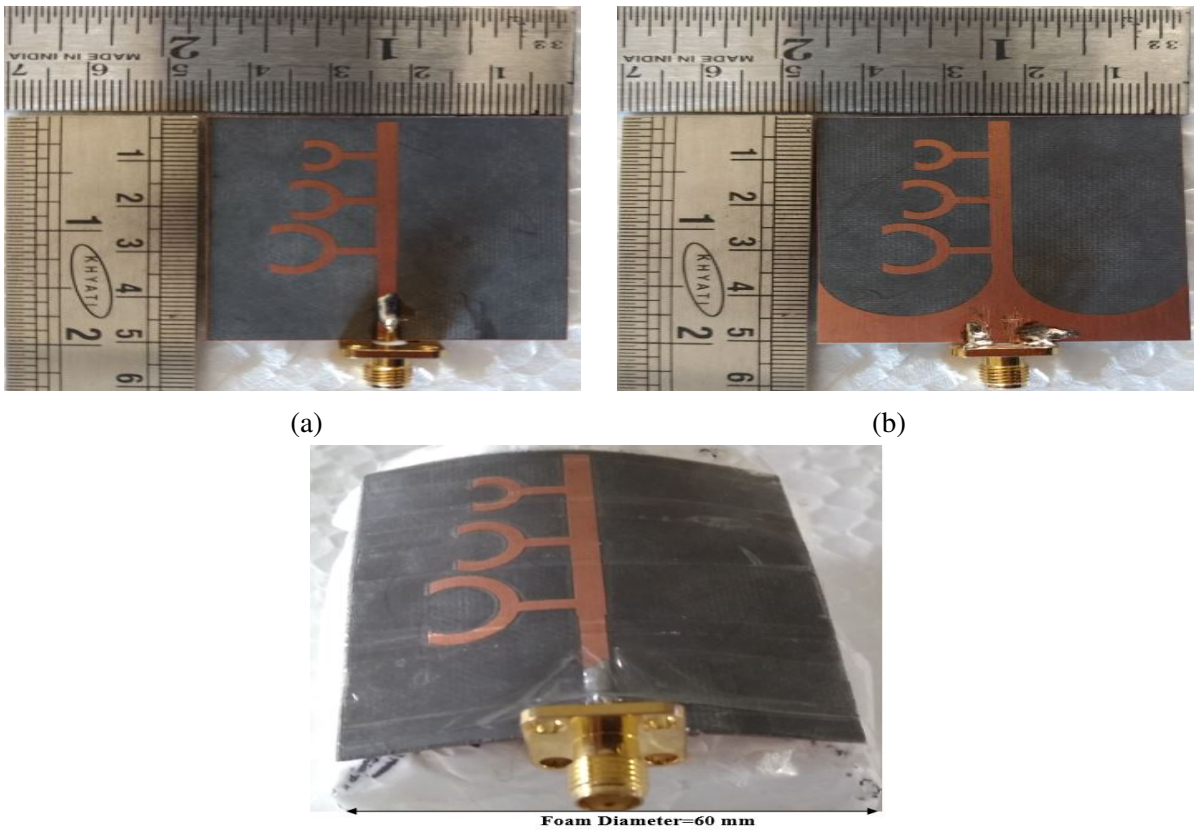

(a) (b)

(c)

Figure 4.19 Photograph of the fabricated basic antenna (a) microstrip line side of planar antenna (b) ground plane side of planar antenna (c) microstrip line side of cylindrical conformal antenna.

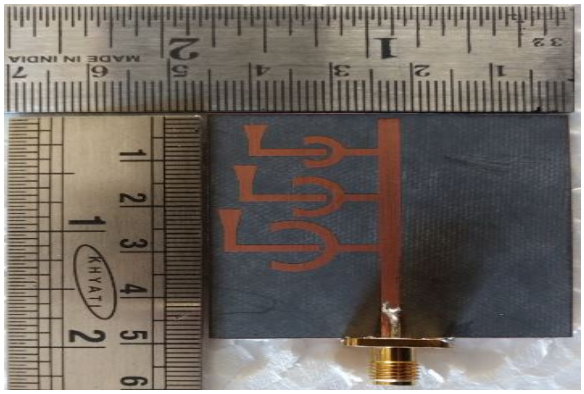

(a)

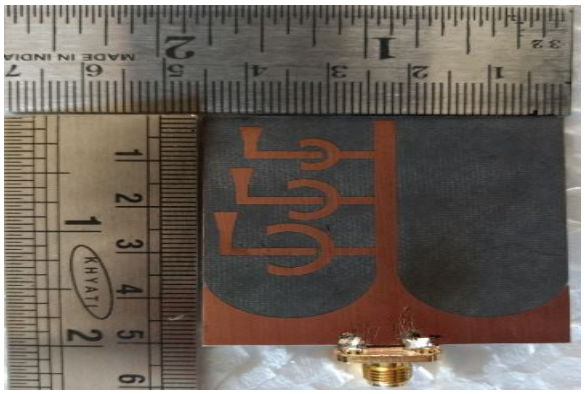

(b)

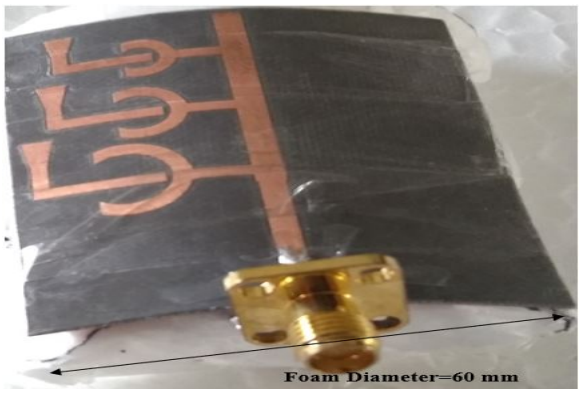

(c)

Figure 4.20 Photograph of the fabricated antenna loaded with triangular shaped parasitic elements (a) front view of planar antenna (b) back view of planar antenna (c) front view of cylindrical conformal antenna.

In the experiment, the standard horn antenna is used, whose gain is known. The measured gain is effectively increased in the proposed conformal antenna which is shown in Figure 4.22(b). It is clear that the gain of the proposed conformal antenna is enhanced by 1.8 dBi as compared with basic antenna.

The conformal antenna integrated with triangular shaped parasitic elements and metamaterial unit cells with different bending angles is also measured. The measured input reflection coefficient is shown Figure 4.23(a) and is observed that resonant frequency is slightly changed due to bending of the antenna. The experimental gain is also changed as in Figure 4.23(b) with the variation of bending angles.

The two-dimensional patterns of the antenna are obtained in an anechoic chamber. To measure the radiation pattern, a standard horn antenna is used at the transmitter and a conformal antenna is connected to the receiver. The conformal antenna radiation pattern is measured in receiving mode. The normalized radiation pattern of the conformal antenna integrated with

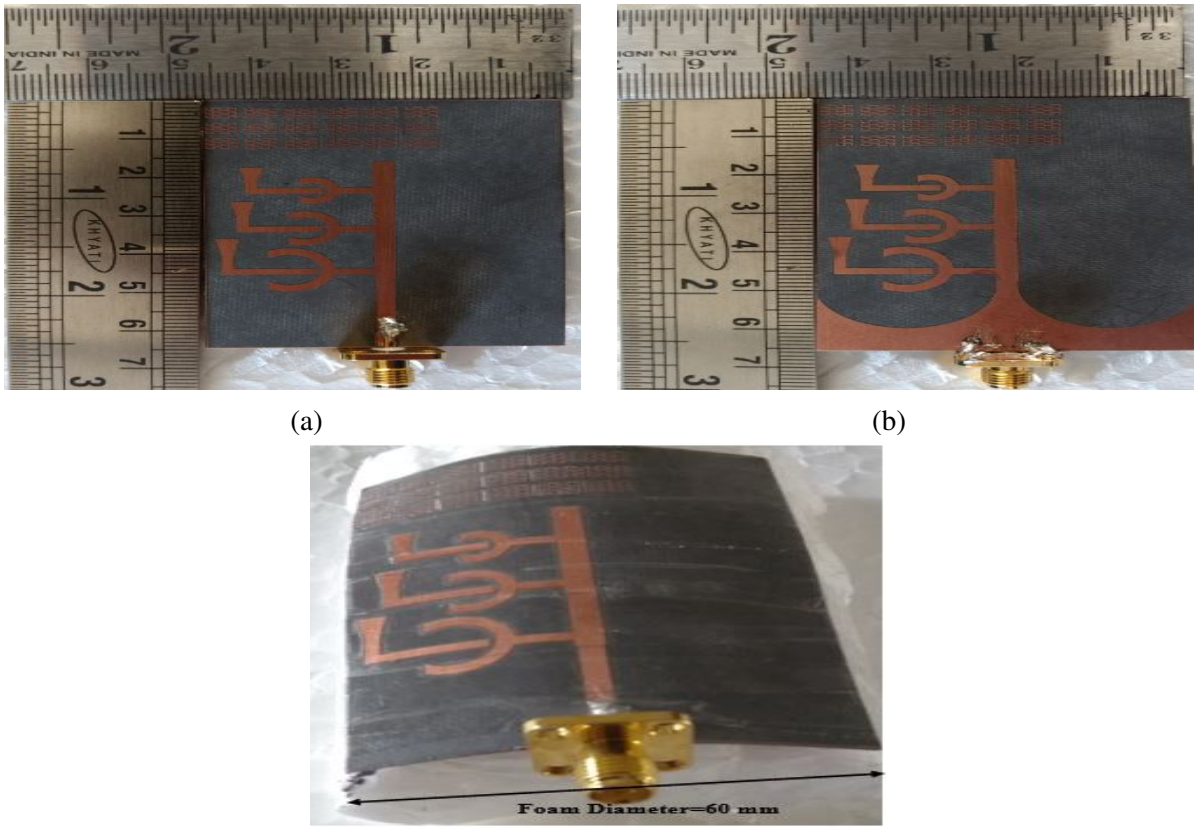

(a) (b)

(c)

Figure 4.21 Photograph of the fabricated proposed antenna integrated with triangular shaped parasitic elements and metamaterial unit cells (a) microstrip line side of planar antenna (b) ground plane side of planar antenna (c) microstrip line side of cylindrical conformal antenna.

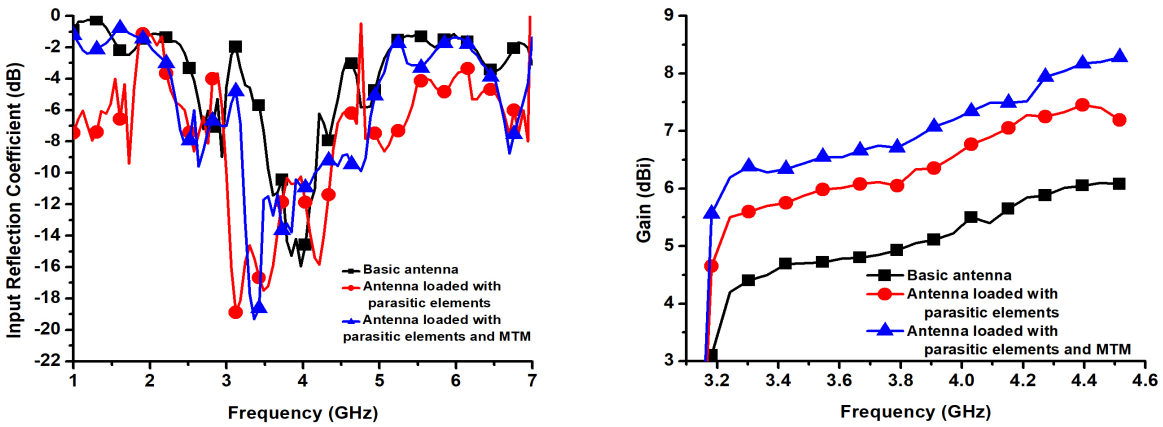

(a) (b)

Figure 4.22 Measured results comparison of the basic antenna and antenna with triangular shaped parasitic elements and MTM (a) input reflection coefficient (b) gain.

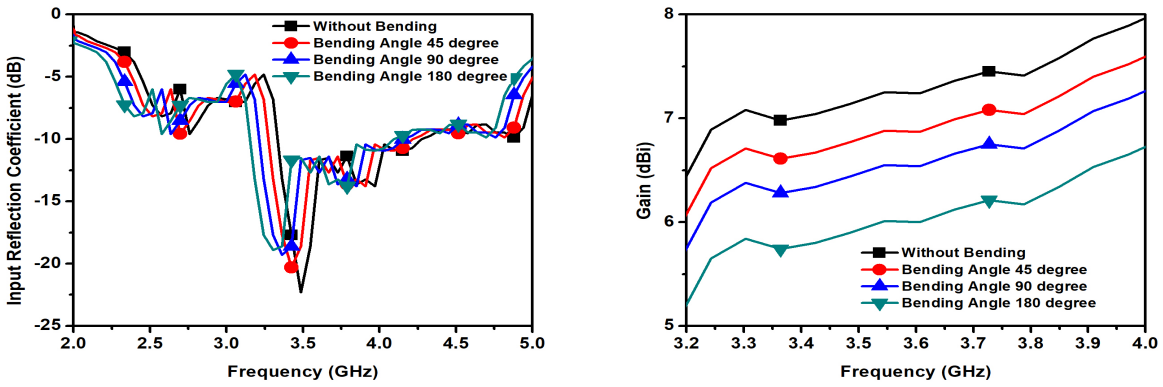

(a) (b)

Figure 4.23 Experimental results comparison of the conformal antenna integrated with triangular shaped parasitic elements and metamaterial unit cells with different bending angle (a) input reflection coefficient (b) gain.

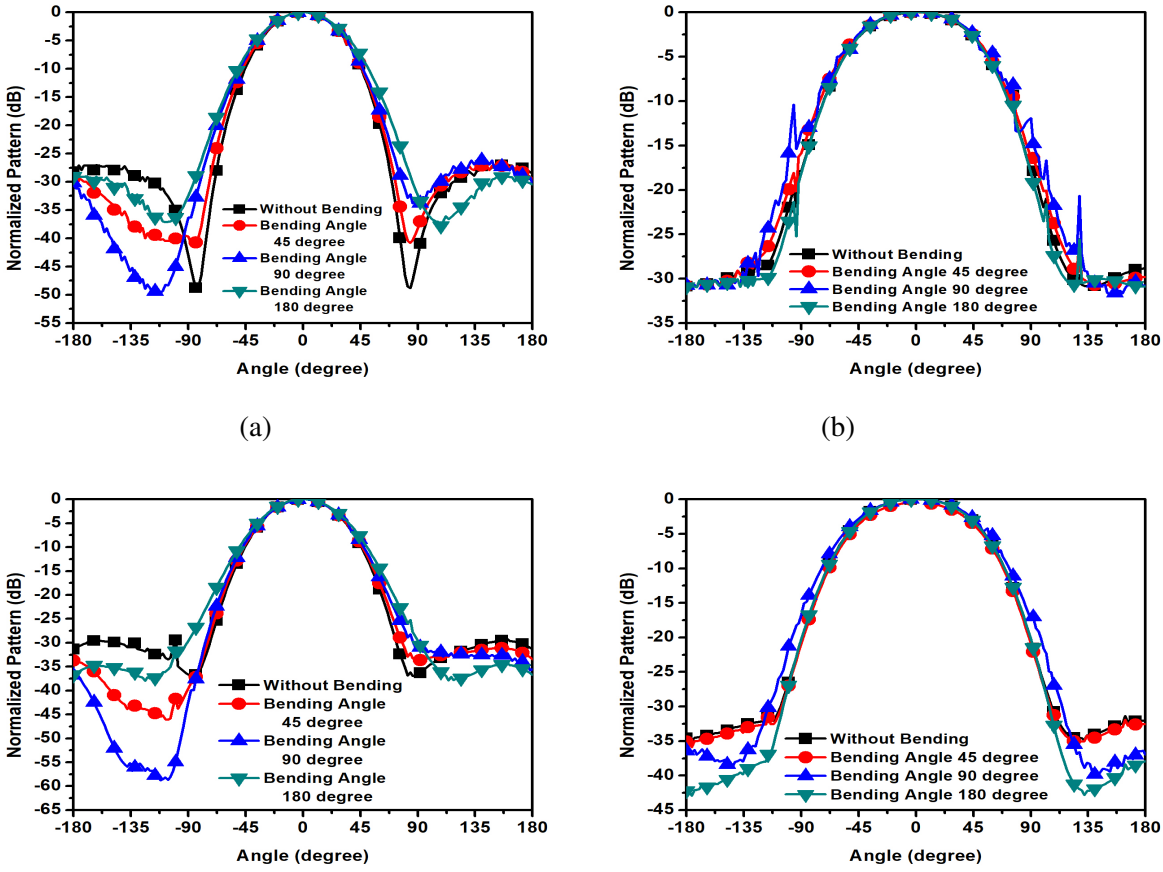

(a) (b)

(c) (d)

Figure 4.24 Experimental radiation pattern comparison of the conformal antenna integrated with triangular shaped parasitic elements and metamaterial unit cells with different bending angle (a) E-plane at 3.3 GHz (b) H-plane at 3.3 GHz (c) E-plane at 3.5 GHz (d) H-plane at 3.5 GHz.

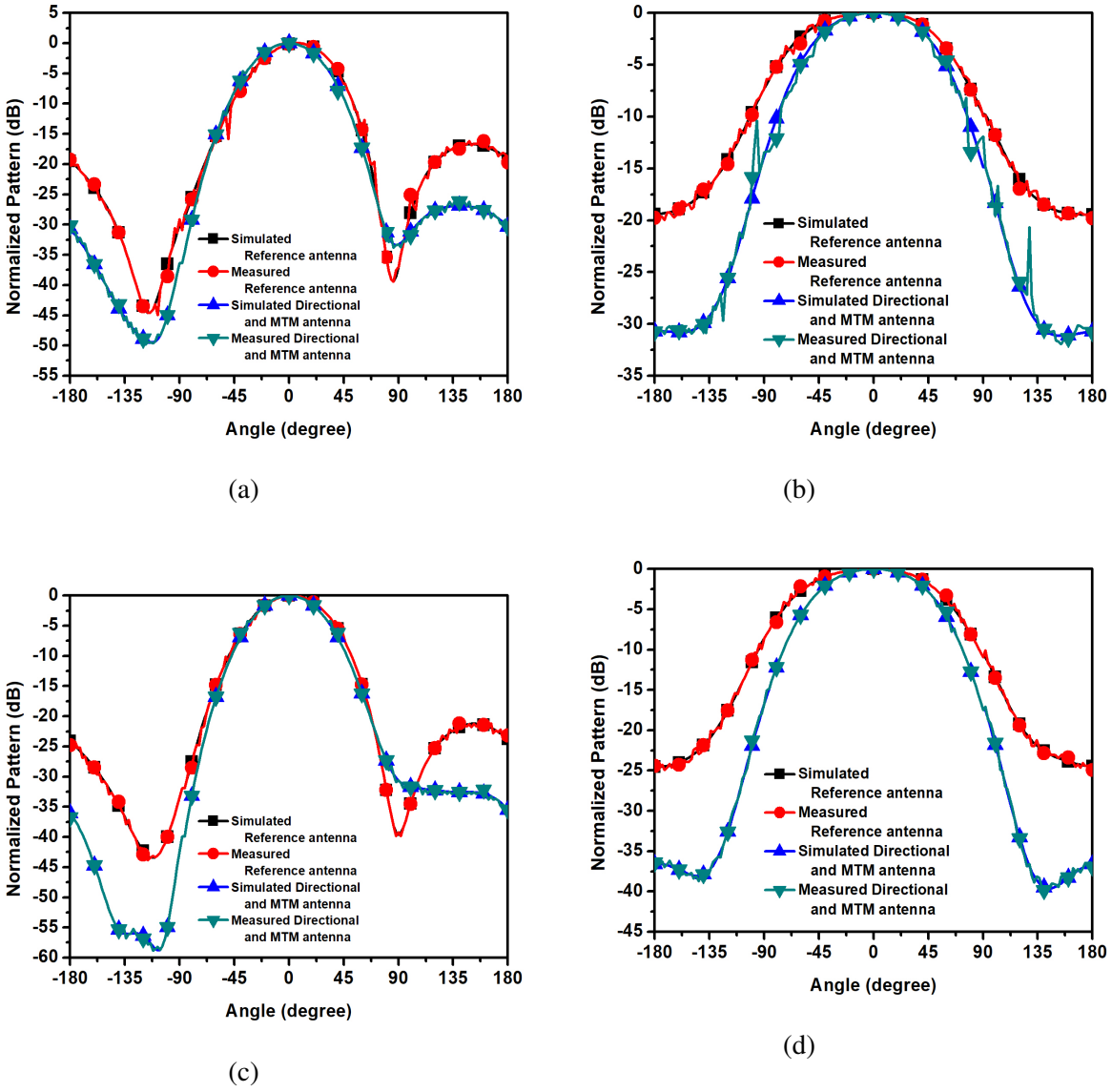

Figure 4.25 Simulation and Experimental radiation pattern comparison of the conformal antenna with 30 mm radius of curvature which is equivalent to 85.90 of bending angle (a) E-plane at 3.3 GHz (b) H-plane at 3.3 GHz (c) E-plane at 3.5 GHz (d) H-plane at 3.5 GHz.

triangular shaped parasitic elements and metamaterial unit cells in the H-plane and E-plane are plotted for 3.3 GHz and 3.5 GHz respectively with different bending angles in Figure 4.24.

The measured normalized radiation pattern of the fabricated conformal antenna in the H-plane and E-plane are plotted for 3.3 GHz and 3.5 GHz respectively in Figure 4.25 and Table 4.3 illustrates the comparison between antenna parameters. The HPBW of the conformal antenna integrated with triangular shaped parasitic elements and low index metamaterial is substantially less than the basic antennas which shows that the pattern becomes more directive.

Table 4.3 Comparison of measured antenna parameters.

Antenna	**Bandwidth**	**Resonant frequency (GHz)**	**Gain (dBi) at 3.5 GHz**	**HPBW(θ_H) at 3.3 GHz**	**HPBW(θ_E) at 3.3 GHz**	**HPBW(θ_H) at 3.5 GHz**	**HPBW(θ_E) at 3.5 GHz**
Basic antenna	3.28-4.24 GHz =960 MHz	3.93	4.7	122.96	56.76	116.82	57.93
Antenna with parasitic elements	3.1-3.74 GHz =640 MHz	3.18	5.7	108.93	55.65	100.38	54.32
Antenna with parasitic elements and metamaterials	3.1-3.88 GHz =780 MHz	3.18	6.5	99.106	54.76	92.47	53.49

Table 4.4 Comparison of the proposed cylindrical conformal antenna with existing in literature.

Antenna	**Size (mm^3)**	**Frequency (GHz)**	**-10dB bandwidth**	**Gain (dBi)**
Proposed work	65×45×0.787	3.5	22.3 %	6.5
[76]	85×25×1.6	3.5	5.1%	6.95
[39]	60×66×1.6	2.96	–	4.4
[91]	50×54×1.5	5.2 / 6.75	2.14% / 2%	8.2
[96]	45×28×0.787	7.6	51.4%	4

The overall performances of the proposed cylindrical conformal antenna integrated with parasitic elements and metamaterial unit cells are compared with those of existing literature in Table 4.4. The proposed antenna provides competitively better performance.

4.6 Conclusion

In this chapter, a basic conformal antenna is proposed. The gain enhancement and narrow beamwidth of the basic conformal antenna are achieved by integrating triangular shaped parasitic elements and low index metamaterial unit cells. The experimental results of the fabricated antennas demonstrated that the gain is enhanced by 1.8 dBi with reduced HPBW by 24^0 in H-plane. The proposed conformal antenna has wideband, high gain and directional radiation pattern in the entire operating frequency range from 3.1 GHz to 3.88 GHz, which is suitable for wideband WiMAX applications.

Chapter 5

Metamaterial Inspired and Slotted Conformal Antenna for Wi-Fi and WiMAX Applications

5.1 Introduction

Wi-Fi and WiMAX have potential application in military and commercial communications. In some applications, these antennas are required to be conformal to the device to make it less visible to the human eye [10, 11, 103]. As space constraints on the device are always a limitation for antenna design, a compact dual-band structure is required. Designing of a dualband conformal antenna which operates in two different important band like Wi-Fi and WiMAX applications is a challenging task. Spectrum of these two important bands like Wi-Fi and WiMAX is shown in Figure 5.1.

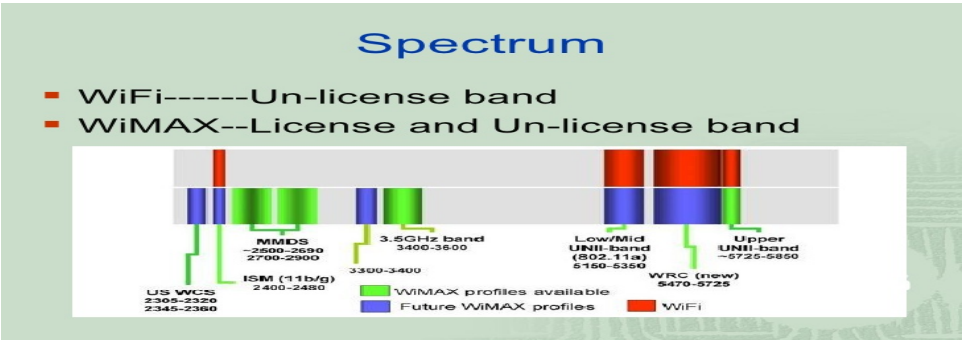

Figure 5.1 Spectrum of Wi-Fi and WiMAX.

The microstrip patch antenna is the most suitable for microwave frequency band for modern wireless communications [104]. The miniaturization of the patch antenna is the desired property and many efforts have been made for this purpose, such as using shorted pin [43, 105, 106], employing substrate with high dielectric constant [44] and utilizing loaded slots and capacitances [45, 107]. If the dielectric constant of the substrate is increased, the size of the antenna reduces but with an increase in quality factor and decrease in operating bandwidth. Compact four-element SRR-loaded dual-band MIMO antenna is designed for WLAN/WiMAX/WiFi/4G-LTE and 5G applications in [[108]. Compactness is achieved in an antenna by employing a modified meandered slot, a slotted Y-shaped monopole, and a trident-shaped feed strip in [109]. A dual-band CP planar monopole antenna is designed for WLAN/Wi-Fi/WiMAX/Bluetooth applications [110]. Research methods are developed to simultaneously increase the bandwidth and minimize the size of the patch antenna. This is a very challenging task but useful for many applications such as handset internal antennas, RF front-end antennas and antennas for millimeter waves. Moreover, miniaturization will reduce system requirements [108, 109, 110, 111, 112, 113].

Since the inception of metamaterials (MTM), the demand for compact and wideband antenna has increased [114]. There is always a trade-off between bandwidth and size in the conventional antennas, which makes them unsuitable for platforms like moving vehicles, missiles and hand held devices. Metamaterials give compactness by loading conventional antennas with single or numerous unit cells. Mode dispersion and Q factor are significantly influenced by metamaterial unit cells. This unique property gives rise to miniaturization of antennas.

Recently, some studies on bandwidth enhancement and metamaterial antennas on the planar surface are published in the literature [110, 115, 116, 117]. To enhance the bandwidth, J. Zhu and G. V. Eleftheriades implemented a transmission line metamaterial antenna of size 50 $\times$ 50 mm^2 operating at 3.3 GHz. A fractional bandwidth of 3.1% is attained by loading shunt spiral inductors but the design is complex due to the presence of vias [115].

P. L. Chi and Y. S. Shih designed a Zero order resonance antenna of size 32.2 $\times$ 20 mm^2 operating at 2.16 GHz, using inter digital capacitor as unit cell [116]. In this case, the meander lines type inductor is used which has properties like low inductance and self-resonance frequency. The fractional bandwidth obtained for the monopole antenna is of 15.1% but the actual bandwidth of the antenna is low.

J. K. Ji et al. presented an antenna based on two planar mushroom structure unit cells [117]. The antenna which operates at 1.99 GHz has an overall size of 40 $\times$ 100 mm^2. Frac-

tional bandwidth up to 20.3% is achieved by merging two resonance modes using inductor and capacitor. As the antenna is resonating at two adjacent modes, there is a posibility in the bandwidth reduction for a slight change in resonant modes. Moreover, the fractional bandwidth is comparatively lower and the size of the antenna is also large.

H. Li et al. proposed a dual-band planar antenna loaded by a square patch with a slot on the bottom side. The antenna designed constitutes a composite right and left-handed (CRLH) metamaterial unit cell for WLAN/WiMAX applications [118]. The size of the antenna is 70 × 44 mm^2 and the bandwidths of the dual band are 22.8% and 10.8% respectively. But the size of the antenna is large with low bandwidth.

A dual mode metamaterial antenna with vias was designed by B. D. Bala et al. by merging zeroth order resonance mode and positive order resonance mode [119]. The bandwidth achieved is 39% for the size of 39 × 25 mm^2, but the presence of vias makes the design complex.

In this chapter, a dual U slot cylindrical conformal antenna with various radius of curvatures are designed for Wi-Fi application and results are compared. Also a new cylindrical conformal dual-band antenna with 15 mm radius of curvature for Wi-Fi and WiMAX applications is proposed. In the proposed dualband antenna the concept of inductor loading is applied to achieve more bandwidth in first band and by incorporating metamaterial the size of the antenna is also reduced. Input reflection coefficient is also improved due to the presence of bottom patch with slot. The presence of two meander lines as parasitic elements on the patch resonates the antenna in the second band at 3.5 GHz which can be used for WiMAX applications.

5.2 Cylindrical conformal antenna with a dual U slot

5.2.1 Design of conformal antenna

The antenna is designed on RT Duroid 5880 substrate of permittivity(ε_r) 2.2 and thickness of 0.787mm with microstrip inset feed as shown in Figure 5.2.The dimensions of the proposed antenna are L_1=41.6 mm, W_1=49.3 mm, L_2 =25 mm, W_2=12 mm, L_3=23 mm, W_3=8 mm, L_4=28 mm, W_4=5.5 mm, t=0.5 mm.The main advantages of U-slot patch antenna is that it produces broad band characteristics.A planar dual U slot antenna is designed.The slots are placed at the centre of the patch because of maximum current distribution. The planar antenna is transformed to conformal cylindrical of 25 mm, 45 mm and 60 mm radii.

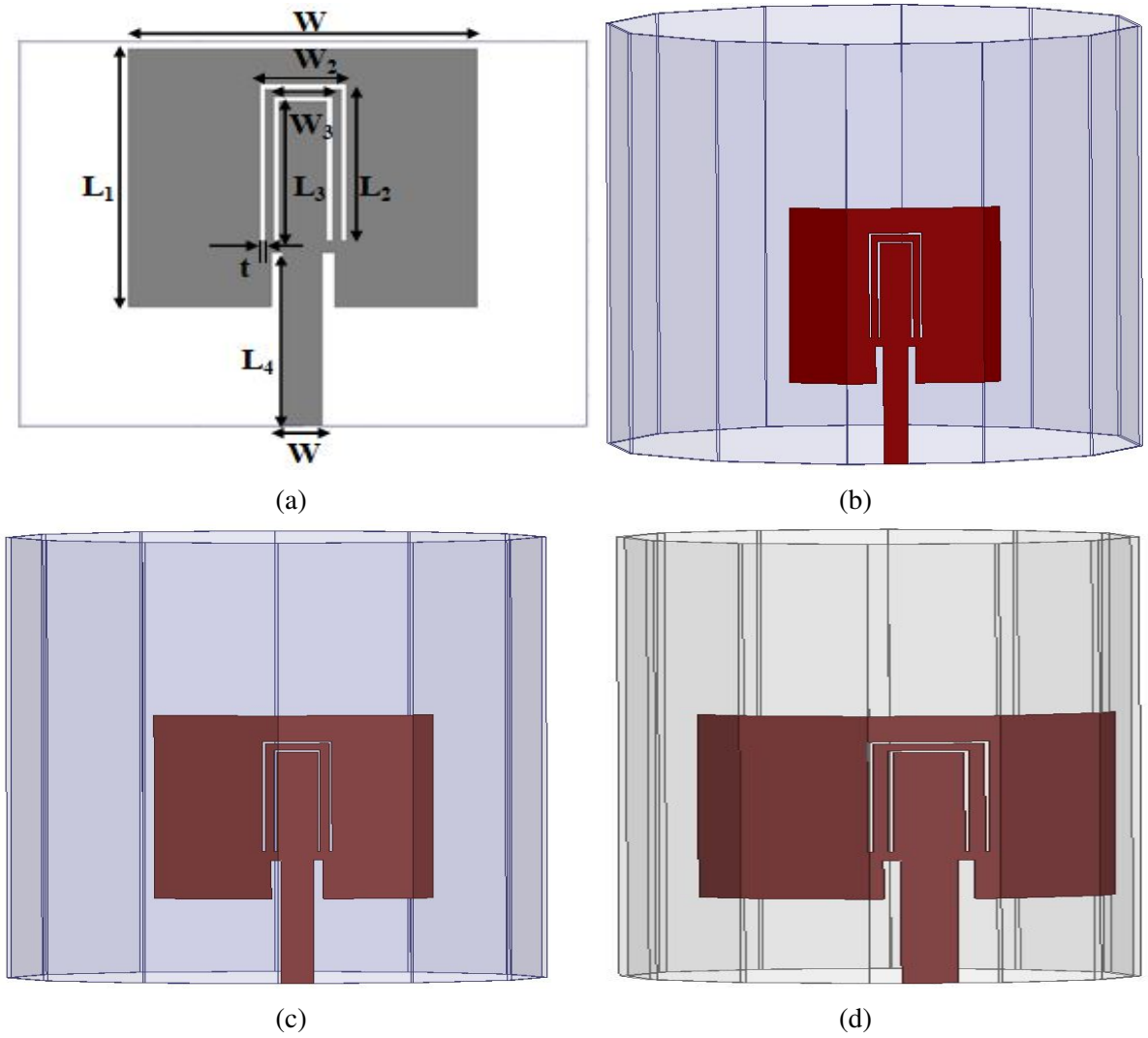

Figure 5.2 Simulated Antennas (a) planar antenna. (b) conformal antenna with 60 mm diameter. (c) conformal antenna with 45 mm diameter. (d) conformal antenna with 25 mm diameter.

Slotted conducting patch used on conducting patch element can cause meandering of excited patch surface current paths and results in lowering of the resonant frequency, which corresponds to the reduction of antenna size and also improvement of bandwidth and gain.

5.2.2 Simulation results

The comparison among the return loss of planar antenna with cylindrical conformal antennas with different radii is shown in Figure 5.3. The simulated return loss is much lower than -10 dB, indicates an acceptable impedance matching between the feeding line and the radiating patch in the curved structure. The resonant frequency of proposed planar antenna is 2.4GHz where as for conformal antenna, it is 2.45 GHz for 25 mm, 45 mm as well as 60 mm radius.

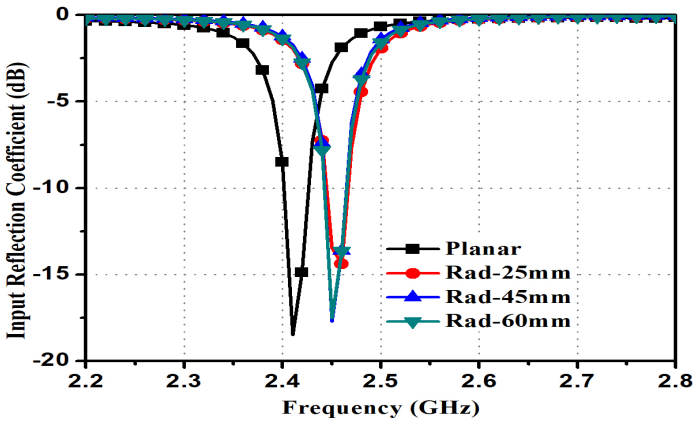

Figure 5.3 Return loss of simulated antenna.

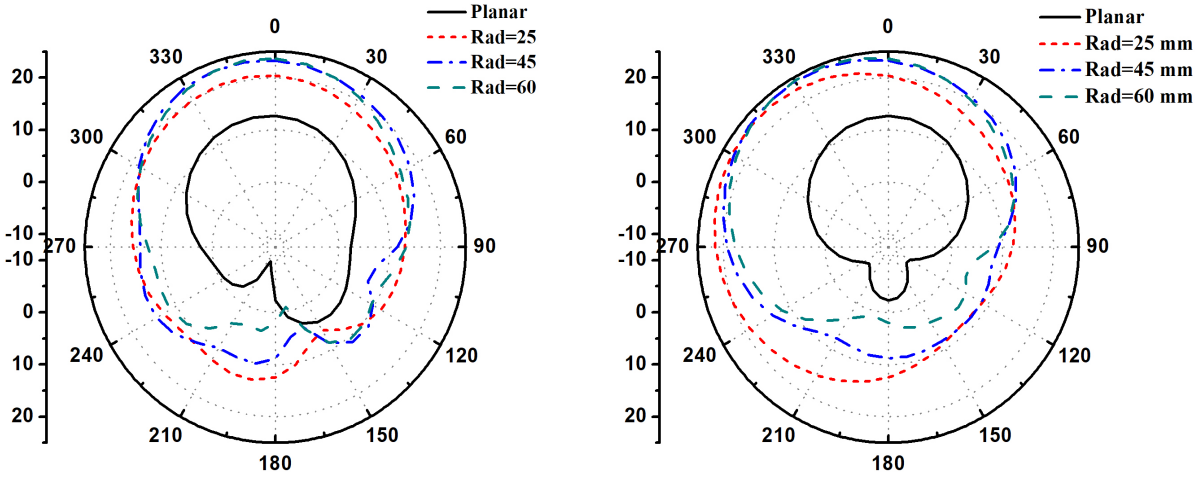

(a) (b)

Figure 5.4 Radiation pattern at 2.4 GHz (a) E-plane (b) H-plane.

There is a change in resonant frequency form planar antenna to conformal antenna which is shown in Figure 5.2.

The comparison between the radiation patterns (E-plane and H-plane) of planar antenna with the cylindrical conformal antennas with different radii are shown in Figure 5.4. For conformal configurations, the pattern changes are expected since the entire surface of the antenna is not parallel to the principal axes.

The comparison of the gain of planar antenna with the cylindrical conformal antennas with different radii is shown in Figure 5.5. For the cylindrical conformal antennas, the simulated gain

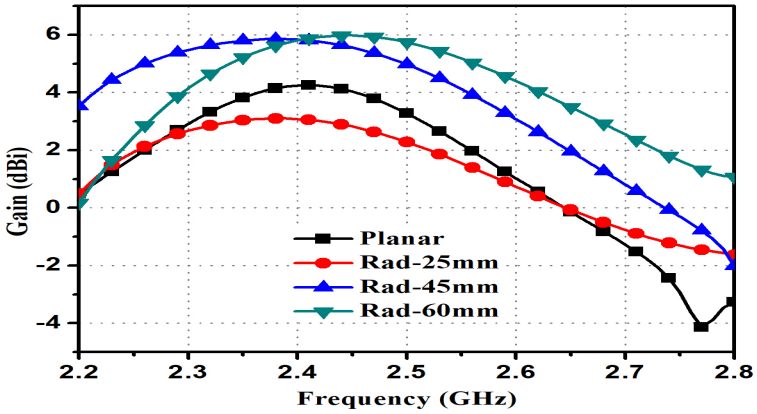

Figure 5.5 Gain of simulated antenna.

values are decreased gradually from 5.9 dB to 2.81dB with the radius of curvature declining from 60 mm to 25 mm.

(a) (b)

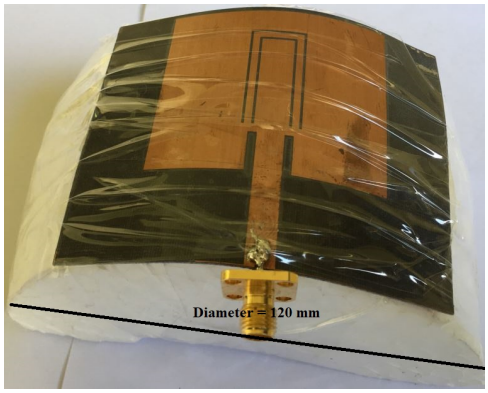

(c)

Figure 5.6 Photographs of fabricated antenna (a) top view of planar antenna (b) bottom view of planar antenna (c) top view of proposed conformal antenna with 60 mm radius of curvature.

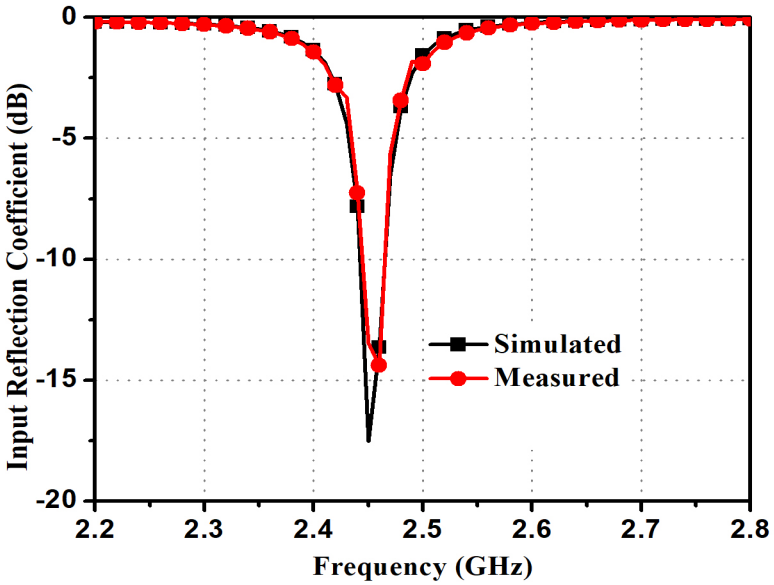

Figure 5.7 The measured magnitude of the reflection coefficient of planar and conformal antenna.

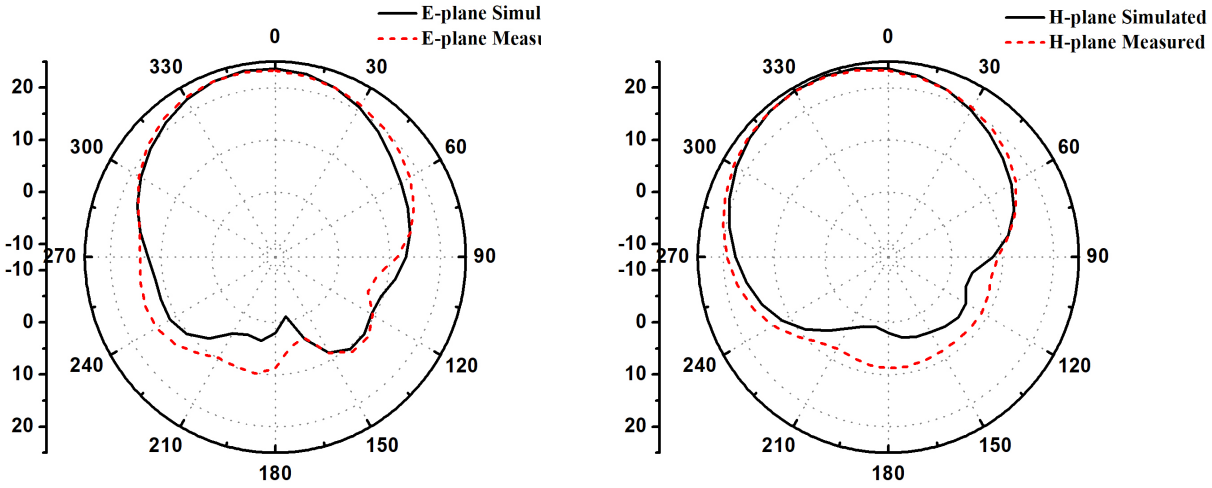

(a) (b)

Figure 5.8 The measured radiation patterns of planar and conformal antenna (a) E-plane pattern at 1.5 GHz (b) H-plane pattern at 1.5 GHz.

5.2.3 Results and discussions

The simulated dual U-slot planar antenna is fabricated on RT/duroid 5880 substrate and it is rolled up to form a cylindrical shape on foam of radius of 45 mm as shown in Figure 5.6. The simulated and measured reflection coefficients of the proposed conformal antenna are compared as shown in Figure 5.7. An impedance bandwidth of 23 MHz is obtained.

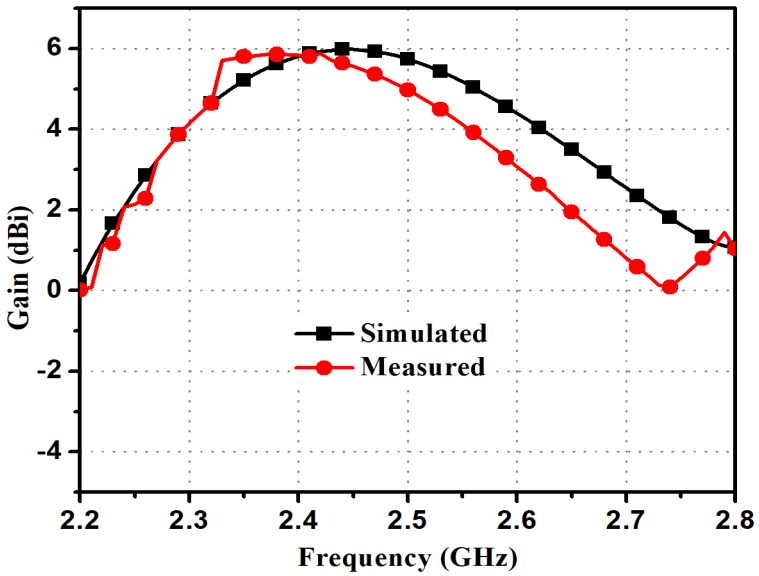

Figure 5.9 The measured gain plot of planar and conformal antenna.

The measurement of radiation patterns for proposed cylindrical conformal at 2.4 GHz frequency is performed in an anechoic chamber. The comparison between simulated and measured E-plane and H-plane of the radiation pattern are illustrated in Figure 5.8. The measured peak gain of the proposed cylindrical conformal antenna is 5.9 dBi as shown in Figure 5.9.

5.3 Design methodology of antenna and parametric study

5.3.1 Design of conventional monopole conformal antenna

A printed monopole antenna is a good candidate for wireless communication services because of its wide impedance bandwidth, omnidirectional radiation pattern, compact structure and ease of fabrication.

The geometry and parameters of the planar antenna are shown in Figure 5.10. The antenna is fed by the coplanar waveguide (CPW) where the ground plane and radiating patch are present on the same side of the substrate for easy fabrication process as compared with microstrip line feed, which requires ground plane on the opposite side of the patch. The shunt capacitance between the ground and top patch can be effectively balanced in CPW feed. Shunt capacitance 'C_R' is formed between the radiating patch and CPW ground which is calculated as [120]

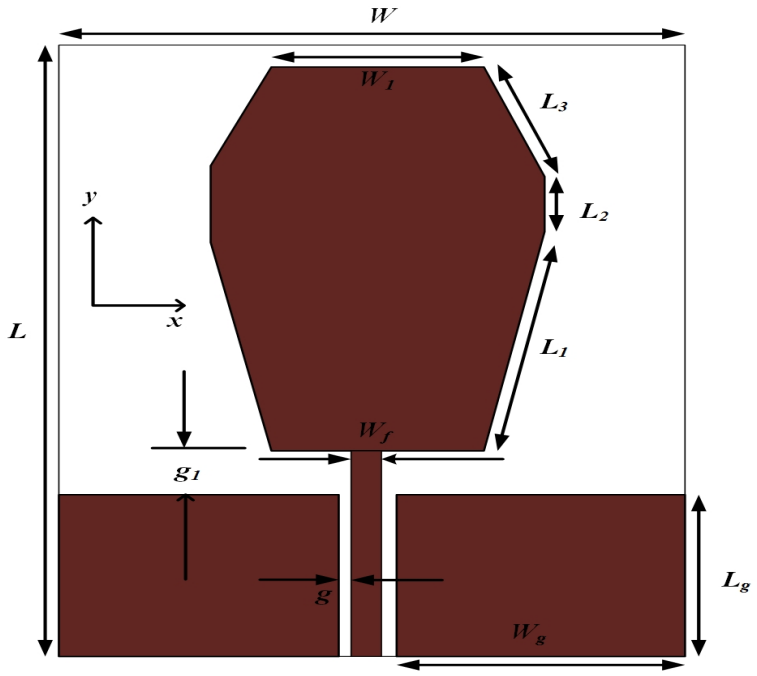

Figure 5.10 Structure of the conventional monopole planar antenna

$$C_R = \frac{10^9 \varepsilon_r \varepsilon_0 A}{D}(pF) \tag{5.1}$$

where ε_r is the relative permittivity, ε_0 is the permittivity in free space, A is the area, D is the gap between the patch and CPW ground.

The antenna is designed at a frequency higher than Wi-Fi frequency (2.45 GHz) because by applying size reduction techniques, the resonant frequency will decrease to Wi-Fi frequency.

RT/duroid 5880 with a dielectric constant (ε_r) of 2.2, thickness of 0.787 mm and dielectric loss tangent of 0.0009 is selected as substrate. The antenna is designed and simulated using commercially available computer simulation technique (CST) software.

A hexagonal shaped antenna is initially selected as it gives a compact structure compared with other shapes. Modification of hexagonal shape is done to incorporate the metamaterial structures for achieving size reduction. So, the hexagonal shape is modified to octagonal. The dimensions of patch 'L_1' and 'L_3 ' are asymmetrical due to optimized positions of the metamaterial unit cell. The dimension of 'L_2' is decided by the size of the metamaterial unit cell to be introduced in the antenna design.

Table 5.1 Optimised dimension of the proposed antenna.

Parameters	Size (mm)	Parameters	Size (mm)
L	40	g_1	2.5
W	30	W_f	2.4
L_1	14.9	L_g	11
L_2	4	W_g	13.45
L_3	7.52	g	0.35
W_1	10	-	-

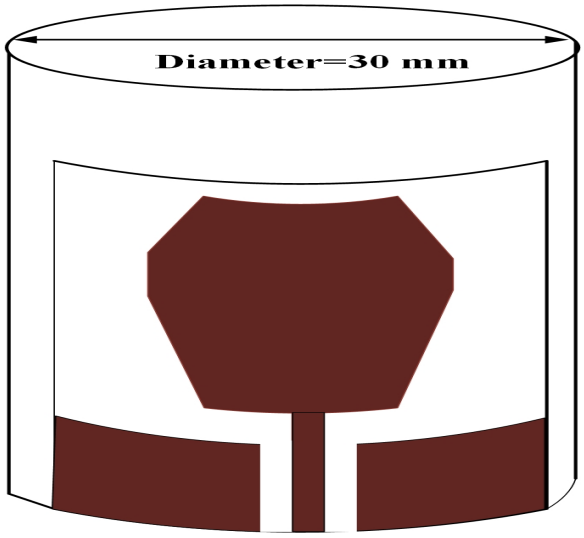

Figure 5.11 Structure of the conventional monopole conformal antenna

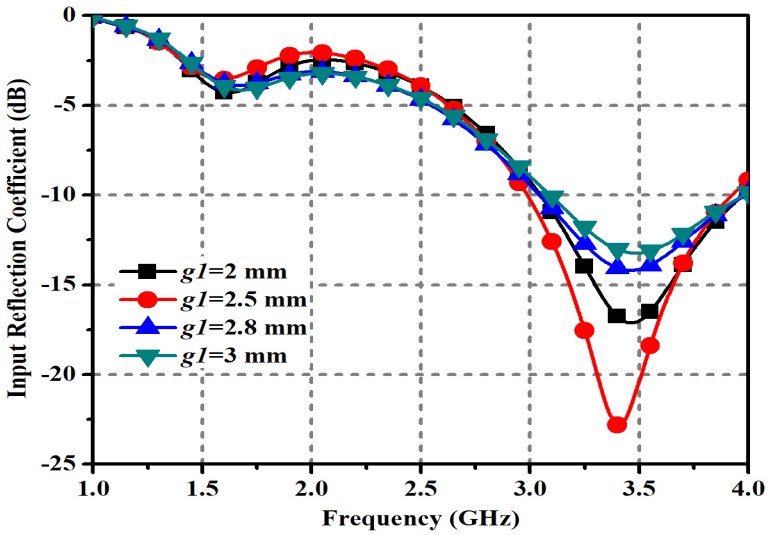

Figure 5.12 The input reflection coefficient (S_{11}) of the conventional monopole conformal antenna with a different value of g_1

The optimized dimensions of the planar antenna in Figure 5.10 are shown in Table 5.1. The planar monopole antenna is transformed to the conformal antenna on a cylinder of radius 15 mm, which is indicated in Figure 5.11. The input reflection coefficient for various values of 'g_1' the distance between the lower edge of the radiating patch and upper edge of the ground plane are observed. The input reflection coefficients of the conformal antenna with different values of 'g_1' are displayed in Figure 5.12. The optimized value of 'g_1' for the proposed antenna is selected as 2.5 mm.

5.3.2 Design of conformal antenna loaded with meander lines

CRLH-TL metamaterial

The parameters of the material like permittivity and permeability depend on the unit cell structure and its periodic arrangement. The design of metamaterial antennas is based on the composite right/left-handed transmission line (CRLH-TL) unit cell shown in Figure 5.13. It is represented as a conventional transmission line with series inductance L_R, series capacitance C_L, shunt inductance L_L and shunt capacitance C_R.

The analytical dispersion equation of the CRLH-TL can be obtained by applying Bloch and Floquet theory to the unit cell as follows [114]:

$$cos(\beta d) = 1 - \frac{1}{2}\frac{(w^2 - w_{se}^2)(w^2 - w_{sh}^2)}{w^2 w_R^2} \tag{5.2}$$

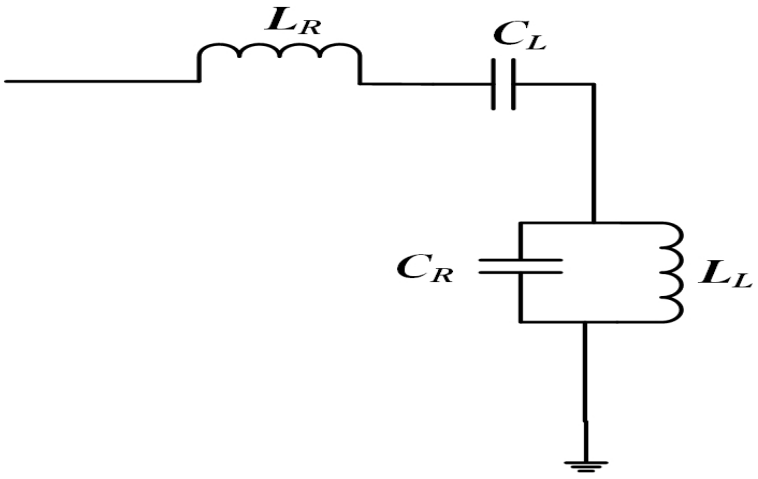

Figure 5.13 Equivalent circuit model of fundamental metamaterial unit cell

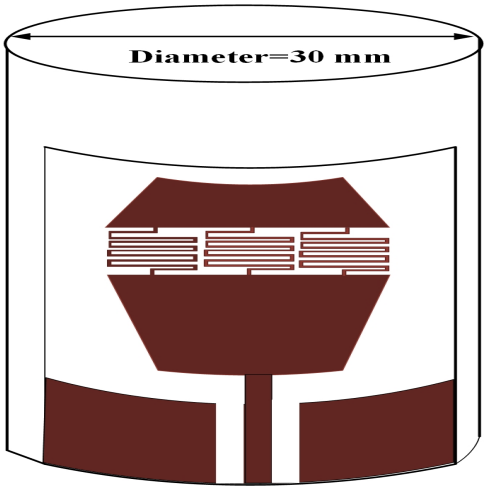

Figure 5.14 Structure of the monopole conformal antenna loaded with meander lines

where $w_{se}=\frac{1}{\sqrt{L_R C_L}}$, $w_{sh}=\frac{1}{\sqrt{L_L C_R}}$, $w_R=\frac{1}{\sqrt{L_R C_R}}$

β is the propagation constant for Bolch waves, and d is the length of the unit cell. The resonance of the CRLH-TL for various modes *'n'* can be obtained by the following condition:

$$\beta_n d = \frac{n\pi d}{l} = \frac{n\pi}{N}, \qquad n = 0, \pm 1, \pm 2....., (N-1) \tag{5.3}$$

where N and l are the total number of the unit cell and the total length of the resonator, respectively.

Design methodology

In the proposed work, the metamaterial concept is applied for compactness, where the size of the antenna can be miniaturized by modifying the patch structure with metamaterial unit cells. Although metamaterials are periodic structures, in the conformal antenna shown in Figure 5.14, only 3 meander lines type unit cells are used as in [112,115]. Meander lines give a compact structure with an increase in current through the zigzag path of the lines. The parameters of the meander line unit cell are the width of the line, the gap between lines and number of fingers. The width of the lines controls the current flow, which in turn governs the inductance of the path. By increasing the number of fingers, the effective electrical length increases with decrease of resonant frequency. More than one unit cell can be incorporated to reduce the size of the antenna.

In the present work, meander line unit cell with a width of 0.2 mm, spacing gap of 0.2 mm and finger length of 5 mm is selected. The finger length 5 mm is equivalent to 0.06 λ_g at 2.45 GHz and satisfies the condition for the average cell size which must be smaller than a quarter of wavelength i.e. $p < \lambda_g/4$. In the equivalent circuit model indicated in Figure 5.13, it can be interpreted that series inductance L_R and series capacitance C_L are decided by the meander lines. In this model, the series capacitance C_L is the interdigital capacitance due to meander lines and the series inductance L_R is due to the current flow on meander lines. The extracted values for parameters C_L and L_R in this model are given below [120]

$$C_L = (\varepsilon_r + 1)l(N-1)A_1 + A_2(pF) \tag{5.4}$$

$$A_1 = 4.409.tanh[0.55(\frac{h}{W})^{0.45}]10^{-6}(pF/\mu\text{m}) \tag{5.5}$$

$$A_2 = 9.92.tanh[0.52(\frac{h}{W})^{0.5}]10^{-6}(pF/\mu\text{m}) \tag{5.6}$$

where 'ε_r' is the relative permittivity, *'l'* is the length of finger, *'N'* is number of finger, *'h'* is the height of substrate, *'W'* is the width of one finger.

$$L_R = 2.6{a_1}^{0.0603}{h_1}^{0.4429}{N_1}^{0.954}{d_1}^{0.606}{W_1}^{-0.173}(nH) \tag{5.7}$$

where 'N_1' is number of turns,'a_1' is the length of a lead, 'h_1' is the height of the meander, 'd_1' is the width of the meander, 'W_1' is the width of the printed strip.

To evenly distribute the meander line along the patch structure, three unit cells are considered. To observe the effect of number of fingers in the meander lines, the simulated input reflection coefficients for the proposed conformal antenna are shown in Figure 5.15. It is found that the resonant frequency of the proposed antenna is decreasing from 3.4 to 2.76 GHz while increasing the number of fingers from 0 to 5 in the meander lines. It indicates that the antenna in Figure 5.11 which is operating at 3.4 GHz before introducing meander lines is operating at 2.76 GHz after implementing meander lines, as shown in Figure 5.14. Initially, the number of fingers is considered as four and on further increasing the number of fingers beyond four, it is observed that gain is decreased, as illustrated in Figure 5.16.

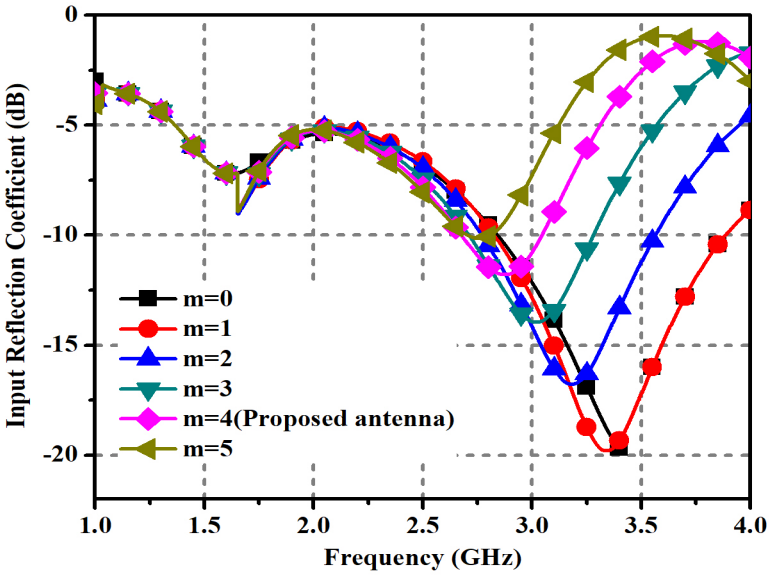

Figure 5.15 The simulated input reflection coefficient of the conformal antenna with a different number of fingers m

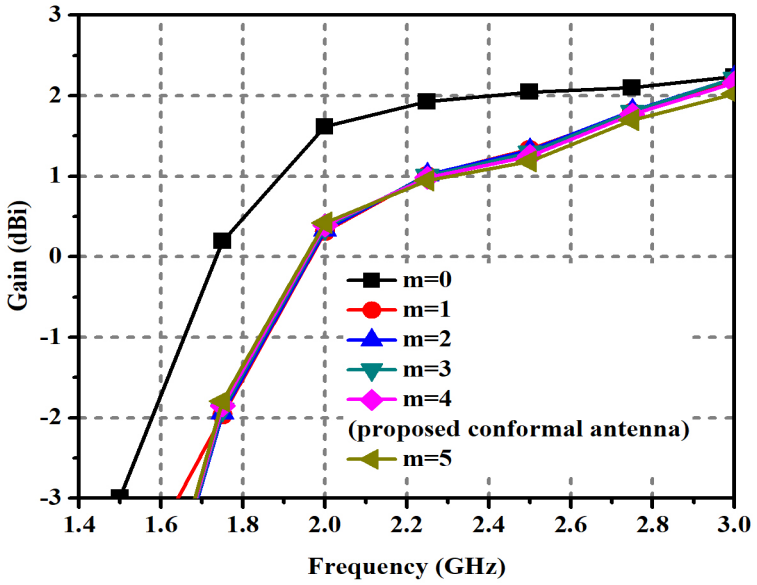

Figure 5.16 The simulated Gain of the conformal antenna with a different number of fingers 'm'

The dispersion characteristics of the proposed CRLH-TL unit cell obtained by using simulated S-parameters are shown in Figure 5.17. The dispersion curve relates frequency and phase constant, which depends on the inductance and capacitance values of CRLH-TL unit cells. It shows that there is a smooth transition from the right-handed pass-band and left-handed pass-band at ZOR of 2.45 GHz. From the dispersion characteristics, the proposed antenna can be

realized as Zero order resonant (ZOR) antenna. The metamaterial-Zero order resonant antenna can be realized using the CRLH transmission structure.

The Q factor and the fractional bandwidth of the Zero Order Resonant (ZOR) circuit are given in [111]

$$Q = \frac{1}{G}\sqrt{\frac{C_R}{L_L}} \tag{5.8}$$

$$BW = G\sqrt{\frac{L_L}{C_R}} \tag{5.9}$$

Compared to conventional resonant antennas, ZOR antennas are known to have narrow bandwidth issue due to small L_L and large C_R. The antenna structure follows the open ended boundary condition. The ZOR frequency is controlled by distributed shunt elements like L_L and C_R of the transmission line. With a specific end goal to enhance the bandwidth of the structure, material with low permittivity and high thickness is utilized. However, this reduces the design freedom and causes fabrication difficulties. An antenna with an increase in L_L is suggested in the proposed work by adding inductance which results in enhanced bandwidth without decreasing the efficiency.

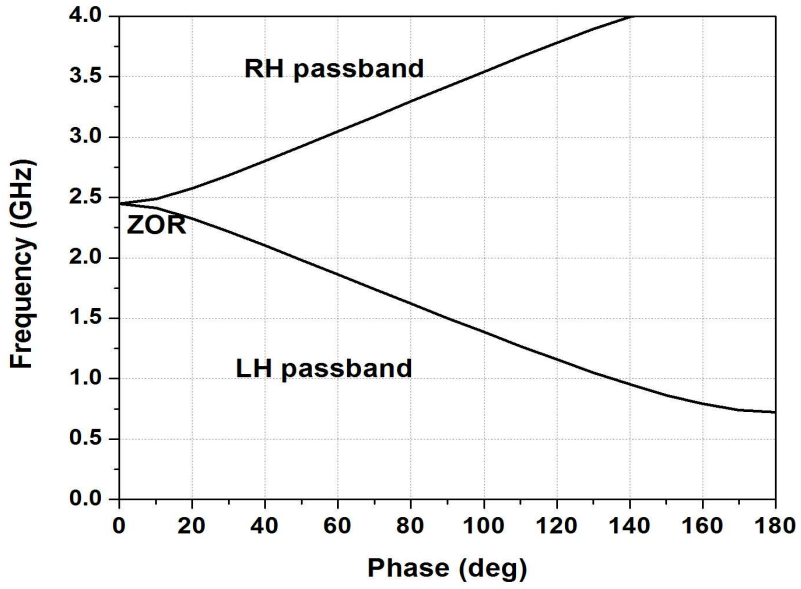

Figure 5.17 Dispersion diagram of the proposed unit cell

5.3.3 Design of conformal antenna loaded with fractal inductor

The antenna can be made compact by reducing the resonant frequency by lumped impedance loading. This is attempted by adding an additional inductor to the patch which is not reported in the published literature. The inductor can be considered as strip inductor, circular geometry or meander line. Circular geometry has the best electrical performance, whereas other geometries like meander line inductors are seldom used because of low inductance and self-resonance frequency (SRF). The inductance of circular shaped inductor can be increased by increasing the mean radius of the coil. A fractal inductor is proposed as shown in Figure 5.18 when the mean radius of the coil is large which results in large area of fractal shape when compared with inductor without fractal structure. Circular geometry can be modified as a fractal structure by the repetition of the circular boundary. In the proposed work, circular boundary and the first iteration of the circular boundary, which is named as a fractal inductor, are considered. Also, the proposed fractal structure can be manufactured easily. The presence of fractal inductor is adding shunt inductance L_L in the equivalent circuit model as given in Figure 5.13 and can be calculated as [120]

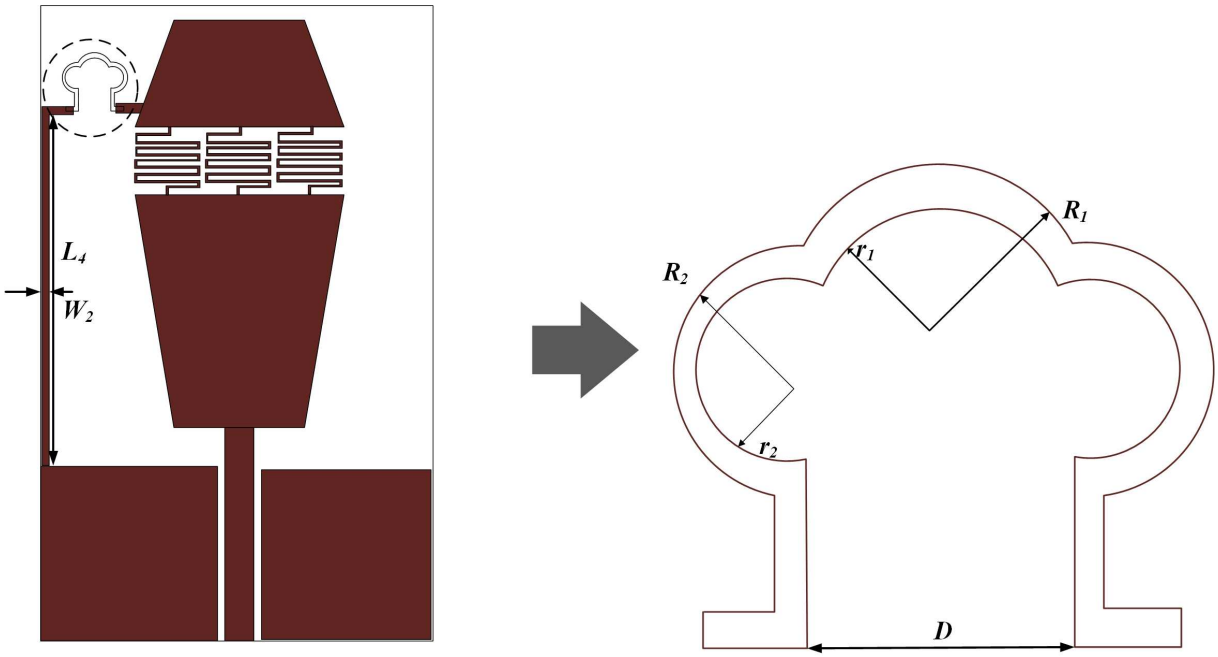

Figure 5.18 Structures of the planar equivalent of the proposed ACPW conformal antenna loaded with meander lines and fractal single turn inductor

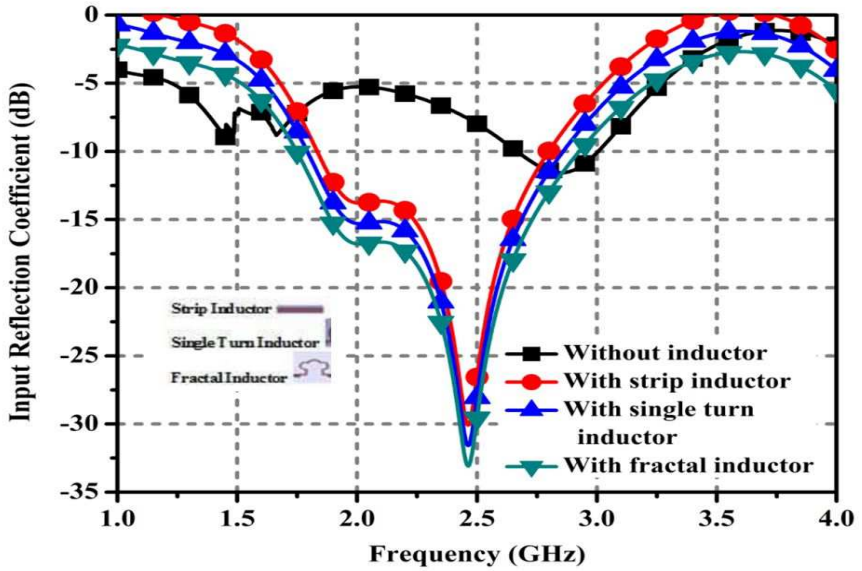

Figure 5.19 The simulated input reflection coefficient of the proposed conformal antenna with different inductor shape

$$L_L = 1.257 \times 10^{-3} \times a \times ln(\frac{a}{W+t}) + 0.078K_g(nH) \tag{5.10}$$

$$K_g = 0.57 - (0.145 \times ln(\frac{W}{h})) \tag{5.11}$$

where a is the mean radius of circular loop, W is the width of loop, t is the thickness of line, h isthe height of the substrate.

For the proposed antenna, equivalent circuit parameters are calculated using (5.1), (5.4), (5.7) and (5.10) which are obtained as C_R=0.7346 pF, C_L=0.1403 pF, L_R=9.6135 nH and L_L=5.5383 nH as given in Figure 5.13.

The variation of simulated input reflection coefficients with frequency for the proposed conformal antenna with different shapes of the inductor are shown in Figure 5.19 for comparison. The resonant frequency of an antenna with an inductor is decreased when compared with that without inductor. The antenna with strip inductor and circular inductor has similar input reflection coefficient variation. But first iteration fractal inductor has better input reflection coefficient at the resonant frequency with an increase in bandwidth. The fractional bandwidth obtained for the antenna without the inductor, strip inductor, single turn inductor, and the fractal inductor is 12%, 43%, 45% and 51.3% respectively. The change in resonant frequency is due to the change in the electrical length of the current path. The fractional bandwidth of the

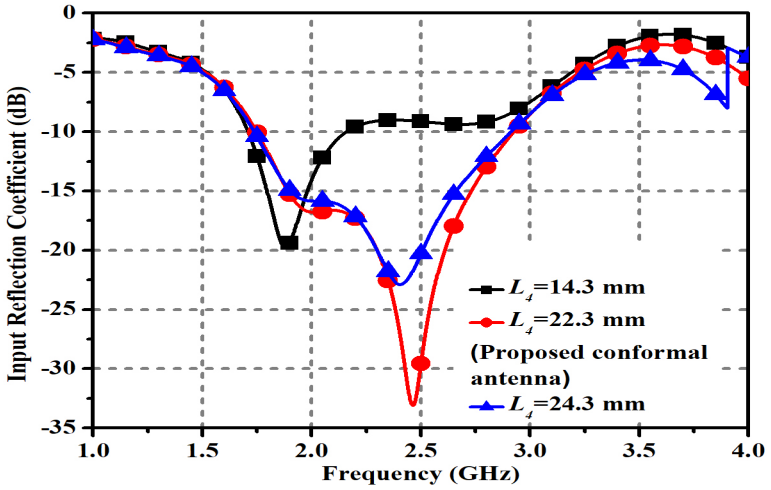

Figure 5.20 The simulated input reflection coefficient of the proposed conformal antenna with different position(L_4) of the fractal inductor

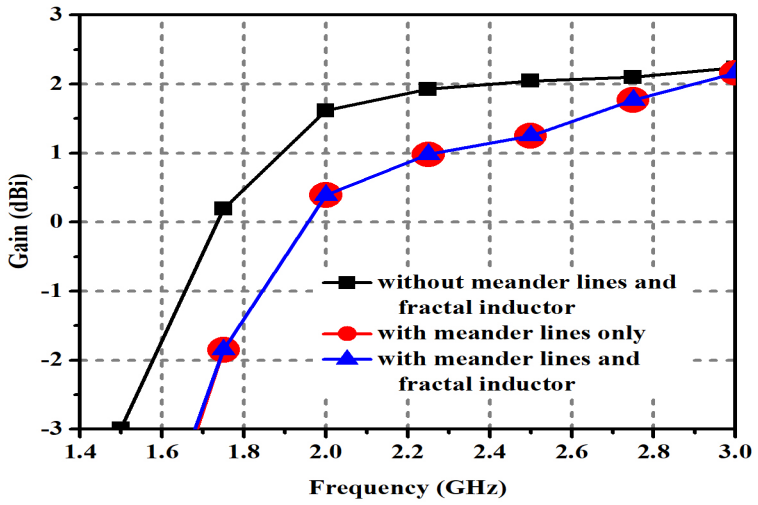

Figure 5.21 The simulated Gain vs. frequency of the conformal antenna with and without meander lines and fractal inductor

proposed cylindrical conformal antenna with a fractal shaped inductor is high when compared to the strip and single turn inductor.

The location of the inductor on the patch also decides the resonant frequency. To observe this effect, the inductor is located at different heights and the simulated input reflection coefficients are plotted in Figure 5.20. It is illustrated that the resonant frequency can be reduced by decreasing the height. When the height L_4 is 22.3 and 24.3 mm, the input reflection coefficient characteristics are similar, but at 24.3 mm the input reflection coefficient is minimum; hence 24.3 mm location is selected as the optimized position.

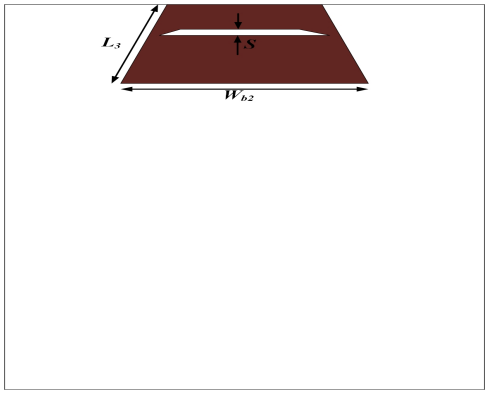

Figure 5.22 Bottom view of the planar equivalent of the proposed conformal antenna

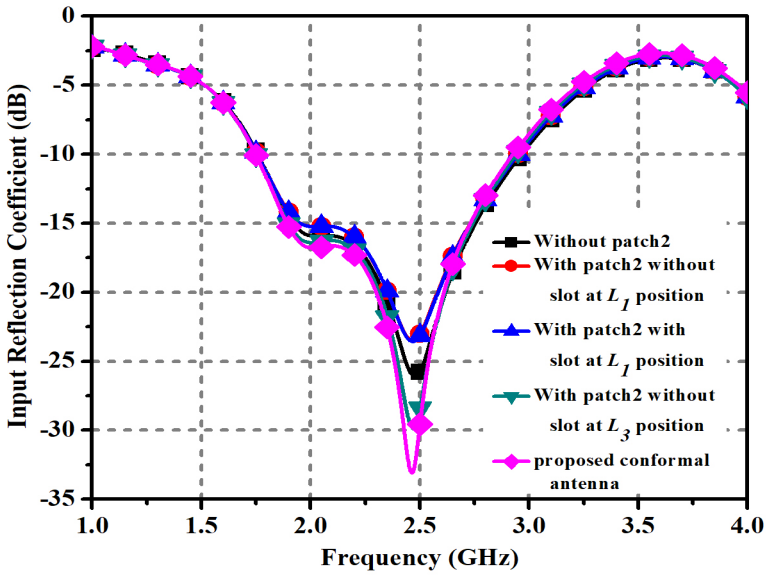

Figure 5.23 The input reflection coefficient (S_{11}) of the proposed conformal antenna with effects of patch2

The simulated gain vs. frequency of the conformal antenna without meander lines and fractal inductor, with meander lines only and the presence of both meander lines and fractal inductor, is compared in Figure 5.21. It can be investigated that the gain of the proposed antenna is reduced due to compactness by introducing meander lines and fractal inductor in the antenna.

5.3.4 Design of conformal antenna loaded with slotted bottom patch

To match the impedance, a novel bottom patch is proposed as shown in Figure 5.22. The bottom patch can be placed either on the lower side ' L_1' or on the upper side ' L_3'. The input reflection coefficients at two locations on the bottom patch, with and without slot, are shown in

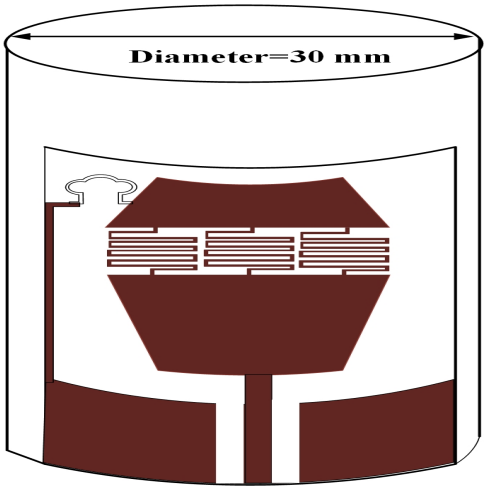

Figure 5.24 Proposed cylindrical conformal antenna with a 15 mm radius of curvature

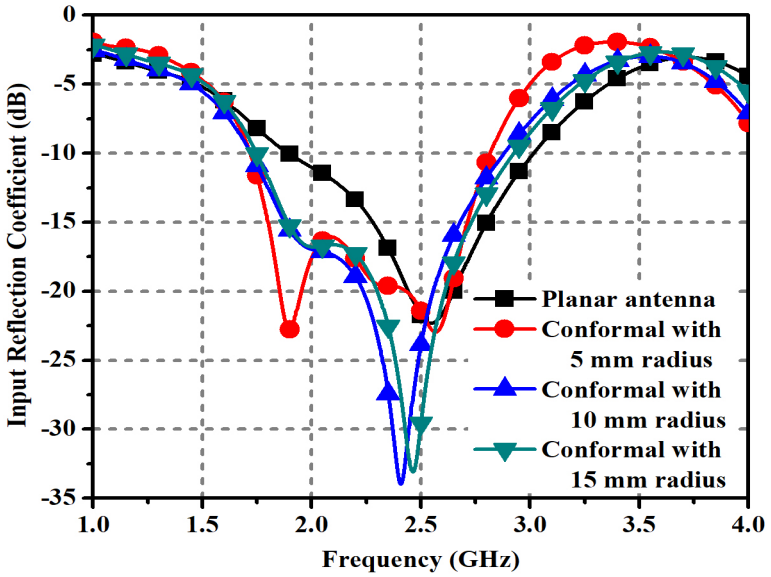

Figure 5.25 The comparison between simulated input reflection coefficient of the planar and conformal antenna with 5, 10 and 15 mm radius of curvature

Figure 5.23. It can be observed that bottom patch below L_3 with slot has less input reflection coefficient at the resonant frequency, hence it is considered in the proposed design.

The proposed antenna which is conformal on a cylindrical device of radius 15 mm is shown in Figure 5.24. The input reflection coefficients of conformal antenna on different radii of curvature are shown in Figure 5.25. The small changes in resonant frequency of the proposed cylindrical conformal antenna from the respective planar antenna is because of bending into conformal, resulting in a change in the effective resonant length. The resonant frequency decreases as the radius of curvature decreases, which is demonstrated in Figure 5.25. In the

Table 5.2 Optimised dimension of the proposed conformal antenna.

Parameters	**Size (mm)**	**Parameters**	**Size (mm**
L	40	g_1	2.5
W	30	L_b	9
L_1	14.9	W_{b1}	4
L_2	4	W_{b2}	16.2
L_3	7.52	S	0.2
W_1	10	R_1	1
W_2	0.5	r_1	0.8
W_f	2.4	R_2	0.6
L_g	11	r_2	0.4
W_g	13.45	D	1.6
g	0.35	L_4	22.3

present paper, the variations of the resonant frequency of conformal antenna on cylinders of different radii are also established. The optimized dimensions of the planar version of the proposed conformal antenna are shown in Table 5.2.

5.3.5 Design of conformal dual-band antenna loaded with meander lines as parasitic elements on patch

The dual-band characteristics of the proposed antenna are obtained by incorporating two meander lines unit cells as parasitic elements. A novel concept of meander lines as parasitic elements is placed in the antenna design for obtaining additional resonant frequency band. The parasitic elements are placed on the right and left most part of the top patch as shown in Figure

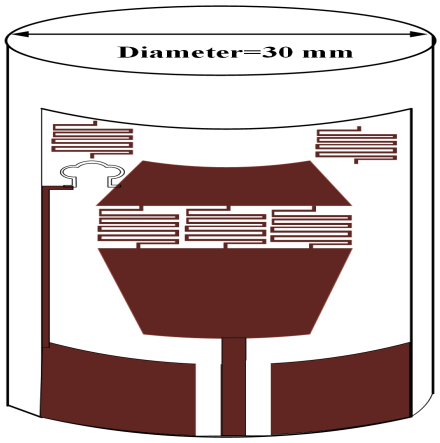

Figure 5.26 Proposed cylindrical conformal dual-band antenna with a 15 mm radius of curvature

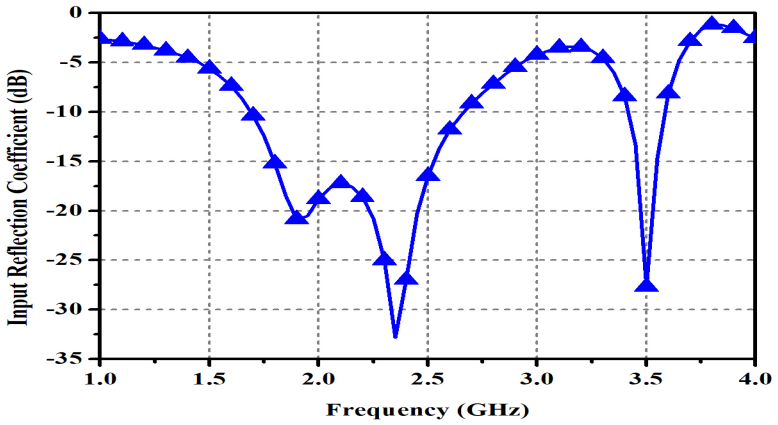

Figure 5.27 The input reflection coefficient (S_{11}) of the proposed conformal dual-band antenna

5.26. The antenna is resonating at 2.45 GHz without parasitic elements as shown in Figure 5.23. The proposed cylindrical conformal antenna is operating in the second band at 3.5 GHz along with the first band at 2.45 GHz as shown in Figure 5.27 by loading meander lines as parasitic elements on patch.

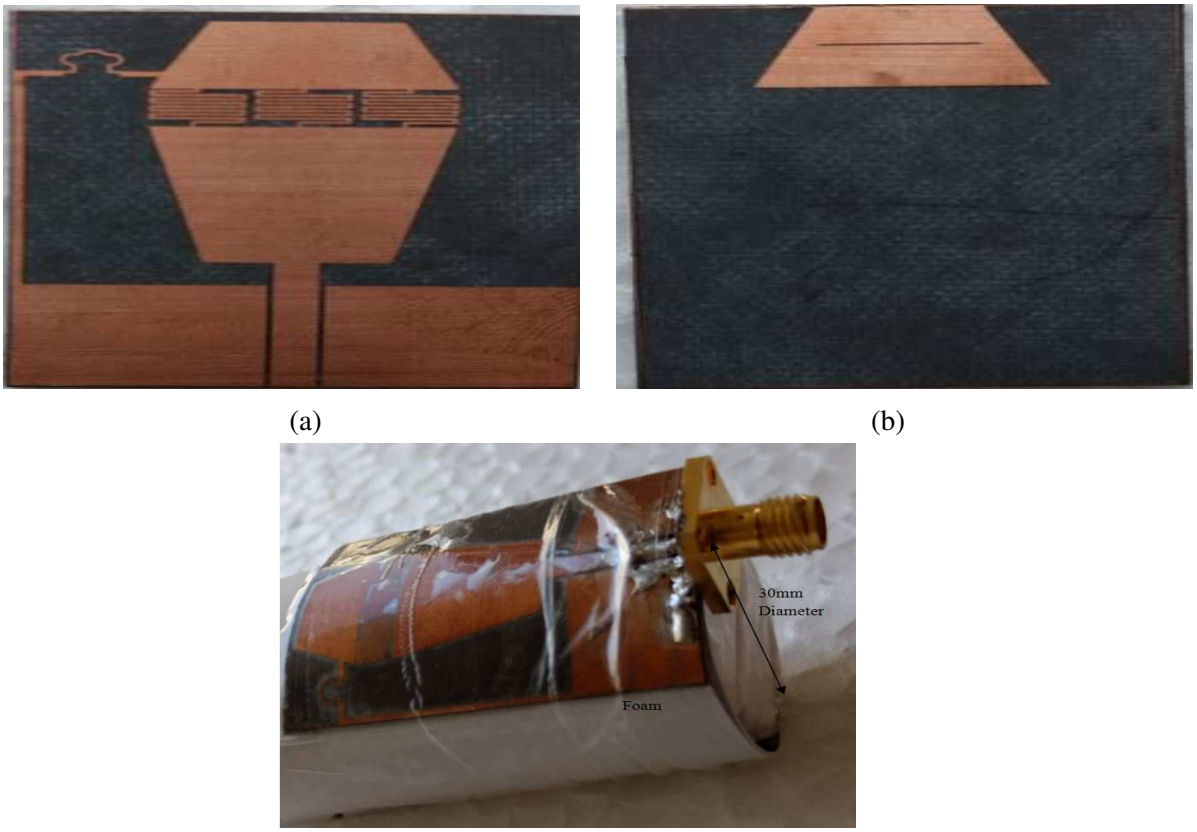

(a) (b)

(c)

Figure 5.28 Photographs of fabricated antenna (a) top view of planar antenna (b) bottom view of planar antenna (c) top view of proposed conformal antenna with 15 mm radius of curvature.

5.4 Results and Discussion

The prototype of the antenna is fabricated using LPKF milling machine S100 on a flat substrate and it is rolled up on a cylindrical shape foam of radius 15 mm as shown in Figure 5.28 and 5.29. The foam material is used as mechanical support and has negligible radiation effect on the antenna.

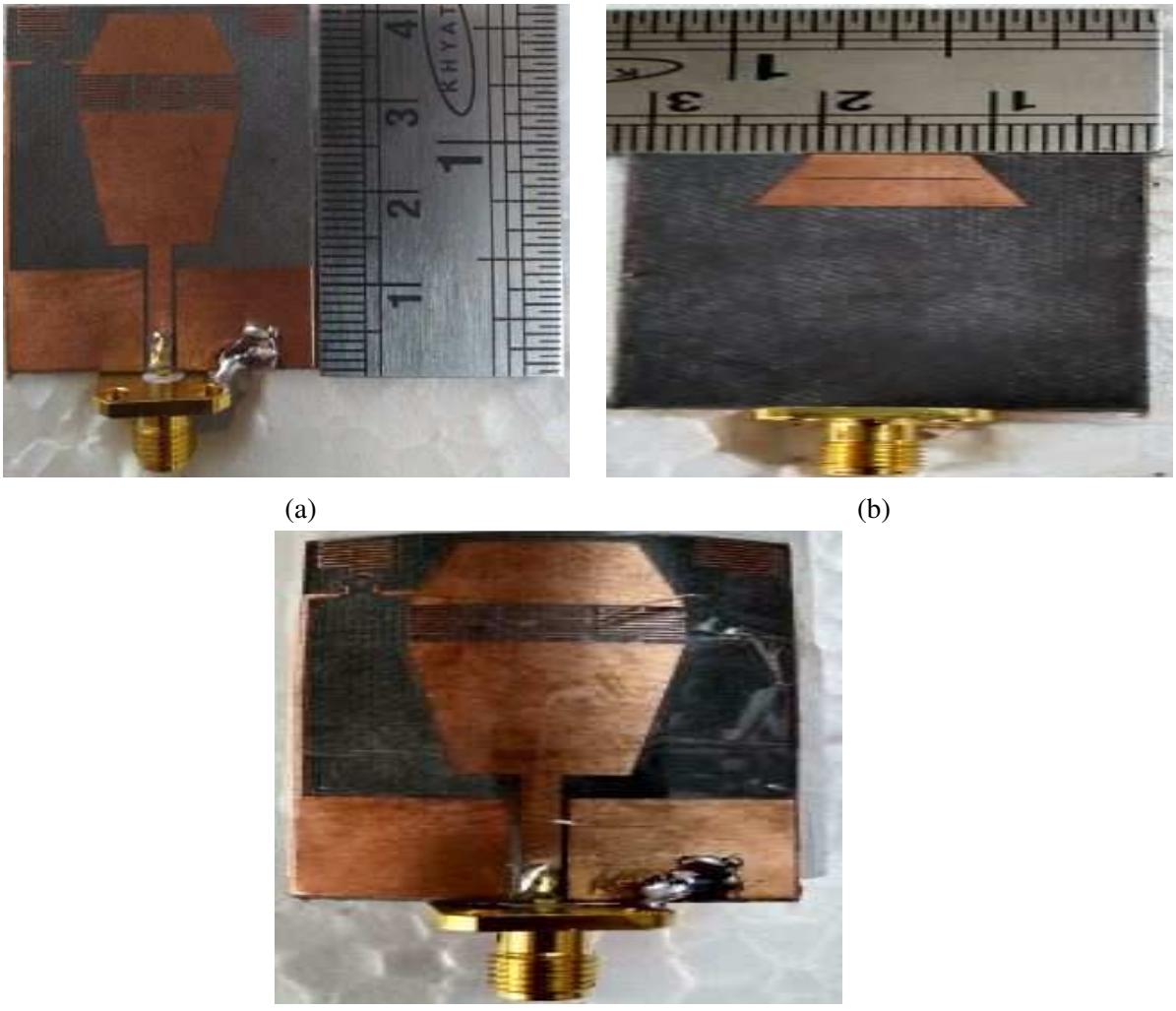

(a) (b)

(c)

Figure 5.29 Photographs of dual-band fabricated antenna (a) top view of planar antenna (b) bottom view of planar antenna (c) top view of proposed conformal antenna with 15 mm radius of curvature.

Both measured and simulated input reflection coefficients (S_{11}) of the proposed cylindrical conformal antenna with and without parasitic elements of a 15 mm radius of curvature are illustrated in Figure 5.30. The simulated input reflection coefficient is obtained using CST STUDIO SUITE 2016 by considering discrete port type with 50 Ω impedance. A four hole round shaped pin with female type SMA connector which is working in the range DC to 18

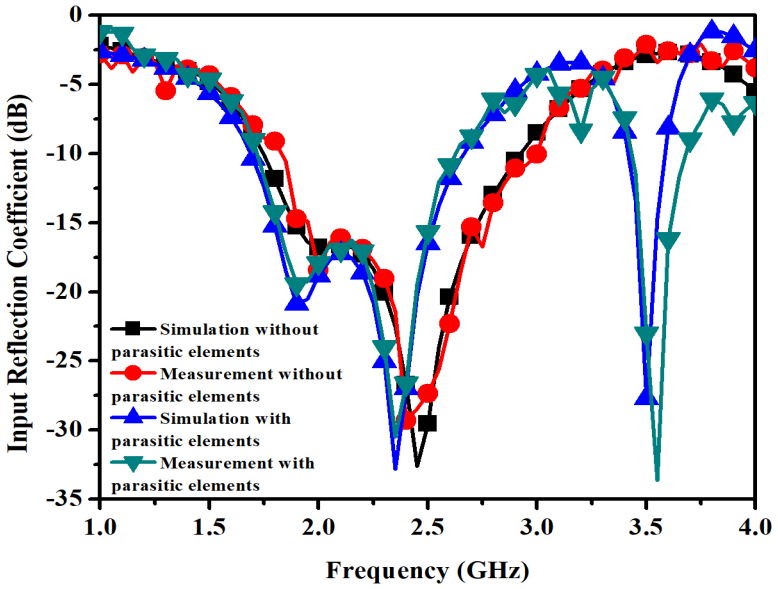

Figure 5.30 The input reflection coefficient of the proposed conformal antenna with and without parasitic elements

GHz is connected to the fabricated antenna. The antennas are measured utilizing HP vector network analyzer within the frequency range of 130 MHz to 13 GHz. The wideband response of the conformal antenna without parasitic elements is achieved by properly choosing the physical

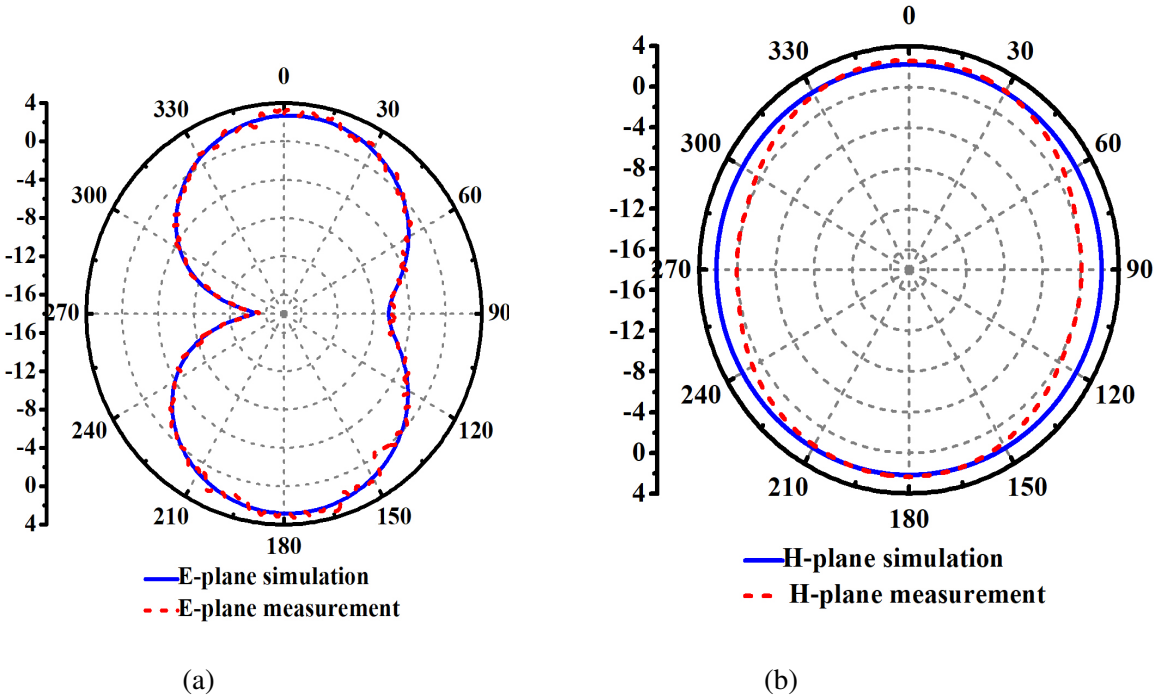

Figure 5.31 Radiation pattern at 2.45 GHz (a)E-plane pattern (b) H-plane pattern.

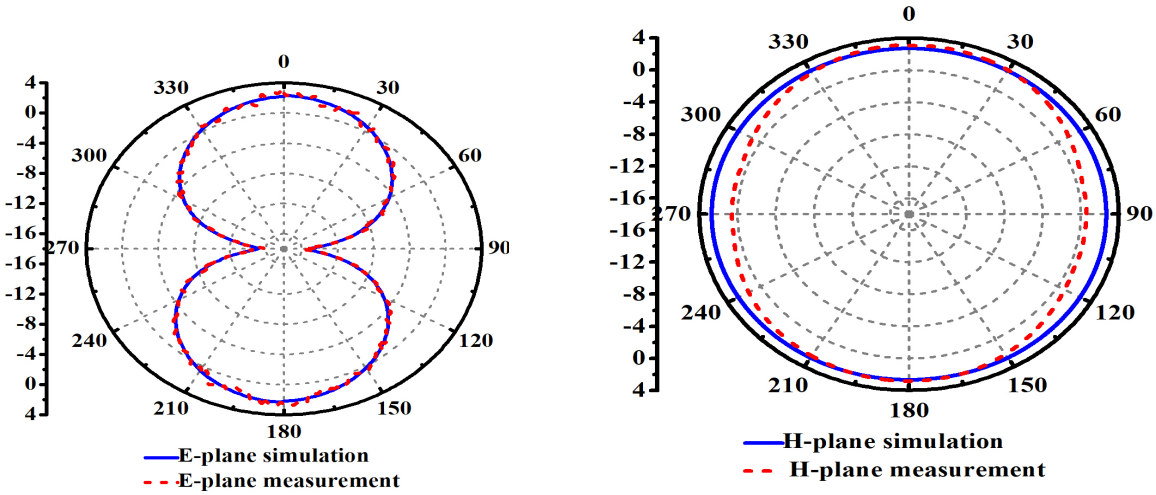

(a) (b)

Figure 5.32 Radiation pattern at 3.45 GHz (a) E-plane pattern (b) H-plane pattern.

dimensions of unit cells and fractal inductor. There is good agreement between simulation and measurement results. The -10 dB input reflection coefficient bandwidth is around 1.17 GHz (1.75 2.92) GHz with a fractional bandwidth of 50.1%. The dual-band characteristic of the conformal antenna is achieved due to the presence of meander lines as parasitic elements. The -10 dB input reflection coefficient bandwidth of the first band is around 970 MHz (1.69 to 2.66) GHz with a fractional bandwidth of 44.5% and for the second band it is around 160 MHz (3.42-3.58) GHz with a fractional bandwidth of 4.5%.

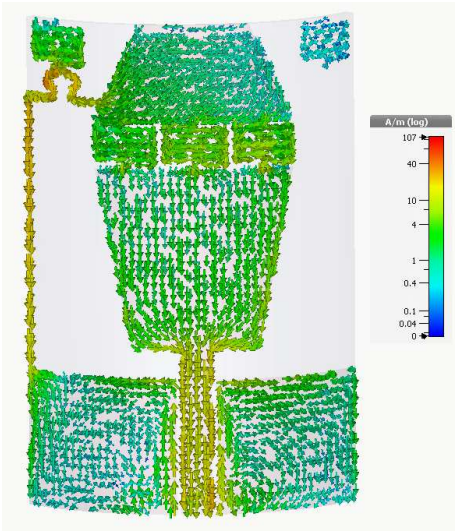

Figure 5.33 The surface current distribution of proposed conformal antenna at 2.45 GHz

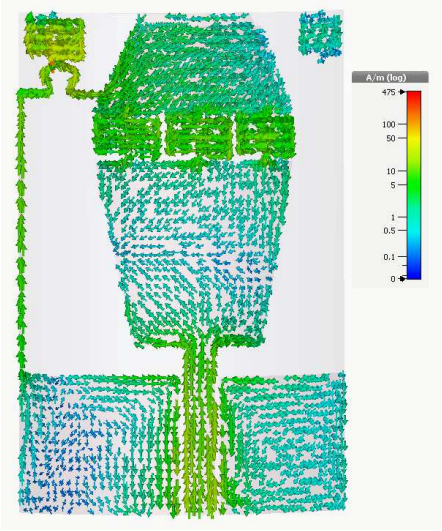

Figure 5.34 The surface current distribution of proposed conformal antenna at 3.5 GHz

The radiation patterns at 2.45 and 3.5 GHz are described in Figure 5.31 and 5.32 respectively for both H-plane and E-plane. The two-dimensional patterns of the antenna are obtained in an anechoic chamber. To measure the radiation pattern, the standard horn antenna is used at the transmitter and the conformal antenna is connected to the receiver. The conformal antenna radiation pattern is measured in receiving mode. A figure of eight shape radiation pattern is obtained in E-plane and omnidirectional pattern in H-plane at the 2.45 as well as 3.5 GHz, respectively. The surface current distribution at 2.45 and 3.5 GHz are shown in Figure 5.33 and 5.34 respectively. It shows how the meander lines on the patch and parasitic meander lines contribute to radiation as the surface current is densely distributed in those areas. In addition, the fractal inductor is also contributing to the radiation part. The surface current distribution

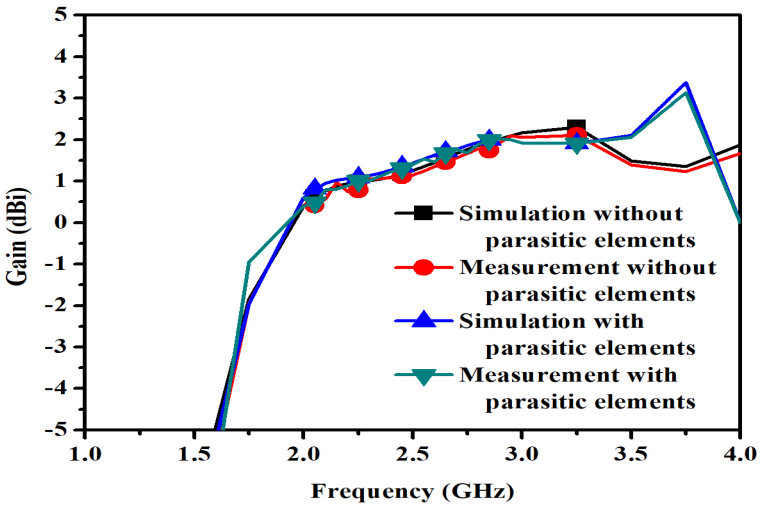

Figure 5.35 The gain of the proposed conformal antenna with and without parasitic elements

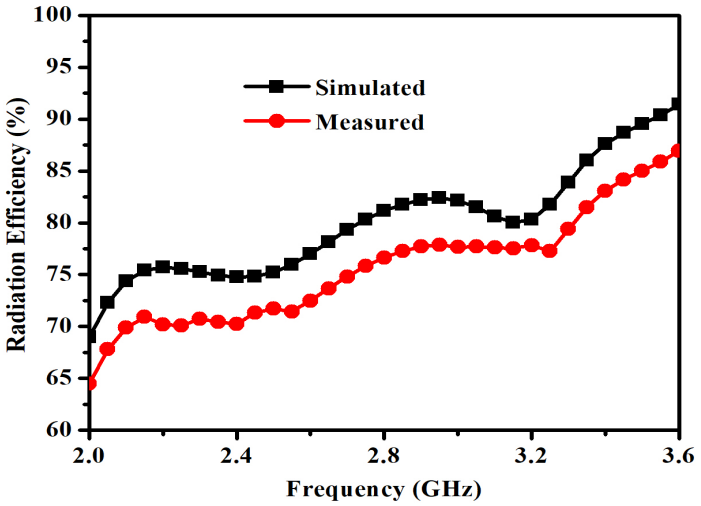

Figure 5.36 The radiation efficiency of the proposed conformal antenna with and without parasitic elements

is also plotted in Figure 5.34 at a frequency of 3.5 GHz for the same antenna to support this discussion. The phase variation of surface current on meander lines is also shown in Figure 5.33 and 5.34. The gain of antenna at 2.45 and 3.5 GHz is shown in Figure 5.35 as 1.26 and 2.2 dBi respectively.

Table 5.3 Comparison of the proposed cylindrical conformal dual-band antenna with planar antenna existing in the literature.

Antenna	**Size (mm^2)**	**Frequency (GHz)**	**-10dB bandwidth**	**Gain (dBi)**	**Radiation efficiency (%)**	**Polarization**
Proposed work	40 × 30	2.45, 3.5	44.5, 4.5	1.26, 2.2	70, 86	LP
[108]	40 × 40	2.93, 5.68	35.21, 6.86	4	89.55, 83.48	LP
[109]	30 × 20	2.975	41.8	2	-	CP
[110]	42.5 × 48	2.38 to 2.75, 4.05 to 6.38	14.4, 44.67	0.88 to 1.4, 3.9 to 4.5	-	CP
[115]	50 × 50	3.30	3.1	0.79	65.8	LP
[116]	32.2 × 20	2.16	15.1	1.62	72	LP
[117]	40 × 100	1.99	20.3	1.05 to 3.35	41.5 to 66.6	LP
[118]	70 × 44	2.5, 5.8	22.8, 10.8	1.5, 4.4	> 94, > 92.1	Dual polarised
[119]	39 × 25	2.5 (ZOR) and 3.32 (POR)	39	1.32	75 (ZOR), 91 (POR)	LP

The simulated and measured results of the radiation efficiency for the proposed conformal dual-band antenna are shown in Figure 5.36. The radiation efficiency (e_{rad}) is calculated with the antenna gain (G) and directivity (D), e_{rad}= G/(D), which is approximately around 75 and 90 % at 2.45 and 3.5 GHz respectively. The measured radiation efficiency is around 70 and 86 % at 2.45 and 3.5 GHz respectively, indicating that low radiation losses are achieved by the antenna. In practical cases, some of the power fed to the antenna terminals is always lost. Moreover, energy is lost in the dielectric material of the antenna and creates unintended heat. Together, these losses lead to situations where the antenna radiated efficiency in actual operation which is always less than the ideal simulation results.

The overall performance of the proposed conformal dual-band antenna is compared with that of previously reported planar antennas [108-119] and [115-119] in Table 5.3. The proposed antenna is realized without vias and it also provides competitively wide bandwidth in the first band. Moreover, the size is also more compact than for antennas published in [108], [110], [115], [117], and [118].

5.5 Conclusion

A compact metamaterial based cylindrical conformal dual-band antenna is designed, fabricated and validated experimentally. The proposed cylindrical conformal antenna with 15 mm radius of curvature is compared with existing planar antenna. It offers a wideband fractional bandwidth of about 44.5% in the first band and 4.5% in the second band which covers the bandwidth requirements of the standard Wi-Fi and WiMAX applications respectively. There is good agreement between simulation and experimental results. Furthermore, the antenna has an omnidirectional radiation pattern in both bands with a gain of about 1.26 and 2.2 dBi respectively. The measured radiation efficiency is 70 and 86 % at 2.45 and 3.5 GHz respectively.

Chapter 6

Conclusions and Scope of Work

6.1 Research findings of the thesis

In the present thesis, cylindrical conformal antennas with omnidirectional and directional radiation pattern are investigated. The analysis and design of conformal antennas and performance improvement in terms of compact size, bandwidth and gain enhancement are illustrated. The design of cylindrical conformal antennas are carefully considered for GPS, Wi-Fi and WiMAX applications. Since, the fabrication of conformal antenna is somehow difficult as compared with planar one, so selection of the dielectric material for the cylindrical conformal antenna also plays a significant rule to get accurate results. Therefore, dielectric material like RT/duroid 5880 of thickness 0.787 mm which is easy to bend into cylindrical conformal is used for fabrication of prototype antenna throughout the thesis.

In chapter 2, cylindrical conformal antennas with different slots on a cylinder of 60 mm radius of curvature are designed and fabricated for GPS application. The designed cylindrical conformal antenna with dumbbell-shaped slot and partial ground offers a good wideband fractional bandwidth of about 75.94% with a gain of about 2.09 to 4.9 dBi within the operating frequency range of 1.056 to 2.349 GHz. The cylindrical conformal antenna with printed cross-slot on the patch and partial ground plane achieves wideband fractional bandwidth of about 79.28% with a gain of about 2.37 to 5.33 dBi within the operating frequency range of 1.09 to 2.525 GHz. A bow-tie shaped wideband conformal antenna with a wide slot is designed, simulated and fabricated. The operating bandwidth of the proposed bow-tie shaped conformal antenna with wide-slot is obtained as 81.4% with a gain of about 3.5 to 4.78 dBi in the whole

operating frequency range of 0.75 to 1.78 GHz. All the designed antennas have improved gain compared to existing literature. By incorporating different slots on radiating patch, better impedance matching is obtained.The wideband characteristics are obtained by incorporating partial ground concept and wide slot on ground plane.

Chapter 3 presents the design of fractal based planar as well as a conformal antenna with a 60 mm radius of curvature. The designed cylindrical conformal antenna with Koch fractal is operating at 1.575 GHz and with a bandwidth of 20 MHz. The proposed conformal antenna with Minkowski fractal is compared with the existing references of the planar antenna at GPS frequency. It offers a good wideband fractional bandwidth of about 43.72%. Furthermore, the antenna size is reduced by 34% and has an omnidirectional radiation pattern with a gain of about 2.3dBi to 3.5dBi within the operating frequency range of 1.09 GHz to 1.7 GHz. Fractal concepts are implemented on radiating patch for compactness of the proposed cylindrical conformal antenna. The partial ground concept is used to enhance the bandwidth.

Chapter 4 deals with the gain enhancement of conformal wideband antenna with parasitic elements and low index metamaterial for WiMAX application. A wideband conformal antenna with directional radiation pattern is proposed as a basic antenna which consists of an array of three fork shaped elements. Three printed triangular shaped metallic parasitic elements are incorporated on both sides of substrate in the unfilled space of fork shaped element for enhancement of the conformal antenna's directional properties. The half power bandwidth (HPBW) of basic antenna in H-plane is around 123^0 which decreases to 108^0, while in E-plane it decreases from 57^0 to 55^0at 3.3 GHz after loading with parasitic elements. Similarly at 3.5 GHz, the HPBW of basic antenna is around 117^0 which decreases to 100^0 in H-plane, though in E-plane it decreases from $58^0$to 54^0. For further enhancement of the directional properties of the proposed cylindrical conformal antenna, the substrate length is extended up to 15 mm to integrate the metamaterial unit cell in both sides of the substrate. As a result, the proposed antenna is more directive with narrow beamwidth and the half power beamwidth is reduced by 24^0 in the H-plane. The gain of the proposed conformal antenna which is integrated with parasitic elements and metamaterial unit cells is enhanced by 1.8 dBi compared to basic conformal antenna. The impedance bandwidth of the proposed conformal antenna achieves a bandwidth of 22.3% from 3.1 to 3.88 GHz.

Cylindrical conformal antennas are designed for Wi-Fi and WiMAX applications in Chapter 5. The conformal antennas with dual U slot on the patch are designed with a various radius of curvatures for Wi-Fi application. The conformal antenna is designed with a single band at 2.45 GHz which can be suitable for Wi-Fi applications. Also, a novel metamaterial inspired com-

pact cylindrical conformal dual-band antenna with a shunt fractal inductor and a bottom patch is designed. The metamaterial concept is applied for modification and compactness, where the size of the antenna can be miniaturized by modifying the patch structure with metamaterial unit cells. To improve the operating bandwidth in the first band i.e at 2.45 GHz, a shunt fractal inductor with large inductance is designed. A similar patch with a slot along the bottom side is additionally used for better impedance matching. The second band at 3.5 GHz is obtained due to the loading of two meander line unit cells on the patch as parasitic elements. The designed conformal antenna is placed on a 15 mm radius cylinder whose equivalent planar dimension is $0.48\lambda_g \times 0.36\lambda_g$ (where λ_g is the guided wavelength). Measurement results showed that the proposed cylindrical conformal antenna achieves a wideband -10 dB fractional bandwidth of 44.5% and a gain of 1.26 dBi at the operating frequency of 2.45 GHz and 4.5% of bandwidth and a gain of 2.2 dBi at the 3.5 GHz. The radiation efficiency is 70 and 86% at the said frequencies respectively.

At the end of the chapter, all the designed antennas are compared in terms of size, bandwidth and gain.

6.2 Future scope

In the 21^{st} century, the cylindrical conformal antennas are widely used for commercial and military applications. Designed and presented cylindrical conformal antennas in this thesis are good candidates for GPS, Wi-Fi and WiMAX applications. The proposed conformal antenna structures are not applied over the other shapes of conformal except cylindrical structure. For the future work, the present work can be extended for conformal geometries for military and commercial applications. The work can be extended to conformal antenna array for different application. Implementation of the conformal beam steering antenna using metamaterial can be the future scope of the present work.

References

[1] Y. Huang and K. Boyle, *Antennas: from theory to practice*. John Wiley & Sons, 2008.

[2] C. A. Balanis, *Antenna theory: analysis and design*. John wiley & sons, 2016.

[3] J. R. James, *Handbook of microstrip antennas*. IET, 1989, vol. 1.

[4] D. R. Jackson and N. G. Alexopoulos, "Simple approximate formulas for input resistance, bandwidth, and efficiency of a resonant rectangular patch," *IEEE Transactions on Antennas and Propagation*, vol. 39, no. 3, pp. 407–410, 1991.

[5] R. Garg, P. Bhartia, I. J. Bahl, and A. Ittipiboon, *Microstrip antenna design handbook*. Artech house, 2001.

[6] Z. N. Chen and M. Y. W. Chia, *Broadband Planar Antennas*. Wiley Online Library, 2006.

[7] S. Schneider, C. Bozada, R. Dettmer, and J. Tenbarge, "Enabling technologies for future structurally integrated conformal apertures," in *IEEE Antennas and Propagation Society International Symposium. 2001 Digest. Held in conjunction with: USNC/URSI National Radio Science Meeting (Cat. No. 01CH37229)*, vol. 2. IEEE, 2001, pp. 330–333.

[8] M. Hopkins, J. Tuss, A. Lockyer, K. Alt, R. Kinslow, J. Kudva, M. Hopkins, J. Tuss, A. Lockyer, K. Alt *et al.*, "Smart skin conformal load-bearing antenna and other smart structures developments," in *38th Structures, Structural Dynamics, and Materials Conference*, 1997, p. 1163.

[9] D. Wingert and B. Howard, "Potential impact of smart electromagnetic antennas on aircraft performance and design," in *Proc. NATO Workshop on Smart Electromagnetic Antenna Structures*, 1996, pp. 1–10.

[10] R. E. Munson, "Conformal microstrip antennas," *Microwave Journal*, vol. 31, p. 91, 1988.

[11] L. Josefsson and P. Persson, *Conformal array antenna theory and design*. John wiley & sons, 2006, vol. 29.

[12] M. Kanno, T. Hashimura, T. Katada, M. Sato, K. Fukutani, and A. Suzuki, "Digital beam forming for conformal active array antenna," in *Proceedings of International Symposium on Phased Array Systems and Technology*. IEEE, 1996, pp. 37–40.

[13] G. Caille, E. Vourch, M. Martin, J. Mosig, and M. Polegre, "Conformal array antenna for observation platforms in low earth orbit," *IEEE Antennas and Propagation Magazine*, vol. 44, no. 3, pp. 103–104, 2002.

[14] E. A. Navarro, A. Luximon, I. J. Craddock, D. L. Paul, and M. Dean, "Multilayer and conformal antennas using synthetic dielectric substrates," *IEEE Transactions on Antennas and Propagation*, vol. 51, no. 4, pp. 905–908, 2003.

[15] H. Zhu, X. Liang, S. Ye, R. Jin, and J. Geng, "A cylindrically conformal array with enhanced axial radiation," *IEEE Antennas and Wireless Propagation Letters*, vol. 15, pp. 1653–1656, 2016.

[16] M. V. T. Heckler, J. da S Lacava, and L. Cividanes, "Design of a circularly polarized microstrip array mounted on a cylindrical surface," in *2005 IEEE Antennas and Propagation Society International Symposium*, vol. 2. IEEE, 2005, pp. 266–269.

[17] M. Xiaoping, G. Xueyuan *et al.*, "Design of cylindrical conformal microstrip gps antenna arrays," in *2009 International Conference on Microwave Technology and Computational Electromagnetics (ICMTCE 2009)*. IET, 2009, pp. 105–108.

[18] S. M. Saeed, C. A. Balanis, and C. R. Birtcher, "Inkjet-printed flexible reconfigurable antenna for conformal wlan/wimax wireless devices," *IEEE Antennas and Wireless Propagation Letters*, vol. 15, pp. 1979–1982, 2016.

[19] R. Zentner, Z. Sipus, N. Herscovici, and J. Bartolic, "Omnidirectional stacked patch antenna printed on circular cylindrical structure," in *IEEE Antennas and Propagation Society International Symposium (IEEE Cat. No. 02CH37313)*, vol. 2. IEEE, 2002, pp. 272–275.

[20] J.-H. Bang, W.-J. Kim, and B.-C. Ahn, "Two-element conformal antenna for multi-gnss reception," *IEEE Antennas and Wireless Propagation Letters*, vol. 16, pp. 796–799, 2016.

[21] N. Herscovici, Z. Sipus, and P.-S. Kildai, "The cylindrical omnidirectional patch antenna," in *IEEE Antennas and Propagation Society International Symposium 1997. Digest*, vol. 2. IEEE, 1997, pp. 924–927.

[22] K. A. Yinusa, "A dual-band conformal antenna for gnss applications in small cylindrical structures," *IEEE Antennas and Wireless Propagation Letters*, vol. 17, no. 6, pp. 1056–1059, 2018.

[23] R. Munson, "Conformal microstrip antennas and microstrip phased arrays," *IEEE Transactions on Antennas and propagation*, vol. 22, no. 1, pp. 74–78, 1974.

[24] X. Wang, M. Zhang, and S.-J. Wang, "Practicability analysis and application of pbg structures on cylindrical conformal microstrip antenna and array," *Progress In Electromagnetics Research*, vol. 115, pp. 495–507, 2011.

[25] Z. Zhang, X. Gao, W. Chen, Z. Feng, and M. F. Iskander, "Study of conformal switchable antenna system on cylindrical surface for isotropic coverage," *IEEE Transactions on Antennas and Propagation*, vol. 59, no. 3, pp. 776–783, 2010.

[26] Y. Bayram, Y. Zhou, B. S. Shim, S. Xu, J. Zhu, N. A. Kotov, and J. L. Volakis, "E-textile conductors and polymer composites for conformal lightweight antennas," *IEEE Transactions on Antennas and Propagation*, vol. 58, no. 8, pp. 2732–2736, 2010.

[27] C.-H. Ahn, Y.-J. Ren, and K. Chang, "A dual-polarized cylindrical conformal array antenna suitable for unmanned aerial vehicles," *International Journal of RF and Microwave Computer-Aided Engineering*, vol. 21, no. 1, pp. 91–98, 2011.

[28] J.-W. Niu and S.-S. Zhong, "Cylindrical conformal bow-tie microstrip antennas with small curvature radius," *Microwave and Optical Technology Letters*, vol. 39, no. 6, pp. 511–514, 2003.

[29] N. Herscovici, "New considerations in the design of microstrip antennas," *IEEE Transactions on Antennas and Propagation*, vol. 46, no. 6, pp. 807–812, 1998.

[30] K. Luk, X. Guo, K. Lee, and Y. Chow, "L-probe proximity fed u-slot patch antenna," *Electronics letters*, vol. 34, no. 19, pp. 1806–1807, 1998.

[31] Y.-X. Guo, C.-L. Mak, K.-M. Luk, and K.-F. Lee, "Analysis and design of l-probe proximity fed-patch antennas," *IEEE Transactions on Antennas and Propagation*, vol. 49, no. 2, pp. 145–149, 2001.

[32] M. G. de Aza, J. Zapata, and J. A. Encinar, "Broad-band cavity-backed and capacitively probe-fed microstrip patch arrays," *IEEE transactions on Antennas and Propagation*, vol. 48, no. 5, pp. 784–789, 2000.

[33] K.-L. Wong and Y.-F. Lin, "Small broadband rectangular microstrip antenna with chip-resistor loading," *Electronics Letters*, vol. 33, no. 19, pp. 1593–1594, 1997.

[34] T. Huynh and K.-F. Lee, "Single-layer single-patch wideband microstrip antenna," *Electronics letters*, vol. 31, no. 16, pp. 1310–1312, 1995.

[35] C.-K. Wu and K.-L. Wong, "Broadband microstrip antenna with directly coupled and parasitic patches," *Microwave and Optical Technology Letters*, vol. 22, no. 5, pp. 348–349, 1999.

[36] E. Chang, S. Long, and W. Richards, "An experimental investigation of electrically thick rectangular microstrip antennas," *IEEE Transactions on antennas and propagation*, vol. 34, no. 6, pp. 767–772, 1986.

[37] H. F. Pues and A. R. Van De Capelle, "An impedance-matching technique for increasing the bandwidth of microstrip antennas," *IEEE transactions on antennas and propagation*, vol. 37, no. 11, pp. 1345–1354, 1989.

[38] S.-Y. Ke, "Broadband proximity-coupled microstrip antennas with an h-shaped slot in the ground plane," in *IEEE Antennas and Propagation Society International Symposium (IEEE Cat. No. 02CH37313)*, vol. 2. IEEE, 2002, pp. 530–533.

[39] Y. Tawk, J. Costantine, and C. Christodoulou, "Reconfiguring the frequency and directive behavior of a printed v–shaped structure," *IEEE Transactions on Antennas and Propagation*, vol. 65, no. 5, pp. 2655–2660, 2017.

[40] G. Zhai, Y. Cheng, Q. Yin, S. Zhu, and J. Gao, "Gain enhancement of printed log-periodic dipole array antenna using director cell," *IEEE Transactions on Antennas and Propagation*, vol. 62, no. 11, pp. 5915–5919, 2014.

[41] J. H. Kim, C.-H. Ahn, and J.-K. Bang, "Antenna gain enhancement using a holey superstrate," *IEEE Transactions on Antennas and Propagation*, vol. 64, no. 3, pp. 1164–1167, 2016.

[42] S. Enoch, G. Tayeb, P. Sabouroux, N. Guérin, and P. Vincent, "A metamaterial for directive emission," *Physical Review Letters*, vol. 89, no. 21, p. 213902, 2002.

[43] R. Chair, K. Lee, C. Mak, K. Luk, and A. Kishk, "Wideband half u-slot patch antennas with shorting pin and shorting wall," in *IEEE Antennas and Propagation Society Symposium, 2004.*, vol. 4. IEEE, 2004, pp. 4132–4135.

[44] T. Lo, Y. Hwang, E. Lam, B. Lee *et al.*, "Miniature aperture-coupled microstrip antenna of very high permittivity," *Electronics Letters*, vol. 33, no. 1, pp. 9–10, 1997.

[45] J. H. Lu and K. L. Wong, "Slot-loaded meandered rectangular microstrip antenna with compact dual-frequency operation," *Electronics Letters*, vol. 34, no. 11, pp. 1048–1049, 1998.

[46] J.-Y. Sze and K.-L. Wong, "Bandwidth enhancement of a microstrip-line-fed printed wide-slot antenna," *IEEE Transactions on Antennas and Propagation*, vol. 49, no. 7, pp. 1020–1024, 2001.

[47] Y.-W. Jang, "Experimental study of large bandwidth three-offset microstripline-fed slot antenna," *IEEE microwave and wireless components letters*, vol. 11, no. 10, pp. 425–427, 2001.

[48] M. K. Kim, K. Kim, Y. H. Suh, and I. Park, "A t-shaped microstrip-line-fed wide slot antenna," in *IEEE Antennas and Propagation Society International Symposium. Transmitting Waves of Progress to the Next Millennium. 2000 Digest. Held in conjunction with: USNC/URSI National Radio Science Meeting (C*, vol. 3. IEEE, 2000, pp. 1500–1503.

[49] P. H. Rao, "Feed effects on the dimensions of wideband slot antennas," *Microwave and Optical Technology Letters*, vol. 40, no. 1, pp. 77–79, 2004.

[50] P. Rao, V. Fusco, and R. Cahill, "Linearly polarised radial stub fed high performance wideband slot antenna," *Electronics Letters*, vol. 37, no. 6, pp. 335–337, 2001.

[51] Y. Jang, "Broadband cross-shaped microstrip-fed slot antenna," *Electronics Letters*, vol. 36, no. 25, pp. 2056–2057, 2000.

[52] M. Yang and Y. Chen, "A novel u-shaped planar microstrip antenna for dual-frequency mobile telephone communications," *IEEE Transactions on Antennas and Propagation*, vol. 49, no. 6, pp. 1002–1004, 2001.

[53] Y. Liu, K. Lau, Q. Xue, and C. Chan, "Experimental studies of printed wide-slot antenna for wide-band applications," *IEEE Antennas and Wireless Propagation Letters*, vol. 3, no. 1, pp. 273–275, 2004.

[54] P. Li, J. Liang, and X. Chen, "Ultra-wideband elliptical slot antenna fed by tapered microstrip line with u-shaped tuning stub," *Microwave and optical technology letters*, vol. 47, no. 2, pp. 140–143, 2005.

[55] A. Dastranj, A. Imani, and M. Naser-Moghaddasi, "Printed wide-slot antenna for wide-band applications," *IEEE Transactions on Antennas and Propagation*, vol. 56, no. 10, pp. 3097–3102, 2008.

[56] Z. Li, L. Tan, X. Kang, J. Su, Q. Guo, Y. L. Yang, and J. Wang, "A novel wideband end-fire conformal antenna array mounted on a dielectric cone." *Applied Computational Electromagnetics Society Journal*, vol. 31, no. 8, 2016.

[57] R. Bala, R. Singh, A. Marwaha, and S. Marwaha, "Wearable graphene based curved patch antenna for medical telemetry applications." *Applied Computational Electromagnetics Society Journal*, vol. 31, no. 5, 2016.

[58] H.-M. Chen, Y.-F. Lin, C.-H. Chen, C.-Y. Pan, and Y.-S. Cai, "Miniature folded patch gps antenna for vehicle communication devices," *IEEE transactions on antennas and propagation*, vol. 63, no. 5, pp. 1891–1898, 2014.

[59] M. Bilgic and K. Yegin, "Modified annular ring antenna for gps and sdars automotive applications," *IEEE Antennas And Wireless Propagation Letters*, vol. 15, pp. 1442–1445, 2015.

[60] E. Wang and Q. Liu, "Gps patch antenna loaded with fractal ebg structure using organic magnetic substrate," *Progress In Electromagnetics Research*, vol. 58, pp. 23–28, 2016.

[61] M.-S. Wang, X.-Q. Zhu, Y.-X. Guo, and W. Wu, "Compact circularly polarized patch antenna with wide axial-ratio beamwidth," *IEEE Antennas and Wireless Propagation Letters*, vol. 17, no. 4, pp. 714–718, 2018.

[62] Wang, Meng-Shuang, Zhu, Xiao-Qi and Guo, Yong-Xin, and Wu, Wen, "Miniaturized dual-band circularly polarized quadruple inverted-f antenna for gps applications," *IEEE Antennas and Wireless Propagation Letters*, vol. 17, no. 6, pp. 1109–1113, 2018.

[63] V. Pathak, S. Thornwall, M. Krier, S. Rowson, G. Poilasne, and L. Desclos, "Mobile handset system performance comparison of a linearly polarized gps internal antenna with a circularly polarized antenna," in *IEEE Antennas and Propagation Society International Symposium. Digest. Held in conjunction with: USNC/CNC/URSI North American Radio Sci. Meeting (Cat. No. 03CH37450)*, vol. 3. IEEE, 2003, pp. 666–669.

[64] F. Scire-Scappuzzo and S. N. Makarov, "A low-multipath wideband gps antenna with cutoff or non-cutoff corrugated ground plane," *IEEE transactions on antennas and propagation*, vol. 57, no. 1, pp. 33–46, 2009.

[65] M. Albooyeh, N. Kamjani, and M. Shobeyri, "A novel cross-slot geometry to improve impedance bandwidth of microstrip antennas," *Progress In Electromagnetics Research*, vol. 4, pp. 63–72, 2008.

[66] A. C. Durgun, C. A. Balanis, C. R. Birtcher, and D. R. Allee, "Design, simulation, fabrication and testing of flexible bow-tie antennas," *IEEE Transactions on Antennas and Propagation*, vol. 59, no. 12, pp. 4425–4435, 2011.

[67] Durgun, Ahmet C, Balanis, Constantine A, Birtcher, Craig R, and Allee, David R, "Radiation characteristics of a flexible bow-tie antenna," in *2011 IEEE International Symposium on Antennas and Propagation (APSURSI)*. IEEE, 2011, pp. 1239–1242.

[68] J. George, M. Deepukumar, C. Aanandan, P. Mohanan, and K. Nair, "New compact microstrip antenna," *Electronics Letters*, vol. 32, no. 6, pp. 508–509, 1996.

[69] B. E. Garibello and S. E. Barbin, "A single element compact printed bowtie antenna enlarged bandwidth," in *SBMO/IEEE MTT-S International Conference on Microwave and Optoelectronics, 2005.* IEEE, 2005, pp. 354–358.

[70] H. L. Dholakiya and D. A. Pujara, "Improving the bandwidth of a microstrip antenna with a circular-shaped fractal slot," *Microwave and Optical Technology Letters*, vol. 55, no. 4, pp. 786–789, 2013.

[71] A. Karmakar, R. Ghatak, D. Poddar, and U. Banerjee, "Complementary stacked patch antenna with fractal shape defect for wideband characteristics," *Microwave and Optical Technology Letters*, vol. 56, no. 4, pp. 944–947, 2014.

[72] C. Mahatthanajatuphat, S. Saleekaw, P. Akkaraekthalin, and M. Krairiksh, "A rhombic patch monopole antenna with modified minkowski fractal geometry for umts, wlan, and mobile wimax application," *Progress In Electromagnetics Research*, vol. 89, pp. 57–74, 2009.

[73] R. Ataeiseresht, C. Ghobadi, and J. Nourinia, "A novel analysis of minkowski fractal microstrip patch antenna," *Journal of Electromagnetic Waves and Applications*, vol. 20, no. 8, pp. 1115–1127, 2006.

[74] S. Manafi and H. Deng, "Design of a small modified minkowski fractal antenna for passive deep brain stimulation implants," *International Journal of Antennas and Propagation*, vol. 2014, 2014.

[75] J. Brégains, L. Castedo, and F. Ares-Pena, "A wimax conformal broad-beam antenna [antenna designer's notebook]," *IEEE Antennas and Propagation Magazine*, vol. 52, no. 6, pp. 106–109, 2010.

[76] C. Meagher, R. Olsen, C. Cirullo, R. C. Ferro, N. Stevens, and J. Yu, "Directional ad hoc networking technology (dante) performance at sea," in *2011-MILCOM 2011 Military Communications Conference*. IEEE, 2011, pp. 950–955.

[77] M. S. M. Mollaei, E. Zanganeh, and M. F. Farahani, "Enhancement of patch antenna gain using cylindrical shell-shaped superstrate," *IEEE Antennas and Wireless Propagation Letters*, vol. 16, pp. 2570–2573, 2017.

[78] T. Cao, C.-w. Wei, R. E. Simpson, L. Zhang, and M. J. Cryan, "Broadband polarization-independent perfect absorber using a phase-change metamaterial at visible frequencies," *Scientific reports*, vol. 4, p. 3955, 2014.

[79] N. Landy and D. R. Smith, "A full-parameter unidirectional metamaterial cloak for microwaves," *Nature materials*, vol. 12, no. 1, p. 25, 2013.

[80] K. Song, S.-H. Lee, K. Kim, S. Hur, and J. Kim, "Emission enhancement of sound emitters using an acoustic metamaterial cavity," *Scientific reports*, vol. 4, p. 4165, 2014.

[81] R. Liu, Q. Cheng, T. Hand, J. J. Mock, T. J. Cui, S. A. Cummer, and D. R. Smith, "Experimental demonstration of electromagnetic tunneling through an epsilon-near-zero metamaterial at microwave frequencies," *Physical review letters*, vol. 100, no. 2, p. 023903, 2008.

[82] W. X. Jiang, C.-W. Qiu, T. C. Han, Q. Cheng, H. F. Ma, S. Zhang, and T. J. Cui, "Broadband all-dielectric magnifying lens for far-field high-resolution imaging," *Advanced Materials*, vol. 25, no. 48, pp. 6963–6968, 2013.

[83] H. Zhou, Z. Pei, S. Qu, S. Zhang, J. Wang, Z. Duan, H. Ma, and Z. Xu, "A novel high-directivity microstrip patch antenna based on zero-index metamaterial," *IEEE Antennas and wireless propagation letters*, vol. 8, pp. 538–541, 2009.

[84] Z.-B. Weng, Y. Song, Y.-C. Jiao, and F.-S. Zhang, "A directive dual-band and dual-polarized antenna with zero index metamaterial," *Microwave and Optical Technology Letters*, vol. 50, no. 11, pp. 2902–2904, 2008.

[85] Y. Liu, X. Guo, S. Gu, and X. Zhao, "Zero index metamaterial for designing high-gain patch antenna," *International Journal of Antennas and Propagation*, vol. 2013, 2013.

[86] D. Li, Z. Szabó, X. Qing, E.-P. Li, and Z. N. Chen, "A high gain antenna with an optimized metamaterial inspired superstrate," *IEEE transactions on antennas and propagation*, vol. 60, no. 12, pp. 6018–6023, 2012.

[87] Y.-L. Lv, F.-Y. Meng, J. Hua, and M.-L. Chen, "A wideband zero index metamaterial lens for directive emission based on z-shaped meta-atom," in *Proceedings of 2012 5th Global Symposium on Millimeter-Waves*. IEEE, 2012, pp. 418–421.

[88] Q. W. Hou, Y. Y. Su, and X. P. Zhao, "A high gain patch antenna based pn zero permeability metamaterial," *Microwave and Optical Technology Letters*, vol. 56, no. 5, pp. 1065–1069, 2014.

[89] P. K. Panda and D. Ghosh, "Isolation and gain enhancement of patch antennas using emnz superstrate," *AEU-International Journal of Electronics and Communications*, vol. 86, pp. 164–170, 2018.

[90] K. Yu, Y. Li, and X. L. Liu, "A high gain patch antenna using near zero-index metamaterial coating," in *2017 IEEE International Symposium on Antennas and Propagation & USNC/URSI National Radio Science Meeting*. IEEE, 2017, pp. 2175–2176.

[91] X.-J. Gao, T. Cai, and L. Zhu, "Enhancement of gain and directivity for microstrip antenna using negative permeability metamaterial," *AEU-International Journal of Electronics and Communications*, vol. 70, no. 7, pp. 880–885, 2016.

[92] K. Yu, Y. Li, and X. Liu, "Mutual coupling reduction of a mimo antenna array using 3-d novel meta-material structures," *Applied Computational Electromagnetics Society Journal*, vol. 33, no. 7, pp. 758–763, 2018.

[93] K. Yu, X. L. Liu, and Y. Li, "Mutual coupling reduction of microstrip patch antenna array using modified split ring resonator metamaterial structures," in *2017 IEEE International Symposium on Antennas and Propagation & USNC/URSI National Radio Science Meeting*. IEEE, 2017, pp. 2287–2288.

[94] B. Hazarika, B. Basu, and J. Kumar, "A multi-layered dual-band on-body conformal integrated antenna for wban communication," *AEU-International Journal of Electronics and Communications*, vol. 95, pp. 226–235, 2018.

[95] B. Zhou, H. Li, X. Zou, and T.-J. Cui, "Broadband and high-gain planar vivaldi antennas based on inhomogeneous anisotropic zero-index metamaterials," *Progress In Electromagnetics Research*, vol. 120, pp. 235–247, 2011.

[96] S.-W. Qu, J.-L. Li, Q. Xue, and C.-H. Chan, "Wideband periodic endfire antenna with bowtie dipoles," *IEEE Antennas and Wireless Propagation Letters*, vol. 7, pp. 314–317, 2008.

[97] R. S. Kshetrimayum, "A brief intro to metamaterials," *IEEE Potentials*, vol. 23, no. 5, pp. 44–46, 2004.

[98] J.-S. G. Hong and M. J. Lancaster, *Microstrip filters for RF/microwave applications*. John Wiley & Sons, 2004, vol. 167.

[99] X. Chen, T. M. Grzegorczyk, B.-I. Wu, J. Pacheco Jr, and J. A. Kong, "Robust method to retrieve the constitutive effective parameters of metamaterials," *Physical review E*, vol. 70, no. 1, p. 016608, 2004.

[100] D. Smith, D. Vier, T. Koschny, and C. Soukoulis, "Electromagnetic parameter retrieval from inhomogeneous metamaterials," *Physical review E*, vol. 71, no. 3, p. 036617, 2005.

[101] S. Jahani and Z. Jacob, "All-dielectric metamaterials," *Nature nanotechnology*, vol. 11, no. 1, p. 23, 2016.

[102] S. K. Mishra, R. K. Gupta, A. R. Vaidya, and J. Mukherjee, "Printed fork shaped dual band monopole antenna for bluetooth and uwb applications with 5.5 ghz wlan band notched characteristics," *Progress In Electromagnetics Research*, vol. 22, pp. 195–210, 2011.

[103] F. Xu, B. Wei, W. Li, J. Liu, W. Liu, and Y. Qiu, "Cylindrical conformal single-patch microstrip antennas based on three dimensional woven glass fiber/epoxy resin composites," *Composites Part B: Engineering*, vol. 78, pp. 331–337, 2015.

[104] D. Pozar, "Input impedance and mutual coupling of rectangular microstrip antennas," *IEEE Transactions on Antennas and Propagation*, vol. 30, no. 6, pp. 1191–1196, 1982.

[105] B. Jung, M.-J. Park, J. Byun, S. Han, and B. Lee, "Triple band internal antenna with a novel feeding structure," in *IEEE Antennas and Propagation Society Symposium, 2004.*, vol. 4. IEEE, 2004, pp. 4300–4303.

[106] R. B. Waterhouse, S. Targonski, and D. Kokotoff, "Design and performance of small printed antennas," *IEEE Transactions on Antennas and Propagation*, vol. 46, no. 11, pp. 1629–1633, 1998.

[107] H.-T. Chen, "Compact circular microstrip antenna with embedded chip resistor and capacitor," in *IEEE Antennas and Propagation Society International Symposium. 1998 Digest. Antennas: Gateways to the Global Network. Held in conjunction with: USNC/URSI National Radio Science Meeting (Cat. No. 98CH36*, vol. 3. IEEE, 1998, pp. 1356–1359.

[108] D. Sarkar and K. Srivastava, "Compact four-element srr-loaded dual-band mimo antenna for wlan/wimax/wifi/4g-lte and 5g applications," *Electronics Letters*, vol. 53, no. 25, pp. 1623–1624, 2017.

[109] X. Fang, G. Wen, D. Inserra, Y. Huang, and J. Li, "Compact wideband cpw-fed meandered-slot antenna with slotted y-shaped central element for wi-fi, wimax, and 5g applications," *IEEE Transactions on Antennas and Propagation*, vol. 66, no. 12, pp. 7395–7399, 2018.

[110] Q. Li, Y. Wei, C. Ding, M. Tan, L. Zhang, X. Lei, G. Wu, Z. Wang, Z. Lu, and Y. Gong, "Dual-band circularly polarised planar monopole antenna for wlan/wi-fi/bluetooth/wimax applications," *IET Microwaves, Antennas & Propagation*, vol. 12, no. 6, pp. 972–976, 2017.

[111] Y. P. Zhang, "Finite-difference time-domain analysis of integrated ceramic ball grid array package antenna for highly integrated wireless transceivers," *IEEE Transactions on Antennas and Propagation*, vol. 52, no. 2, pp. 435–442, 2004.

[112] D.-U. Sim, J.-I. Moon, and S.-O. Park, "An internal triple-band antenna for pcs/imt-2000/bluetooth applications," *IEEE Antennas and Wireless Propagation Letters*, vol. 3, pp. 23–25, 2004.

[113] R. Carrillo-Ramirez and R. W. Jackson, "A highly integrated millimeter-wave active antenna array using bcb and silicon substrate," *IEEE transactions on microwave theory and techniques*, vol. 52, no. 6, pp. 1648–1653, 2004.

[114] T. Jang, J. Choi, and S. Lim, "Compact coplanar waveguide (cpw)-fed zeroth-order resonant antennas with extended bandwidth and high efficiency on vialess single layer," *IEEE Transactions on Antennas and Propagation*, vol. 59, no. 2, pp. 363–372, 2010.

[115] J. Zhu and G. V. Eleftheriades, "A compact transmission-line metamaterial antenna with extended bandwidth," *IEEE antennas and wireless propagation letters*, vol. 8, pp. 295–298, 2008.

[116] P.-L. Chi and Y.-S. Shih, "Compact and bandwidth-enhanced zeroth-order resonant antenna," *IEEE Antennas and Wireless Propagation Letters*, vol. 14, pp. 285–288, 2014.

[117] J. K. Ji, G. H. Kim, and W. M. Seong, "Bandwidth enhancement of metamaterial antennas based on composite right/left-handed transmission line," *IEEE antennas and wireless propagation letters*, vol. 9, pp. 36–39, 2010.

[118] H. Li, Q. Zheng, J. Ding, and C. Guo, "Dual-band planar antenna loaded with crlh unit cell for wlan/wimax application," *IET Microwaves, Antennas & Propagation*, vol. 12, no. 1, pp. 132–136, 2017.

[119] B. D. Bala, M. K. A. Rahim, and N. A. Murad, "Dual mode metamaterial antenna for wideband applications," *Microwave and Optical Technology Letters*, vol. 56, no. 8, pp. 1846–1850, 2014.

[120] I. J. Bahl, *Lumped elements for RF and microwave circuits*. Artech house, 2003.

List of Publications

International Journals

1. Ratikanta Sahoo and D. Vakula, “Compact metamaterial inspired conformal dual-band antenna loaded with meander lines and fractal shaped inductor for Wi-Fi and WiMAX applications,” *IET Microwaves, Antennas & Propagation*, vol. 13, no. 13, pp. 2349-2359, 2019. (SCI)

2. Ratikanta Sahoo, Damera Vakula, "Gain enhancement of conformal wideband antenna with parasitic elements and low index metamaterial for WiMAX application," *AEU-International Journal of Electronics and Communications*, vol.105, pp. 24-35,2019.(SCI)

3. Ratikanta Sahoo, Damera Vakula, "Bow-tie-shaped wideband conformal antenna with wide-slot for GPS application", *Turkish Journal of Electrical Engineering & Computer Sciences*, vol. 27, no. 1, pp.80-93, 2019. (SCI)

4. Ratikanta Sahoo, Damera Vakula, and NVSN Sarma, “Printed Cross-Slot Wideband Conformal Antenna for GPS Application,” *Applied Computational Electromagnetics Society Journal*, vol. 33, no. 10, pp.1175–1181, 2018. (SCI)

5. Ratikanta Sahoo and D. Vakula, “ A cylindrical wideband conformal fractal antenna for GPS application,” *Advanced Electromagnetics*, vol. 6, no. 3, pp. 64-69, 2017. (ESCI)

International Conferences

1. Ratikanta Sahoo, D. Vakula, NVSN Sarma, "A wideband conformal slot antenna for GPS application," *Progress in Electromagnetics Research Symposium-Fall (PIERS-FALL)*, 19-22 Nov, 2017, Singapore, (IEEE Xplore).

2. Ratikanta Sahoo, D. Vakula. "A cylindrical conformal antenna for GPS application," *8th International Conference on Computing, Communication and Networking Technologies (ICCCNT)*,3-5 Jul, 2017, IIT Delhi,(IEEE Xplore).

3. Ratikanta Sahoo, D. Vakula, NVSN Sarma . "A dual U slot conformal antenna for Wi-Fi application," *Antenna Measurement Techniques Association(AMTA 2016)*,30 Oct.-3 Nov, 2016, Austin, USA,(IEEE Xplore).